Deltares

Eemshaven: Site evaluation

Geological and geotechnical characteristics and hazards

Eemshaven: Site evaluation
Geological and geotechnical characteristics and hazards

Eemshaven: Site evaluation
Geological and geotechnical characteristics and hazards

Client	Ministerie van Economische Zaken en Klimaat
Contact	
Reference	None
Keywords	Nuclear Power Plant, desk study, geology, geo-engineering, earthquakes, liquefaction

Document control	
Version	1.0
Date	28-07-2025
Project nr.	11209639-013
Document ID	-
Pages	
Classification	
Status	Final

Management Summary

This report describes the site evaluations for three potential nuclear power plant sites in and around the Eemshaven. This includes an evaluation of hazards associated with the build-up of the subsurface, subsidence, settlement, bearing capacity, seismicity and volcanism. No major risks have been identified. It is a first-assessment desk study based on currently available data and does not provide sufficient information for the design phase. The main attention points are:

- There are deposits that are potentially of archaeological interest around -15 to -20 m NAP. If the construction design will lead to significant disturbance of these deposits, archaeological research will need to be executed. It is advised to contact the Cultural Heritage Agency in an early stage of planning.
- The surface has subsided 15 to 20 cm due to gas extraction since the early sixties. Gas production was ceased in 2024, but subsidence will continue into the foreseeable future. Projected subsidence for the Eemshaven area is as follows:
  – ~4-5 cm until 2080 due to continued settlement in the Groningen gas field.
  – ~5 cm in the next 100 years due to glacio-isostatic adjustment.
  – ~3-10 cm due to other causes by 2100.
- Induced seismic activity originating from the Groningen gas field is expected to decline. The government body that monitors Dutch mining activity reports that the probability of an earthquake with a magnitude of $M_L > 4$ is currently 1% at the center of the Groningen field 15-20 km to the southwest of the Eemshaven. It is recommended to conduct a more detailed risk assessment of the effect of earthquakes during the design phase.
- Some findings with regards to the build-up of the shallow subsurface depart significantly from currently available geological models. Although there is enough data to describe the subsurface in this reconnaissance phase of the project, more data is needed when moving to the design phase. This is to better map the thickness of clay layers (notably the ‘NUNAWO’ layer) and buried tidal channels, which will be vital to accurately model differential settlement under heavy loads as well as groundwater flow.
- The bearing capacity of the NUNAWO layer is too low. This implies that ground treatment of the NUNAWO layer is required or that a piled foundation is needed.
- The geotechnical parameters are derived from CPT correlations. Lab testing is required to confirm the parameters derived from the correlations, especially in the layers with alternating thin sand and silt/clay layers.
- No groundwater monitoring wells are present at the potential project sites, which makes the geohydrological evaluation of the sites uncertain. It is advisable to develop and execute a monitoring plan, preferably consisting of multiple monitoring wells per site with filters at different depths, to capture both horizontal and vertical gradients. Monitoring should continue for at least one year to capture seasonal effects. High frequency monitoring would be advisable for at least a short period to capture tidal effects.

Technical summary

This report provides a subsurface site evaluation for the Eemshaven locality, for which three potential nuclear power plant sites were designated (Figure 1.1). This includes a data inventory, a geological desk study, a description of the geohydrological situation and the geotechnical parameters. Within the scope of these studies are the external hazards as described in chapter 5 of IAEA-SSR-1:

- Evaluation of fault capability.
- Evaluation of ground motion hazards (including human induced seismicity).
- Evaluation of volcanic hazards.
- Geotechnical characteristics and geological features of subsurface materials.
- Evaluation of geotechnical hazards and geological hazards.

The evaluation is based on currently available data and encompasses the construction of geological cross sections and first-level assessments of the geohydrological situation, the geotechnical properties of the subsurface and hazards associated with subsidence, seismicity and volcanic activity.

Geological build-up

The upper 500 m of the subsurface is part of an overall prograding sequence going from an open marine environment during the Neogene to Pleistocene fluvial, glacial and aeolian deposits. Neogene marine sediments coarsen upwards from clay to fine to medium sands between -500 and -120 m NAP, followed by predominantly medium to coarse fluvial sands at depths between -120 and -40 m NAP. The area was covered by land ice twice, which in the subsurface of the Eemshaven is mostly marked by glaciofluvial coarse sands and to a lesser extent glaciolacustrine clays and glacial till. Glacial deposits are generally found between -50 and -20 m NAP. The top of the Pleistocene sequence consists of fluvial and aeolian medium to coarse sands found between -25 and -15 m NAP. As most stratigraphic units consist of medium to coarse sands, they are hard to distinguish in boreholes and especially in CPTs.

Early Holocene layers consist of patches of thin basal peat layers (< 40 cm around depths of -12 to -18 m NAP) followed by silty clays that were deposited on supratidal salt marshes (Wormer Member of the Naaldwijk Formation). The Wormer clays are generally 1 to 3 m thick with the notable exception of the southern portion of site 3, where this clay layer is up to 10 m in thickness between -14 and -4 m NAP. The upper ~10 m of Holocene layers consist of a heterogeneous mix of mostly sand layers laminated with thin silt and clay layers. At site 1, there are a few more distinct clayey intervals. Below site 2 a tidal channel was discovered and mapped that locally cuts into the Wormer clays and basal peat. Note that the discovery of thick Wormer clays below site 3 and the presence of an incised tidal channel below site 2 is not captured by the GeoTOP or any other geological model.

Geotechnical properties

With the exception of the landfill, the sand layers are similar for the three sites. The landfill is dense at site 2 and 3 and loose to medium dense at site 1. The natural sand layers below consist mainly of loose to medium dense sands. The NUNAWO clay layer varies significantly in thickness, and can be absent in site 2 and the northern part of site 3. Differential settlements can be expected due to these variations. The bearing capacity of the NUNAWO layer is too low, which implies that ground treatment of the NUNAWO layer is required or that a piled foundation is needed. Such a treatment will also reduce the total expected settlements and the differential settlements. The Eemshaven area is known for soil profiles with layers consisting of alternating sand and silt/clay layers at centimeter scale. These layers are difficult to classify based on CPT data.

The region is known for static liquefaction of the external slopes of the foreshore. This is accounted for in regular evaluations of the flood defenses. However, static liquefaction may need re-evaluation for low likelihood events for a NPP. A stiff overconsolidated clay layer (“Potklei”) is present in the region, which can be identified by a denser CPT grid.

Geohydrological setting
There are no publicly available piezometric measurements at any of the three sites. Modelling results from the national hydrological model LHM suggest that site 1 has a clear division in a part with deeper (north) and shallower (south) groundwater levels, which is explained by variations in soil surface level. Also site 2 shows a large variation in groundwater level depth, with relatively deep levels in the south-west part and shallow levels in the northern part. On average, modelled groundwater levels are deepest at site 3.

Absolute groundwater levels (in m NAP) are lowest at site 1 and highest at site 3. Particularly in the east – southeast part of site 3 the groundwater levels are relatively high; this is due to higher resistance of the Holocene layer here, because of the presence of the clayey Wormer member.

The mean yearly highest groundwater levels (GHG) are particularly relevant in relation to inundation risk. At site 3, the GHG remains well below a depth of 1 meter. At site 1, however, there are areas where the calculated GHG is shallower than 0.5 meter, with most of the terrain having a GHG depth between 0.5 and 1 meter. At site 2 the variation is largest, again due to the large variations in soil surface levels.

It is stressed that, because of the absence of publicly available piezometric data, the modelling results are uncertain and data acquisition is advised.

Hazards associated with subsidence, seismicity and volcanic activity
InSAR measurements of surface motion show subsidence rates of around 3.5 to 6 mm/year for all three potential NPP sites in the Eemshaven area. Subsidence in the area is for the most part caused by gas extraction from the Groningen gas field. The area has been subjected to about 15 to 20 cm of subsidence since the early sixties when production started, which translates to about 3 mm/year. Although gas production ceased in 2024, subsidence will continue into the foreseeable future with another 4 to 5 cm of subsidence to be expected by 2080. Other causes of ground motion are glacio-isostatic adjustment and compaction.

Seismicity in the Eemshaven is also related to the Groningen gas field. The seismicity in the Groningen field is characterized by clustering around large faults in the producing reservoir at a depth of approximately 3 km. Over 1500 events of $M_L > 1$ have been linked to gas production since the 1980ies. The most notable event was the Huizinge earthquake in 2012, with a magnitude of $M_L = 3.6$, about 15 km to the southwest of the Eemshaven. The probability of an earthquake in the central part of the Groningen field with a magnitude of $M_L > 4$ was 5.5% before 2018 and has since declined to 1% in 2025.

There are no hazards associated with volcanic activity.

Need for additional data and analysis
Based on the current assessment of the subsurface at the Eemshaven sites, no additional geological or geotechnical data is needed for the current, reconnaissance, phase of the project.

The parameters derived here are based only on CPT data using correlations and Dutch standards. Additional laboratory testing on local material has not yet been performed. Further investigation is required before more detailed design phases are started. A denser grid of

CPTs penetrating to deeper layers is required to determine the expected (differential) settlements.

For a better characterization of the geohydrological setting, more data are urgently needed. It is advised to install piezometric monitoring wells with filters at different depths as soon as possible, to obtain a sufficiently long time series. Monitoring of groundwater levels should continue for at least one year to capture seasonal effects. While drilling for these monitoring wells, sediment cores should be obtained at predefined depths to perform additional geotechnical laboratory tests. Investigation of the sediment properties for the deep clay layers, particularly their settlement behaviour, is needed to optimise the geotechnical calculations.

For the potential risks associated with seismic hazards a full Probabilistic Seismic Hazard Analysis according to the latest scientific standards and SSHAC recommendations, is recommended. Based on preliminary assumptions it is concluded that the risk of full liquefaction is low. These assumptions need further consideration once the full Probabilistic Seismic Hazard Analysis has been carried out.

Table of Contents

1 Introduction

1.1 Aim of this study

This report provides a subsurface site characterization for three potential nuclear power plant (NPP) sites in and around the Eemshaven port in the northeastern tip of the Netherlands (Figure 1.1). This includes a data inventory, a geological desk study, a description of the geohydrological situation and the geotechnical parameters. Within the scope of this study are the external hazards as described in chapter 5 of IAEA-SSR-1:

- Evaluation of fault capability.
- Evaluation of ground motion hazards (including human induced seismicity).
- Evaluation of volcanic hazards.
- Geotechnical characteristics and geological features of subsurface materials.
- Evaluation of geotechnical hazards and geological hazards.

The geological, geohydrological and geotechnical models and profiles should all be regarded as first assessments to characterize the site, based on the currently available data. In addition, the report provides first assessments of expected rates of subsidence, seismic hazards and volcanic risks. All geological data and interpretations are available in a GIS project that is included as supplementary material to this report.

1.2 Content and structure of this report

This report is divided into ten chapters and two appendices. The introduction (Chapter 1) covers the aim of this study, while Chapter 2 introduces the available datasets and the datasets specifically used for the geological desk study. The desk study is based on publicly available data sources and two private datasets made available by the current operator. In subsequent chapters first the regional geological background is given (Chapter 3), while the creation of the geological cross sections is covered in Chapter 4. Chapter 5 uses, amongst others, the geological model to describe the geohydrological situation, including insights from existing groundwater-level monitoring systems. The geotechnical aspects of the site are described in Chapter 6, that ends with proposed soil profile parameters for the initial design of the site. Chapters 7, 8 and 9 give first assessments of expected rates of subsidence, seismic hazards and volcanic risks. The report finishes with conclusions and recommendations (Chapter 10). In addition to the main text, a detailed written description of key characteristics of geological units is provided in Appendix A. In a separate report, the Royal Netherlands Meteorological Institute (KNMI) describes the seismological and climatological data.

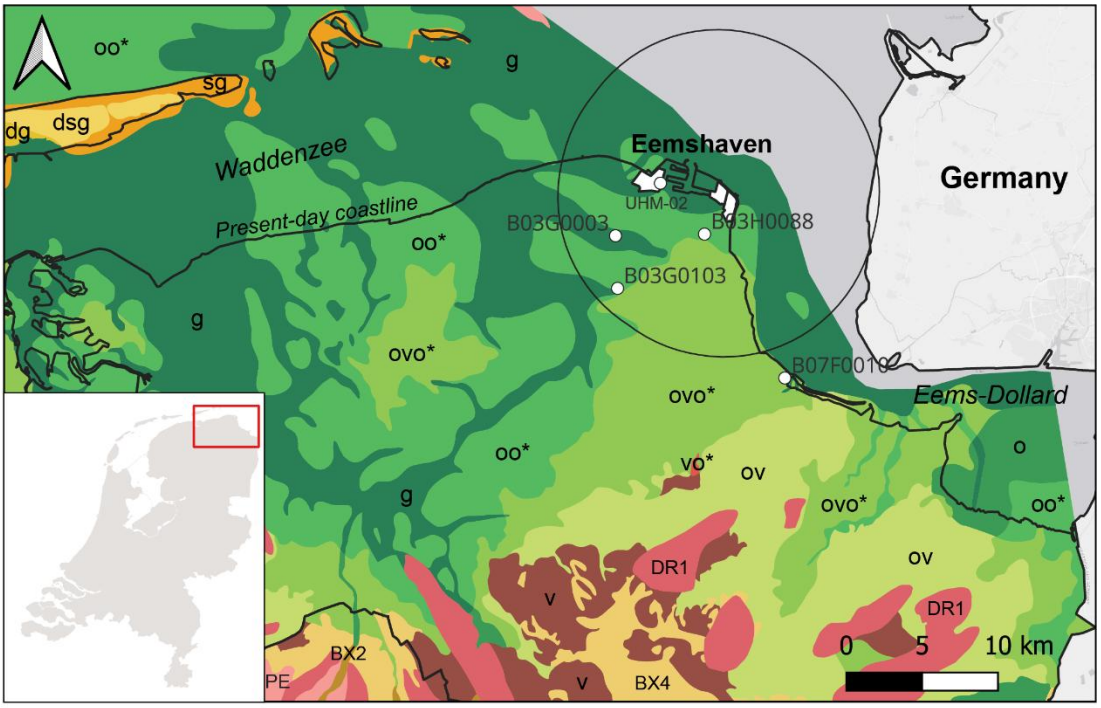

Units geological map

Holocene units

d	Coastal dune sand	dsg	dg			
s	Beach and foreshore deposits	sg				
g	Tidal channel deposits	g				
o	Tidal deposits	o	ov	ovo*	oo*	
v	Coastal peat	v	vo*			

Note: The order of the letters in the multiletter codes indicates the top-to-bottom stacking order of the deposits. e.g. ds = Coastal dune sand (d) on top of beach and foreshore deposits (s). The star behind a letter indicates that this part of the code (e.g. g in ovg) represents older Holocene deposits.*

Pleistocene and older units (onshore and at base of tidal channels)

BX1-4	Various glacial (aeolian) sand units (Boxtel Fm)	BX2	BX4
DR1	Glacial till, partially ice-pushed and/or co-deposited with older deposits (Drente Fm).	DR1	
PE	Glacial deposits, predominantly fine-grained, including 'pot clay'-type glaciolacustrine clays (Peelo Fm).	PE	

Figure 1.1 Geological location map for the North-Groningen region surrounding the Eemshaven potential NPP sites (the white areas, from west to east, S1, S2 and S3) with selected reference boreholes indicated. A 10-km buffer around site S2 is indicated with the black circle for reference. Geological units follow the geological map of the Netherlands (TNO-GDN, 2023).

2 Data sources

2.1 Subsurface data

Subsurface data were retrieved from several databases. The following sections provide a detailed description of the various datasets stored in these databases. Location of all datapoints and outline of the study area is available in a GIS file (see Section 2.5) and is indicated in Figure 2.1.

The Netherlands has multiple open-source databases from which a wide range of subsurface data can be retrieved in standardized format. The 'shallow subsurface' (in the Netherlands typically up to a depth of 500 m below Amsterdam Ordnance Datum zero or Normaal Amsterdams Peil (NAP)) can be obtained from DINOloket (https://www.dinoloket.nl/en). This database is maintained by the Geological Survey of the Netherlands and is actively updated with both new data and digitized legacy data. For an explanation on how data can be retrieved from this database, see https://www.dinoloket.nl/en/help-subsurface-data.

A separate database, NLOG (https://www.nlog.nl/en/welcome-nlog) exists for subsurface data that falls under the Dutch Mining Act (e.g. 2D and 3D seismic surveys and deep boreholes) and provides data that extend below -500 m NAP. This database is not described in the current report because of the limited use within the scope of this report.

2.1.1 Cone Penetration Tests

Geotechnical Cone Penetration Test (CPT) results for the Eemshaven sites are available from several different sources. DINOloket (https://www.dinoloket.nl/en/subsurface-data) provides .gef and .xml data files per CPT in a standardized format available through the Dutch National Key Registry of the Subsurface (BRO – https://basisregistratieondergrond.nl/english/). Within the study area (Figure 2.1) there are about 485 CPTs available this way. Older, manually scanned CPT data are also available at DINOloket, but lack the possibility for easy manipulation of the original data. There are almost 900 of such older CPTs available in the vicinity. A limited subset of these CPTs was used to identify depths of layer tops to aid in the interpretation of the geological profiles.

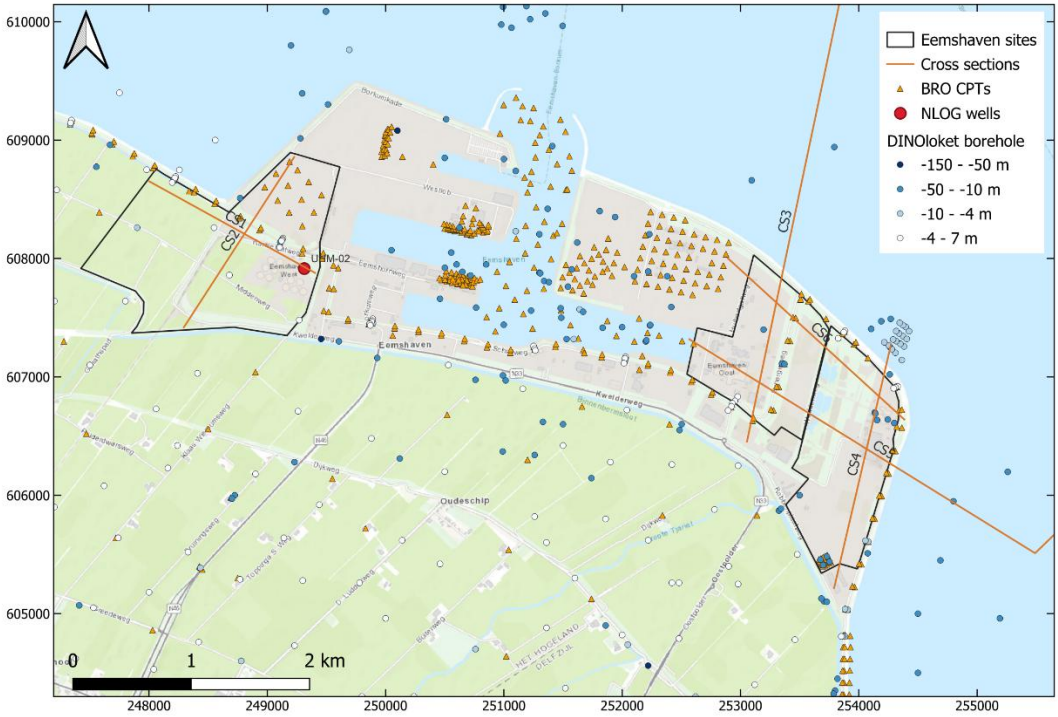

Figure 2.1 Location map of the Eemshaven area, the location of three potential sites S1, S2 and S3 (from west to east) and the publicly available site investigation data that were used in this report.

2.1.2 Borehole data

From DINOloket (https://www.dinoloket.nl/en/subsurface-data) geological borehole descriptions (GDN boreholes) are available for downloading. Some of these boreholes include core photographs and supporting analytical data (chemical and grain size). A total of 375 GDN boreholes were considered in the vicinity of the three Eemshaven sites with core lengths ranging from just a few meters to over 30 m (Figure 2.1). 75 of these boreholes include core photographs, 17 include a grain size analysis and 6 include a chemical analysis. None of the boreholes include (geophysical) well log data.

From the NLOG database there are three investigations all at the same location within the area of Eemshaven site 1. The most complete investigation that was used in this study is a hydrocarbon exploration borehole (Uithuizermeeden-02) down to a depth of 5 km that also includes well log and geophysical data.

Well log descriptions are available as .gef and .xml data files and for some older localities also as scanned pictures of the hand-drawn logs. Since 2000 well log descriptions are performed throughout the Netherlands according to a standardized well description method (Standaard Boor Beschrijvingsmethode – SBB5.1; Bosch, 2000). Geophysical well log data are available as .las files and/or scanned pictures at DINOloket. While these data is provided in a standardized digital format, the type of analytical data that is provided may differ by location.

2.2 Geological maps and models

The data stored in the open-source databases feeds into geological mapping of the surface and subsurface. These models can be visualized using DINOloket (https://www.dinoloket.nl/en/subsurface-models/map), or can be requested to view and use outside DINOloket (https://www.dinoloket.nl/en/request-model-files). Multiple subsurface models designed for specific purposes are available at DINOloket. Explanations on the

intended uses and data underlying the various models can be found at https://www.dinoloket.nl/en/explanation-subsurface-models. Stratigraphic units used in these models are described in the Stratigraphic Nomenclature of the Netherlands (Figure 2.2; https://www.dinoloket.nl/en/stratigraphic-nomenclature).
The relevant models in the current context are briefly discussed in the following paragraphs.

2.2.1 Geological map of the Netherlands

In 2023 an update was made to the Geological map of the Netherlands (TNO-GDN, 2023). For the onshore area, previous geological mapping at a scale of 1:50.000 and the regional 3D subsurface models were used as basis. For a full background on the geological map of the Netherlands, see https://www.dinoloket.nl/en/geological-map.

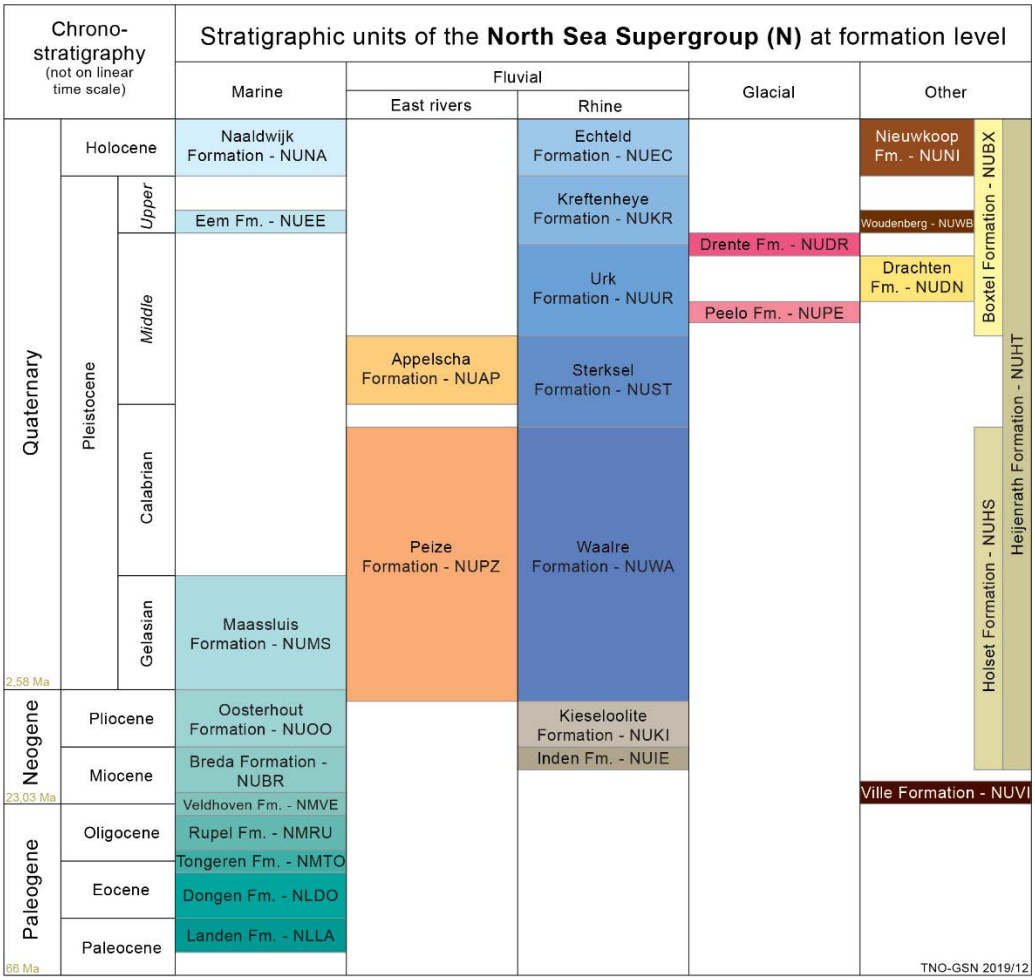

Figure 2.2. Dutch stratigraphic nomenclature as used in this report. Lithostratigraphy of the North Sea Supergroup at formation level (Adapted from Van Adrichem Boogaert & Kouwe, 1993). Stratigraphic units are split in marine and fluvial facies, glacial and glacially altered sediments and other formations with other deposits (e.g. peat), with the fluvial units further separated into units derived from the southeast (e.g. Paleo-Rhine River) and from the east (Baltic River System). For a full written description of these units at the scale of the Netherlands, see https://www.dinoloket.nl/en/stratigraphic-nomenclature.

2.2.2 GeoTOP

The GeoTOP model provides a detailed 3D model of the subsurface down to -50 m NAP to be used as a framework for groundwater management, (shallow) natural resources and infrastructure works. Voxels of 100 by 100 meters horizontally and 0.5 meter vertically provide lithology and lithostratigraphy including the probability of occurrence and uncertainties of each lithological class. The most recent version (v1.6.1) was released in 2025 and covers the Eemshaven area, including the Dutch offshore part that encompasses

the Doekegat, Eems and Bocht van Watum tidal channels. For a full description see https://www.dinoloket.nl/en/detailing-the-upper-layers-with-geotop.

2.2.3 DGM/REGIS

The Digital Geological Model (DGM, https://www.dinoloket.nl/en/the-digital-geological-model-dgm) and the regional hydrological model (REGIS, https://www.dinoloket.nl/en/regis-ii-the-hydrogeological-model) provide regional-scale subsurface interpretations down to approximately -500 m NAP. DGM and REGIS are 3D layer models that classify lithostratigraphic units based on their lithology and other rock properties. DGM/REGIS both use more simplified stratigraphic units compared to GeoTOP. For example: DGM/REGIS classify all Holocene deposits as a single 'complex' stratigraphic unit, whereas GeoTOP details Holocene deposits down to the level of geological formations and layers. Hence GeoTOP should be preferred for interpretations above -50 m NAP.

2.3 Surface elevation and bathymetry

The most recent publicly available digital terrain model (DTM) of the Algemeen Hoogtebestand Nederland (AHN5) at a resolution of 5x5 m was used for the surface elevation of onshore parts. For more information on the AHN, see https://www.ahn.nl/.

Vaklodingen were used for bathymetric data in and around the Eemshaven port area. Vaklodingen are singlebeam surveys that are carried out every three to six years depending on the area by the Directorate General for Public Works and Water Management. In the vicinity of the Eemshaven there are about ten of these surveys available from between 1983 and 2020. For more information on vaklodingen, see https://waterinfo-extra.rws.nl/monitoring/morfologie/

In this study we used a combination of AHN5 and the latest vakloding bathymetry as the current surface. In addition, for offshore parts of cross sections we also indicate the minimum (deepest) and maximum (shallowest) bathymetry based on the available vakloding surveys.

2.4 Data sources incorporated in the developed GIS project

A table listing and explaining the data sources used in the GIS project file has been made. See the attached file data_sources_GIS.xlsx. The GIS data is provided as a QGIS project file (.qgs). It is advised to open and visualize this in QGIS version 3.40.8 'Bratislava'.

3 Regional geological background

3.1 Conceptual model of the depositional history at the Eemshaven locality

Geological-, geotechnical- and geohydrological subsurface models all require a good conceptual knowledge of the interactions between processes that shaped the subsurface and its properties. In the following sections the geological record at the Eemshaven locality are briefly described for five time-intervals. The focus is on the type of sediment that was deposited and in which type of sedimentary environment these sediments originated. These descriptions serve as conceptual background knowledge that was used for the construction of the geological cross sections that are presented in Chapter 4 and as context for the geohydrological and geotechnical characterization in chapters 5 and 6.

In Appendix A, key characteristics of the geological units will be described individually per unit for those units in the shallow subsurface underneath the site location. The chosen unit names follow the Stratigraphic Nomenclature of the Netherlands (https://www.dinoloket.nl/en/stratigraphic-nomenclature) to enable easy comparison with existing subsurface national models such as GeoTOP and REGISII. Key localities outside the study area are used to provide additional detail on the subsurface record expected at the sites. These localities each provide a detailed record of similarly aged sedimentary rocks and sediments as those found at different depth intervals at the Eemshaven sites. The location of these reference localities is indicated in Figure 1.1 and/or Figure 2.1.

In general, the subsurface geological record at the Eemshaven localities represents a depositional history dominated by the gradual retreat of the North Sea after major regional transgression during the Cretaceous on top of the tectonically stable Groningen Platform. This resulted in a nearly 2000 m thick succession of various shallow marine-, and since the Pliocene continental depositional environments. On top of this emerging trend, Pleistocene glaciations left their mark by progressively reaching farther southward from Scandinavia and during multiple phases even covering the northern parts of the Netherlands. The glaciations impacted the previously deposited unconsolidated sediments, for instance by incising deep tunnel valleys underneath the ice sheet or by leaving behind layers of glacial till. Sea-level rise at the beginning of the Holocene caused a return of coastal- and marine environments where the effects of tides left their mark through erosion and deposition. In the last 100’s of years, humans gradually reclaimed land from the sea, creating the present-day landscape.

In the following sections, this brief geological sketch is elaborated and supported with relevant data and/or maps.

3.1.1 Paleozoic and Mesozoic

The geological history of the Eemshaven region is marked by a complex and well-documented stratigraphy, largely due to its proximity to the prolific Groningen gas field (Vis et al., 2025). The Groningen Platform has acted as a persistent structural high since a significant phase of subsidence and sedimentation during the Late Devonian to Carboniferous (Kombrink, 2008). Overlying this ancient basement, a thick succession – approximately 1000 meters – of Permo-Triassic sedimentary rocks was deposited, including the Rotliegend sandstones, Zechstein evaporites, and Lower Germanic Triassic units. The Zechstein interval is notable for the development of salt diapirs and walls, which have influenced subsequent structural evolution. The major regional Hardegsen unconformity at around 2000 meters depth marks a significant hiatus, separating the Triassic from the overlying Cretaceous limestones, which reach a thickness of about 950 meters and represent a later phase of marine sedimentation away from siliciclastic sediment sources.

The oldest sedimentary rocks in the Eemshaven subsurface can be described using the Uithuizermeeden boreholes (Figure 3.1 - https://www.nlog.nl/nlog-mapviewer/brh/106523395?lang=en). These wells are located within the confines of the westernmost site 1. A first hydrocarbon exploration well (UHM-01/UHM-01-S1) was drilled in 1965 down to 3330 m depth. This was followed by a 440 m deep observation well (UHM-OBS) in 1969. More recently, another exploration well down to 5420 m depth (UHM-02, location shown in Figure 2.1) was drilled in 2002.

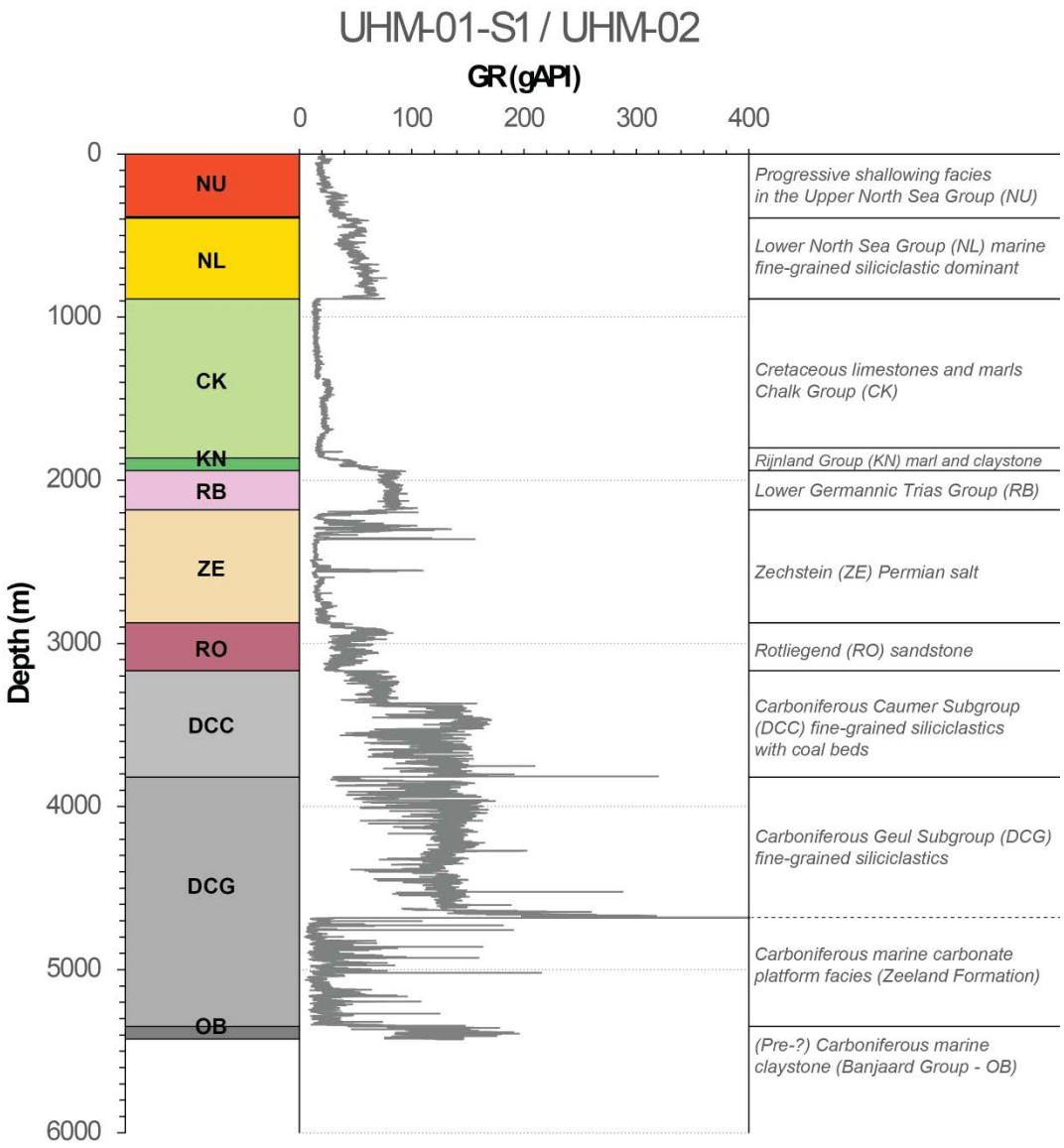

Figure 3.1 Stratigraphic reference composite well Uithuizermeeden (combination of wells UHM-01-S1 / UHM-02) for the deep subsurface at Eemshaven. Stratigraphic units are given at group level.

3.1.2 Paleogene and Neogene

Locality B03G0103 provides the equivalent of Neogene sedimentary rocks encountered below the Eemshaven, namely the Miocene Breda Formation and Pliocene Oosterhout Formation. Paleogene formations are likely to consist of the Rupel, Dongen and Landen formations. There are no cores or geological models that interpret Paleogene formations in the vicinity of the Eemshaven at formation level. The closest borehole that describes Paleogene formations is B06A0076, located about 60 km to the west. It shows a sequence of the Dongen, Rupel and Breda formations. Given the spatial extent of these formations, a similar sequence is also expected to exist in the Eemshaven area.

The Breda and Oosterhout formations in B03G0103 describe an overall prograding sequence and the associated change of depositional environment at this location from a shallow marine environment of the Breda Formation to a deltaic and near-shore environment of the Oosterhout Formation. This is well illustrated in the paleogeographic reconstruction of Gibbard & Lewin (2016) (Figure 3.2).

The Breda Formation is primarily composed of clay, with some more sandy layers towards its top. It is found at depths of around -400 to -130 m NAP according to the DGM model. The glauconite content in the Breda Formation is known to be notably high, which is chemically recognized by higher K_2O to Al_2O_3 ratios compared to glauconite-free sand (Huisman & Kiden, 1998). The presence of potassium as a radioactive element leads to elevated levels of gamma radiation, which may be confused in gamma-ray logs for a higher clay-content. Looking at the gamma-ray log of B03G0103, the sediments of the Breda Formation can clearly be distinguished from those of the overlying Oosterhout Formation by their higher values (Figure 3.3). This high glauconite content is attributed to in situ production, indicating low sedimentation rates in a marine environment. Peaks in glauconite may be associated with marine transgressions (Adriaens et al., 2018).

The Oosterhout Formation is characterized by light grey-green very fine- to medium sand, rich in shells, and can locally be clayey and glauconitic. It is found at depths between -240 and -120 m according to the DGM. The formation unconformably overlies the Breda Formation, which is marked by an angular unconformity known as the Late Miocene Unconformity (LMU) (Munsterman et al., 2019), which is the redefined base of the Oosterhout Formation. It is marked by a sharp decrease in gamma-ray readings (also visible in the gamma-ray log in Figure 3.3). The Oosterhout Formation is associated with deltaic and near-shore depositional environments part of an overall prograding delta system that was mostly fed by the Eridanos river system coming from the east (Gibbard & Lewin, 2016). It is overlain by more proximal deltaic and continental (fluvial) deposits of the Peize Formation as described in the next section.

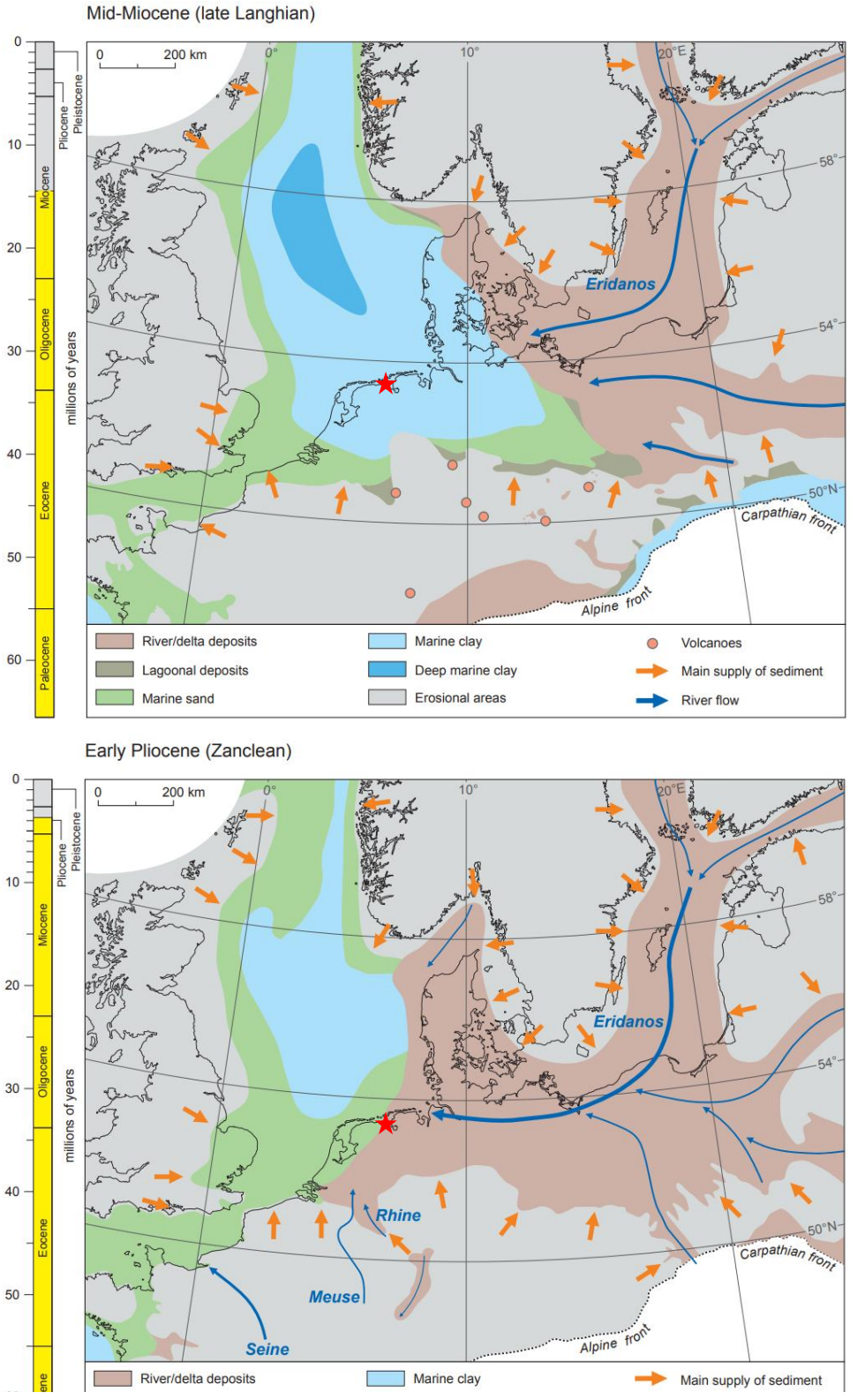

Figure 3.2 Paleogeographic reconstruction in Gibbard & Lewin (2016) focusing on the North Sea basin and its sediment supply systems. The star is the location of Eemshaven. During the Mid-Miocene (upper panel), the Eemshaven area was located in a marine environment in which the Breda Formation clays were deposited. Further progradation of Eridanos-fed delta systems led to near-shore and deltaic conditions during the Pliocene (lower panel).

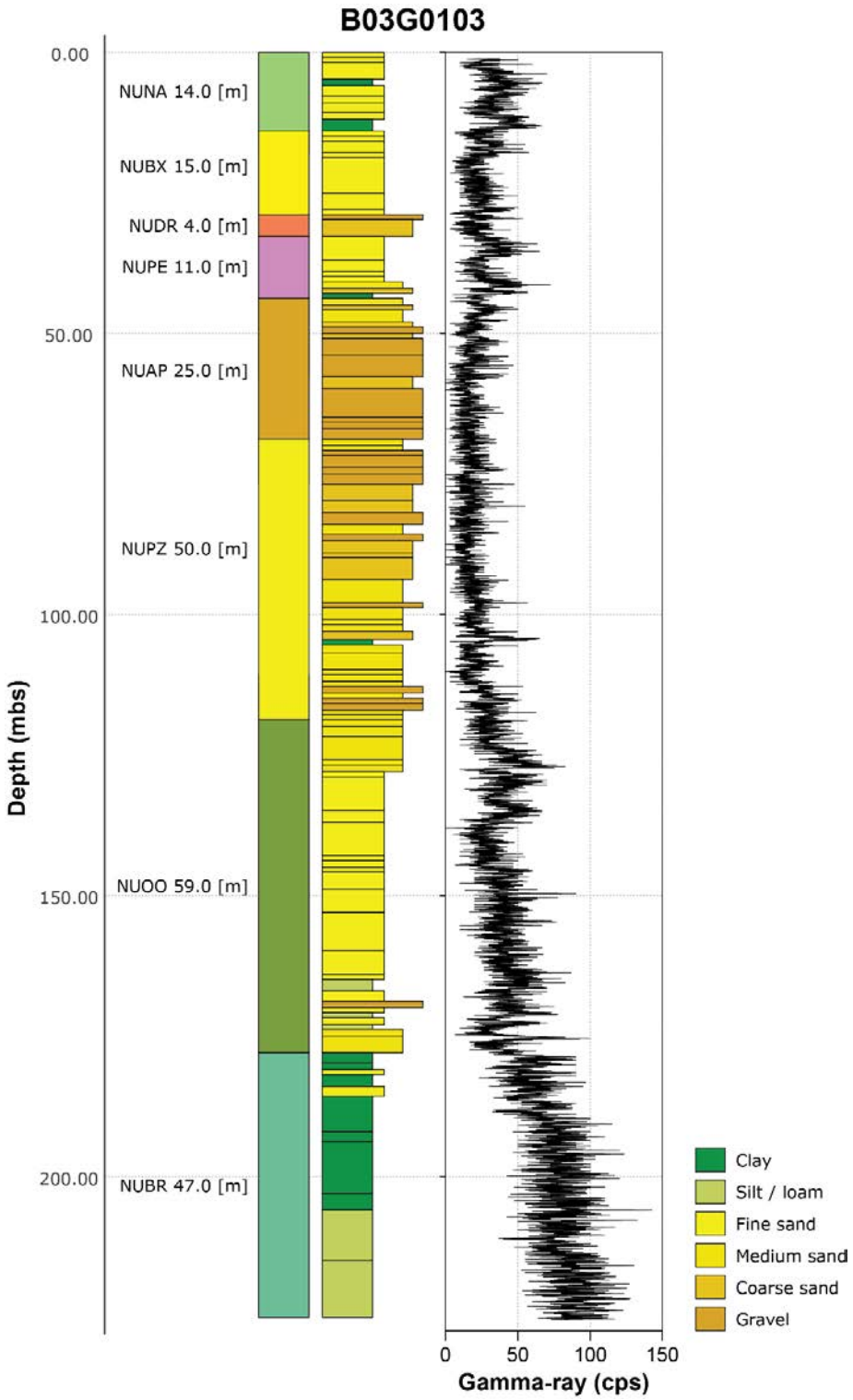

Figure 3.3 Stratigraphic log of well B03G0103 showing a Neogene (Miocene and Pliocene), Pleistocene and Holocene sequence that is typical for this area. Neogene marine deposits of the Breda and Oosterhout formations are overlain by early to middle Pleistocene fluvial deposits of the Peize and Appelscha formations. Middle-Pleistocene Peelo and Drente glaciofluvial deposits are relatively thin in this borehole but may obtain greater thicknesses at Eemshaven. Also note the Gamma-ray log and the difference between NUBR (glauconite-rich) clays, NUOO sands and fluvial sands of the Peize and Appelscha formations. The Neogene to Middle-Pleistocene sequence shows an overall coarsening-upwards trend that represents the transition from a distal offshore environment (NUBR) to a near-shore (NUOO), a deltaic (lower part of NUPZ) and a terrestrial environment (NUPZ and NUAP).

3.1.3 Pleistocene

Sea levels dropped at the onset of the colder Pleistocene epoch, leading to a shallow marine environment transitioning into a more proximal deltaic (delta front to delta top) and later terrestrial environment (Figure 3.4). Early to Middle Pleistocene (2.58 - 0.47 Ma) infill of this part of the North-Sea basin was dominated by large braided river systems. The first of these was the Eridanos- or Baltic river system originating in the Baltic area, which led to the deposition of mostly coarse and distinctly quartz-rich (white) sands. These sands belong to the Peize Formation (NUPZ) which in most places lies unconformably on top of the Late-Pliocene Oosterhout sands. The source of sediment supply shifted around 1 Ma when rivers originating from central- and eastern Germany became more dominant (e.g. the Elbe and Weser rivers) leading to a gradual transition into the Appelscha Formation (NUAP). Locality B03G0103 illustrates the sequence of Peize and Appelscha fluvial sands.

During the middle-Pleistocene, this area is known to have been covered twice by ice sheets during the Elsterian (465 - 418 ka) and Saalian (238 - 126 ka) stages. In the subsurface of the Eemshaven area lies the Peelo Formation (NUPE), which in the direct vicinity mostly consists of glaciofluvial sands that were deposited by glacial outwash as the ice retreated towards the end of the Elsterian. Deep N-S oriented erosional valleys (so-called ‘tunnel valleys’) developed below and in front of the Elsterian ice sheets due to strong subglacial and concentrated meltwater flows. Some of the tunnel valleys were up to 375 m deep and later filled with glaciofluvial sands and glaciolacustrine clays (Kluiving et al., 2003). The latter is often referred to as ‘pot clays’ or ‘pottery clay’ because of their high density and stiffness. One of such tunnel valleys is located to the east of the Eemshaven area (Figure 3.5). Its infill features thick layers of potclay and glaciofluvial sand that belong to the Peelo Formation. Locality B07F0010 near Delfzijl (Figure 3.6) is a good example of the central part of this tunnel valley that was filled with over 40 m of potclay. In the deeper parts of the Eems-Dollard estuary this clay layer is often exposed at the channel floor where it acts as an erosion-resistant layer (Pierik et al., 2022, Van Onselen, 2021). Conversely, Locality B03H0088 closer to the Eemshaven (Figure 3.7) shows a purely sandy glaciofluvial and thinner infill at the margin of the tunnel valley system.

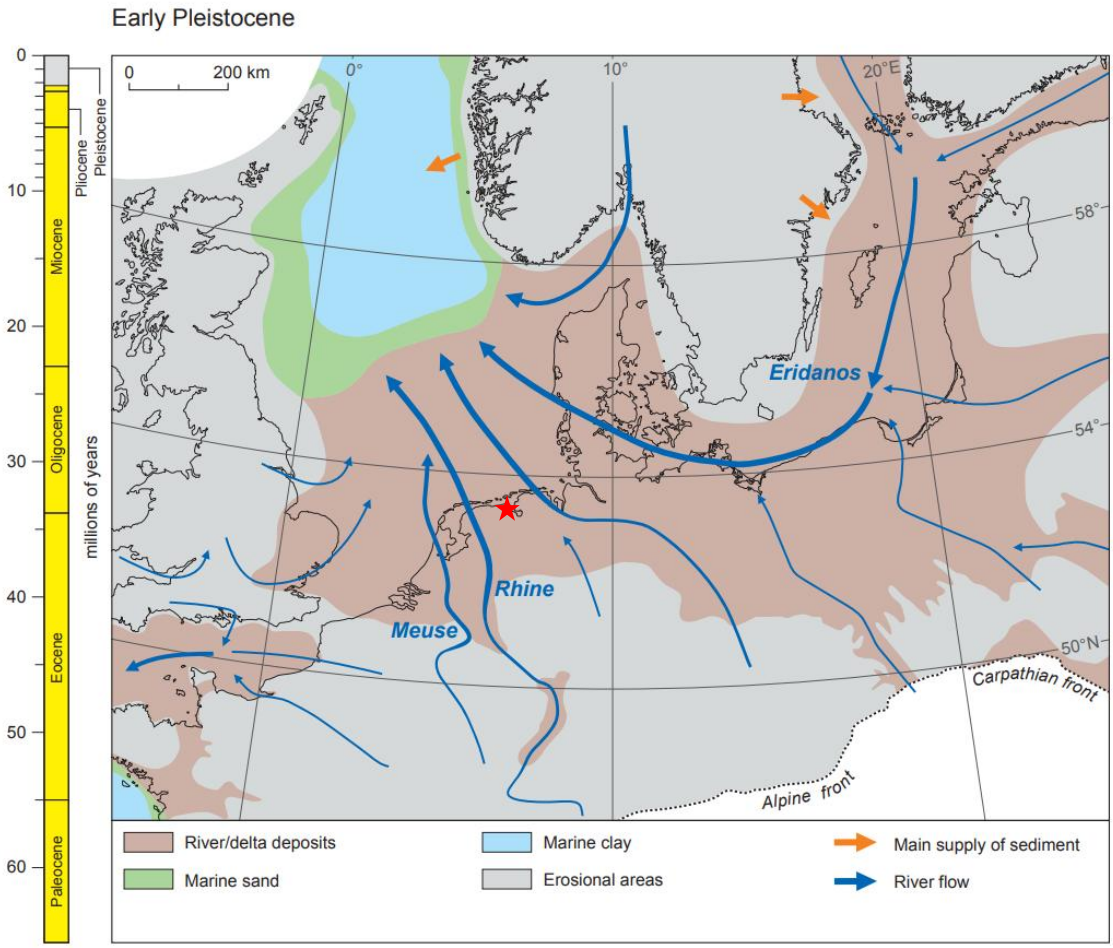

Figure 3.4 Paleogeographic reconstruction of Gibbard & Lewin (2016) focusing on the Nort Sea basin and its sediment supply systems during the Early Pleistocene. The Eemshaven area, marked by the red star, was part of a large river system. Initially, sediment supply was dominantly coming from the Baltic area through the Eridanos river system to the east. This led to the deposition of quartz-rich Peize sands. Later, sediment supply from German rivers to the southeast became more dominant, forming the Appelscha Formation.

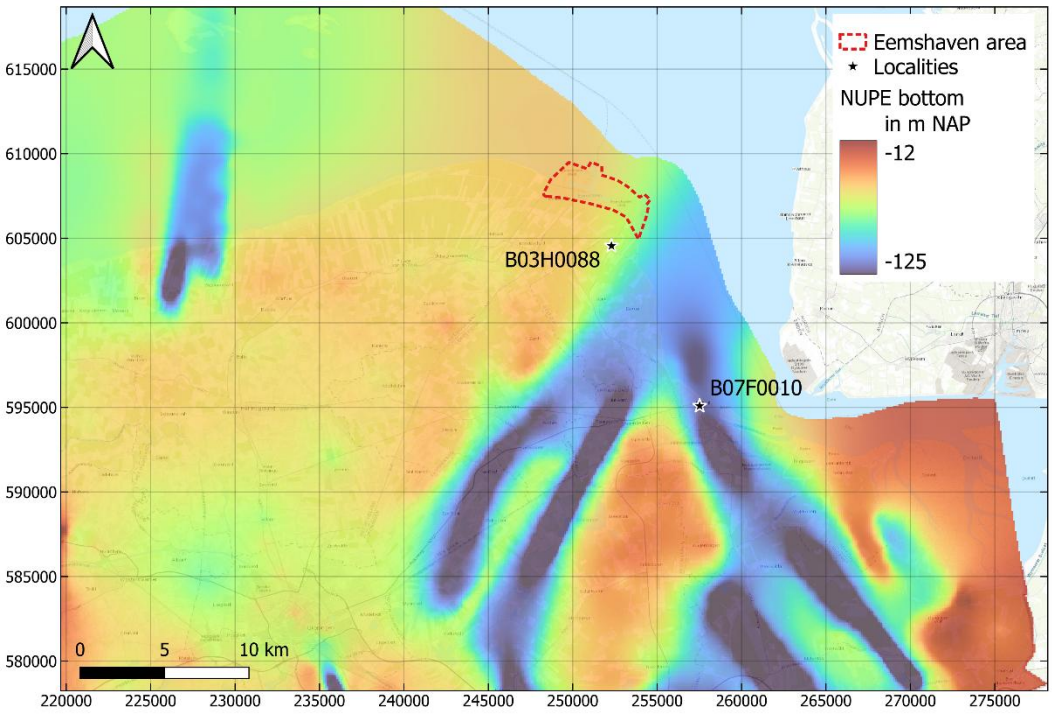

Figure 3.5 The bottom depth of the Peelo Formation according to the DGM model reveals the presence of deeply incised tunnel valleys formed during the Elsterian glaciation in this part of The Netherlands. As shown on the map, a prominent N-S oriented tunnel valley system is located just to the east of the Eemshaven area.

During the Holstein interglacial that followed the Elsterian, the area around the present-day Eemshaven presumably saw a period of fluvial/tidal/shallow marine activity (associated with the Tijnje Member of the Urk Formation, NUURTY) and later aeolian activity (Drachten Formation, NUDN). However, most of the sediment deposited during this period was subsequently reworked and/or eroded by the Saalian ice sheet. Sediments of the Peelo Formation are therefore typically unconformably overlain by glacial till (Gieten Member of the Drente Formation, NUDRGI), glacial outwash (Schaarsbergen Member of the Drente Formation, NUDRSC) or by later Pleistocene deposits. This sequence is well-illustrated in Locality B03G0103 (Figure 3.3).

In the warmer Eemian interglacial stage that followed, global sea levels rose. An extensive tidal system formed along the line of the present-day Lauwerszee and the City of Groningen, which was a lower-lying area at the time (Meijles, 2015). These predominantly tidal deposits are identified as the Eem Formation (NUEE). During the subsequent Weichselian stage, popularly referred to as the ‘last ice age’, the northern ice sheets did not reach this area. Sediment deposited in alternating mix of (periglacial) fluvial, aeolian and lacustrine depositional environments during this time is associated with the Boxtel Formation (NUBX).

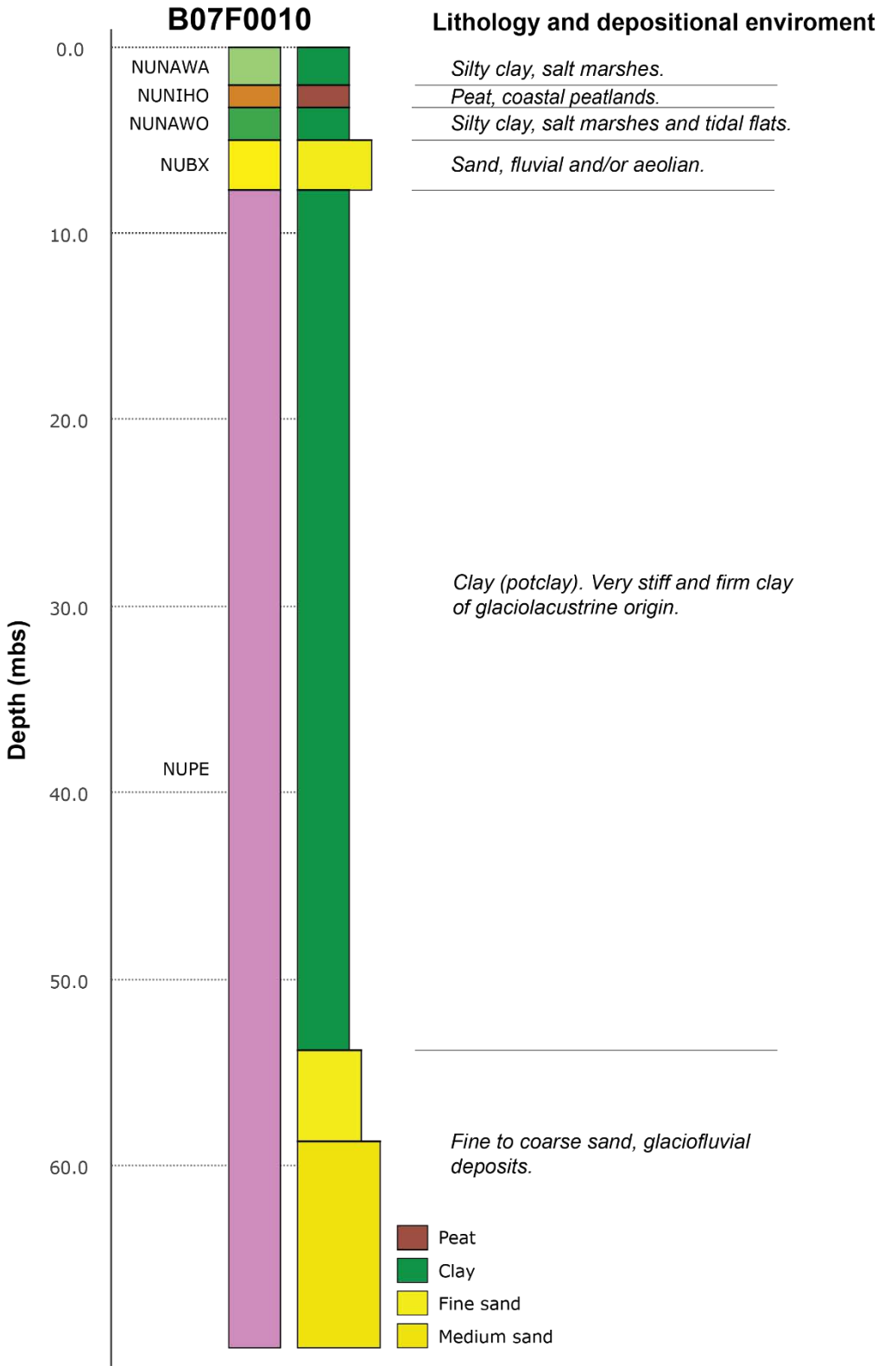

Figure 3.6 Stratigraphic log of GDN borehole B07F0010, about 12 km to the south in the city of Delfzijl. This borehole is located in a tunnel valley (see Figure 3.5) and was filled with glaciolacustrine 'potclay'.

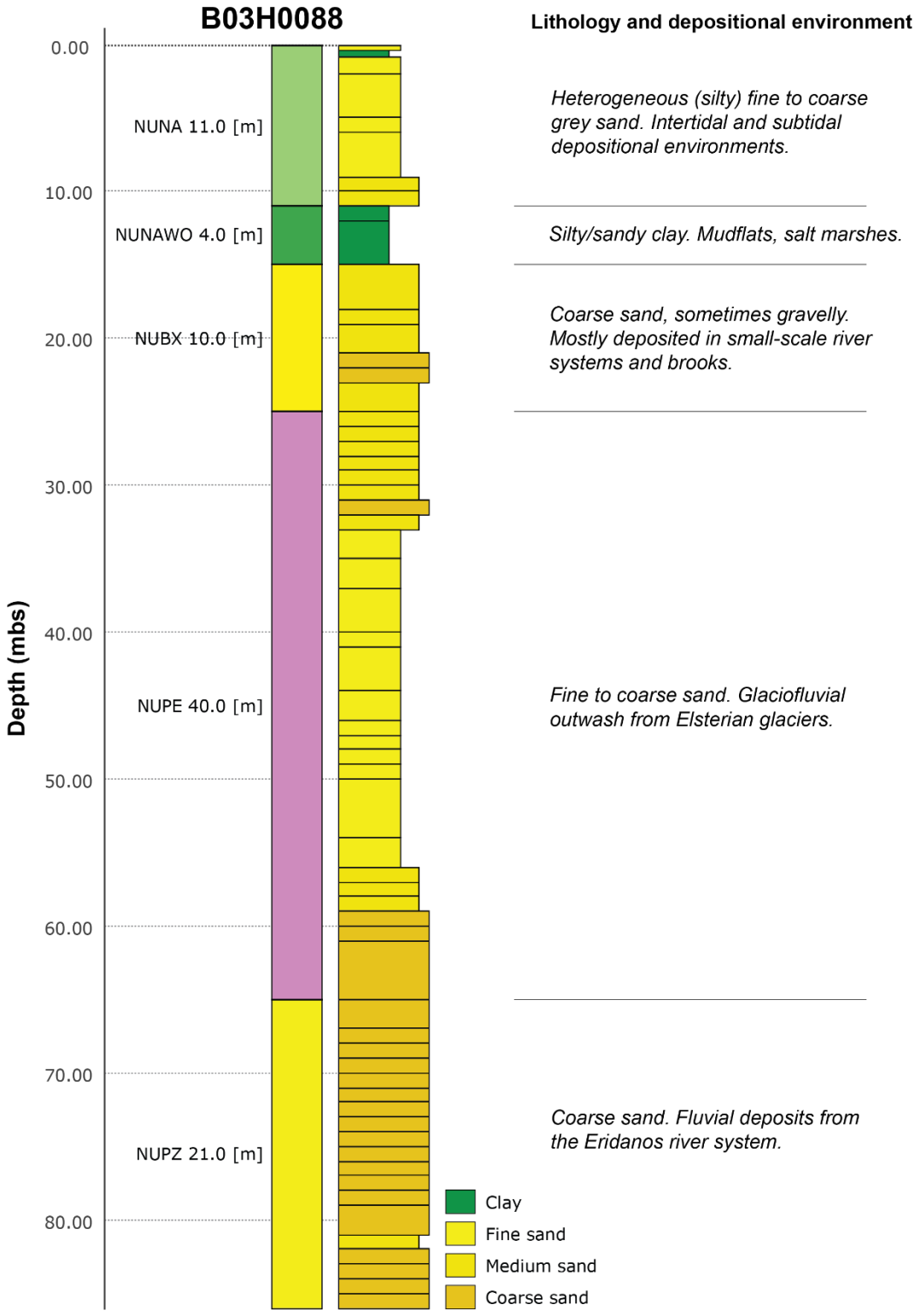

Figure 3.7 Stratigraphic log of GDN borehole B03H0088, 3 km south of the Eemshaven, showing a Pleistocene sequence of fluvial sands of the Eridanos river system (NUPZ) unconformably overlain by glaciofluvial sediments of the Peelo Formation. Compared to B07F0010 (

Figure 3.6), the Peelo Formation is thinner here at the margin of the tunnel valley and consists mostly of sand from glaciofluvial outwash, rather than glaciolacustrine clays.

3.1.4 Holocene

The geological development during the Holocene was strongly influenced by the global sea-level rise after the Last Glacial Maximum (Hijma et al., 2009; Hijma & Cohen, 2019). Rising sea-levels progressively drowned the previously exposed areas (Vos & Van Heeringen, 1997). Initial drowning in the early Holocene is commonly characterized by the thin peat layer known as the Basal Peat Bed of the Nieuwkoop Formation. The overlying clastic tidal deposits of the Wormer Member of the Naaldwijk Formation indicate a further increase in relative sea-level. More peat, in the form of the Hollandveen Member occurs higher in the sequence and is typically followed by more clastic tidal deposits of the Walcheren Member of the Naaldwijk Formation.

Around the Eemshaven, early Holocene deposits mostly consist of (sandy and/or sandy laminated) clays that were deposited in salt marshes and on tidal mud flats. These clays are part of the Wormer Member of the Naaldwijk Formation (NUNAWO) and lie on top of the Late Pleistocene Boxtel sands or above a thin layer of basal peat. Throughout most of the remaining Middle and Late Holocene periods, the area was in an intertidal zone along the Eems-Dollard estuary. Depositional environments alternated between tidal flats, bars, channels and creeks, leaving a heterogeneous unit consisting mostly of sand alternated by relatively thin silt and clay layers and sporadically some very thin peat layers. Locality B03H0449 (Figure 3.8) shows the above described sequence of Holocene deposits.

Locally, deeper tidal channels incised into the upper Pleistocene units (mainly the Boxtel Formation) and eroded the Early Holocene Wormer clay and basal peat in the process. These channels left bed and channel fill deposits consisting of mostly fine sand.

3.1.5 Anthropogenic influence

From 1500 AD onwards, reclamation of salt marshes to create arable farmland and safe places for subsistence shaped the Dutch Wadden Sea coast. By 1750 AD, land reclamation had displaced most natural shore habitats and by 1850 AD the new shoreline was fully protected by dikes (Reise, 2013, De Haas & Schepers, 2022). This new protected shoreline ran along the southern edge of the current Eemshaven port.

The Eemshaven port is located on the former Uithuizer Wad, a mudflat area located between the Doekegat tidal channel of the Eems-Dollard estuary and the protected shoreline at the time. Most of the mud flat area was reclaimed in the early 1970s when construction works began, albeit a small part in the west was already reclaimed in 1953 as part of the Koningin Emma polder. Up to 6 m of sand was added to create the new quays and industrial areas, whereas the man-made levees protecting the port rise up to 15 m above the sea level. The transition from deposits on the Uithuizer mudflat to anthropogenic sand is often marked by a thin layer of sandy clay, clayey sand or silt in CPTs and boreholes.

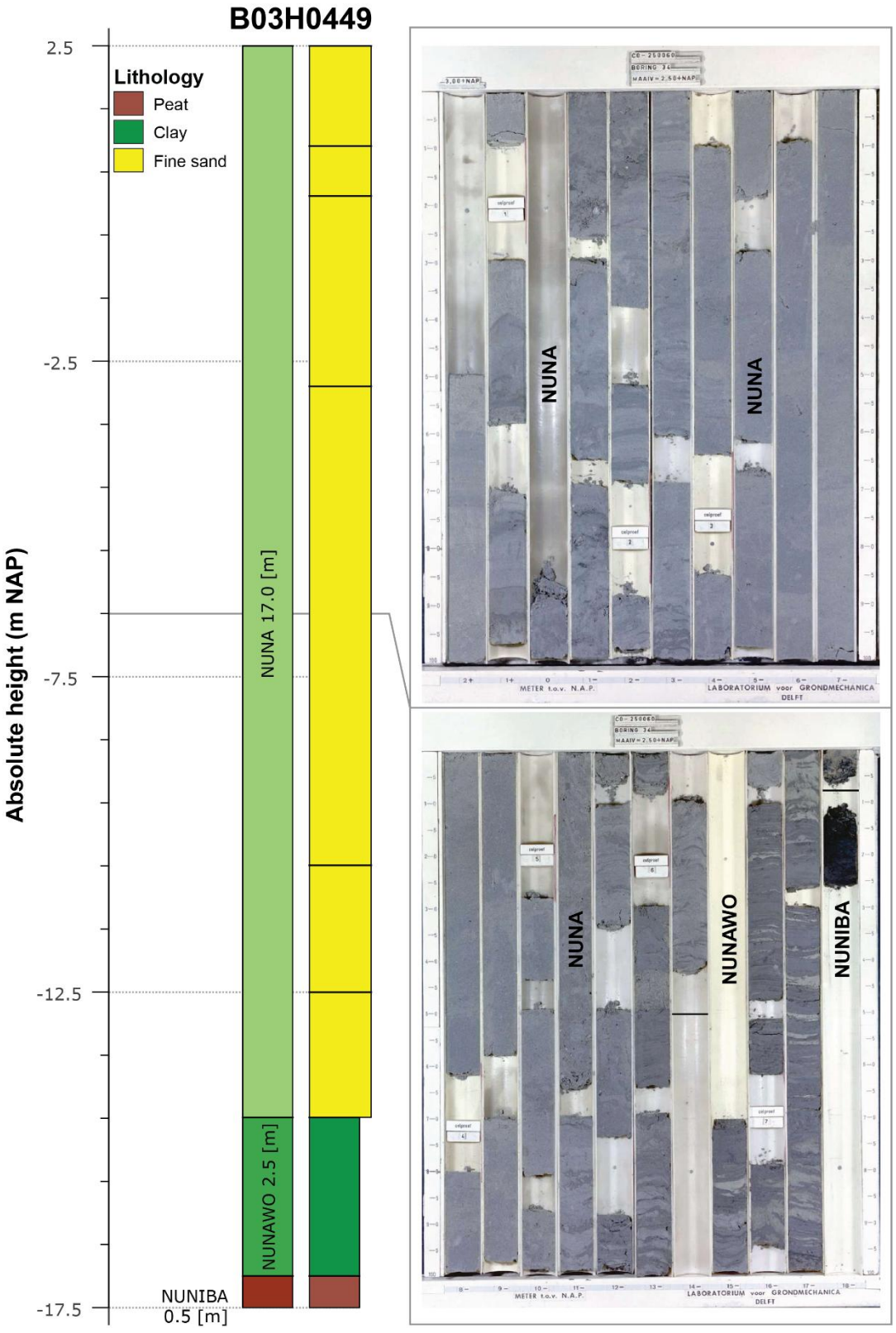

Figure 3.8 Stratigraphic log of GDN borehole B03H0449 showing a the typical sequence of Holocene deposits for the Eemshaven area. A thin layer of NUNIBA basal peat and Early-Holocene NUNAWO clay deposited in an environment of salt marshes followed by NUNA sand deposited on tidal flats and in tidal channels. Although at first glance the material looks quite homogeneous, note the sand and clay laminae, especially in the NUNAWO clay.

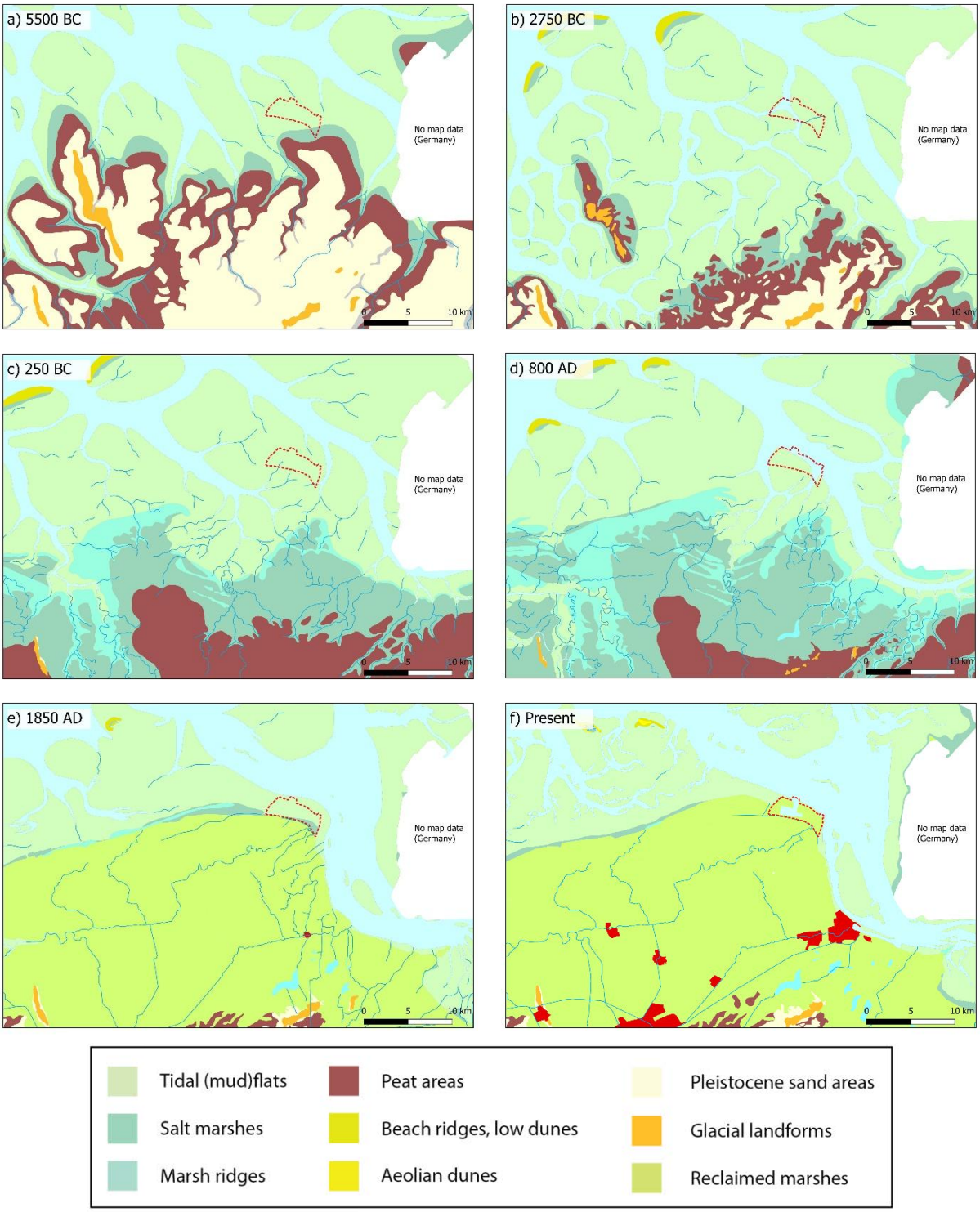

Figure 3.9 Holocene paleoenvironmental reconstructions for the northeastern part of Groningen, around Eemshaven. After Vos et al. (2020). The contours of the Eemshaven area are indicated in red. (a) Salt marshes and tidal flats during the Atlantic chronozone of the Holocene. (b, c and d) intertidal flats, tidal channels and creeks are present in the Eemshaven area up until recent times. Note that the exact locations of these environments throughout time are not certain. (e, f) in recent times, salt marshes and tidal flats were reclaimed and protected by dikes. In 1850 AD (panel e) the Eemshaven area is located on a mud flat called the 'Uithuizer Wad' that was reclaimed in the early 1970s to build the Eemshaven port. See also the historical topographic maps in Figure 3.10.

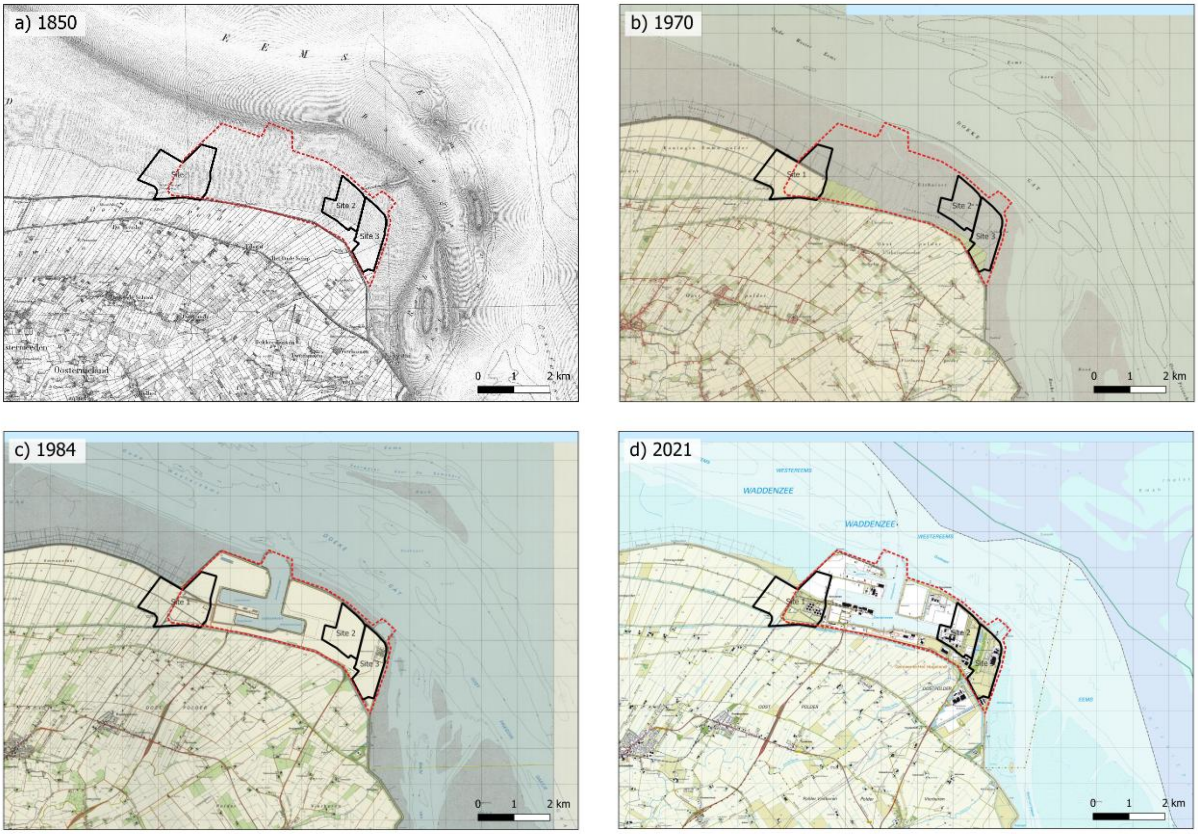

Figure 3.10 Historical topographic maps in relation to the Eemshaven area (red outline) and potential sites 1, 2 and 3 (black outlines). In 1850 (panel a), the entire area was a mudflat (Uithuizer Wad) that separated the Doekegat tidal channel from the reclaimed marshlands. In 1970 (panel b), just before construction of the port commenced, most of the area was still part of this mudflat except for most of site 1, which was already reclaimed in 1953 as part of the Koningin Emma polder. The topographic map of 1984 (panel c) is the earliest available map that shows the completed Eemshaven port area. The most recent map (panel d) additionally shows the new Beatrixhaven that opened in 2008.

4 Geological cross sections

4.1 Construction of the cross sections

A total of six cross sections were produced, covering all three sites in the Eemshaven area with two cross sections additionally including part of the immediate offshore area. All cross sections go down to a depth of -40 m NAP. With little CPT and borehole information reaching the depth of Pleistocene units, GeoTOP has been primarily used to determine the boundaries of the Peelo Formation (NUPE), Eem Formation (NUEE) and the lower boundary of the Boxtel Formation (NUBX). CPT records were used to update the boundaries and presence of Holocene stratigraphic units (NUNA, NUNAWO, NUNIBA), as this information was not taken into account in the GeoTOP model.

In the sections below, the characteristics of stratigraphic units as they appear in the respective cross sections are described in the order from oldest (NUPE) to youngest (NUAAOP).

Findings based on these cross sections, including the discovery of an incised tidal channel running below site 2 and 3, are presented at the end of this chapter in Section 4.4.

4.2 Site 1 cross sections

There are two cross sections covering site 1. CS1 running from northwest to southeast (Figure 4.1) and CS2 from southwest to northeast (Figure 4.2).

4.2.1 Peelo Formation (NUPE)

NUPE is the oldest unit shown in both cross sections and is believed to mostly consist of medium to very coarse sand based on nearby boreholes (e.g. B03G0105, B03H0035 and B03H0034). The only exception is B03G0012, located 1.5 km to the south. This borehole suggests that the top of NUPE consists of clay, presumably potclay (Nieuwolda Member). NUPE lies at a depth of -25 to -30 m NAP for the upper boundary and about -50 m NAP for the lower boundary.

4.2.2 Eem Formation (NUEE)

On top of NUPE lies the Eem Formation. NUEE is interpreted in boreholes to the west (e.g. B03G0057 and B03G0041), but not to the east. It is unknown if this formation reaches the (north)eastern part of the site 1. It is very likely that NUEE wedges out towards the northeast, as shown in the SW-NE cross section (Figure 4.2). NUEE may be found between -22 and -30 m NAP in the southwest of site 1 and is believed to be absent in the northeast. NUEE in this area consists mostly of fine to very coarse sand, but may be clayey at the top (e.g. as in B03G0041). In these cross sections however, there is no indication of such a clay layer.

4.2.3 Boxtel Formation (NUBX)

NUEE is overlain by NUBX and can be found between -16 and -22 m NAP in the southwest, dipping slightly towards the northeast where it is found between -18 and -24 m. The exact depth of the lower boundary is highly uncertain as there is a little data to back this up. NUBX here generally consists of medium to coarse sand with a gravel admixture. Cone resistance reaches upward of 30 MPa in some CPTs (e.g. CPTs 100420 and 100410). NUBX may also contain thin layers of (sandy) clay (e.g. CPT100420 at -22 m NAP).

4.2.4 Nieuwkoop Formation basal peat (NUNIBA)

A thin layer of basal peat (NUNIBA) was found at a depth of -17 to -18 m NAP around where the two cross sections intersect (around B03G0013, CPT100501 and 100420). It is absent in

most other CPTs as seen in the NW-SE cross section (Figure 4.1). The presence of NUNIBA also indicates that the Late-Pleistocene surface had been preserved, which may be of archaeological interest.

4.2.5 Naaldwijk Formation (NUNA and NUNAWO)

The Holocene layers consist of the Wormer Member of the Naaldwijk Formation (NUNAWO) followed by the Naaldwijk Formation (undifferentiated) all the way to either the current land surface or anthropogenic material if present. NUNAWO in this area consists of sandy or silty clay alternated by thin layers of sand. It lies at a depth of around -18 m NAP and has a thickness that ranges from 1 to 3 m. In the easternmost part of the site 1 area NUNAWO reaches a thickness of up to 6 m.

The overlying undifferentiated Naaldwijk Formation predominantly consists of fine to coarse sands with two intervals that are notably more clayey and/or silty in composition. Between -16 and -10 m NAP NUNA consists of medium to coarse sand almost exclusively, suggesting a high-energy depositional environment of tidal channels and (subtidal) bars. The first interval with silt/clay layers is found between -10 and -8 m NAP (e.g. CPT100420). The second clayey/silty interval is found around -5 m NAP and is especially well-developed in the NW part of site 1 (the left half of the NW-SE cross section in Figure 4.1). These fine-grained intervals are associated with more distal environments such as mudflats and salt marshes (i.e. away from main tidal channels and less frequently flooded), whereas intervals of sand are associated with the higher energy conditions of tidal channels, bars and creeks.

4.2.6 Anthropogenic (NUAAOP)

CPT data from anthropogenic material that was used to reclaim and build the Eemshaven area suggests that it does not exclusively consists of sand. In the northeastern tip of site 1, multiple thin clay layers or lenses can be identified, most notably in CPT125965. Although little public information is available on where the material for the Eemshaven was sourced from, it is likely that local sources were used, such as dredging material from the Eems-Dollard navigation channel.

4.3 Site 2 & 3 cross sections

There are four cross sections discussed in this section. CS3 running from south to north, covering Eemshaven site 2 and the Doekegat tidal channel (Figure 4.3). CS4 from south to north only covering Eemshaven site 3 (Figure 4.4). CS5 from west to northeast, covering both sites 2 and 3 and including the offshore east of the Eemshaven area, including (from west to east) the Robbenplaat mudflat, Bocht van Watum tidal channel and Paap mudflat (Figure 4.5). Finally, CS6 runs from west to east along the northern margin of site 2 and 3 (Figure 4.6).

4.3.1 Peelo, Drente and Boxtel Formation (NUPE, NUDR, NUBX)

The exact boundaries of these late-Pleistocene units as drawn in these cross sections are highly uncertain as there is little data available at this depth. Furthermore, both NUBX, NUDR and NUPE consist mostly of sand, making it hard to differentiate between these units based on CPT data alone. NUDR locally appears to consist of coarser sand and gravel (e.g. B03H0021) versus fine to medium sand of NUPE (e.g. B03H0035). NUBX is covered by multiple CPTs along this cross section and generally consists of medium to coarse sand with cone resistance typically ranging between 10 and 20 MPa.

4.3.2 Nieuwkoop Formation basal peat (NUNIBA)

If present, basal peat can be found on-shore at a depth of between -14 and -15 m NAP and is typically only a few tens of centimeters thick. Basal peat is typically absent, such as in B03H0332, CPT100457 where NUBX sand transitions into NUNAWO clays with no sign of peat in between (i.e. a peak in friction ratio for CPT data). In other places it was eroded by a

Holocene tidal channel, as described in section 4.3.3 and 4.4.1. The presence of NUNIBA also indicates that the Late-Pleistocene surface has been preserved, which may be of archaeological interest.

4.3.3 Naaldwijk Formation (NUNA and NUNAWO)

NUNAWO in the site 2 and 3 cross sections consists mainly of (silty) clay and is generally found at depths between -14 and -10 m NAP. The only exception being the southeast of the site 3 area where NUNAWO comprises an up to 10 m thick layer of clay between -14 and -4 m NAP. See CS4 and CS5 where the thick NUNAWO clays are also found offshore. See also section 4.4.2 for a more detailed description of the NUNAWO clay presence at site 3.

Unlike NUNAWO at site 1, there are almost no distinct sand layers at this location, suggesting a more distal depositional environment of salt marshes. The latter agrees with the paleoenvironmental reconstruction that suggests that the (south)eastern half of the Eemshaven area was located closer to the salt marshes and peatlands, whereas the western part was on mudflats closer to tidal channels (Panel a in Figure 3.9). The presence of NUNI peat on top of NUNAWO clay in the southeasternmost part of site 3 and the Eemshaven area also indicates close proximity to peatlands that were outside of the sphere of tidal influence (see CS4). Compared to site 1, the bottom of NUNAWO is found at shallower depth here, suggesting this was a slightly higher supratidal area at the time.

Later NUNA deposits consist almost exclusively of fine to medium coarse sand (e.g. B03H0002, B03H0646 for reference). CPTs along these cross sections suggest that there are some thin (sandy) clay or silt layers, but unlike the situation at site 1, they do not appear in distinct intervals that can be correlated between CPTs and/or boreholes.

The sudden absence of NUNAWO and NUNIBA in CS3, 5 and 6 suggests the incision of a NUNA tidal channel. Among others, CPT100430 and 100489 show a continuous layer of sand at a depth where otherwise low cone resistance/high friction ratio would indicate the presence of clayey material associated with NUNAWO and NUNIBA, such as in CPT100428. The exact depth to which this channel has incised is uncertain. For the interpretation of the cross section, a slight increase of cone resistance and decrease of its variability in e.g. CPTs 100430, 100463 and 100464 was chosen as an indicator of the presence of slightly coarser and non-tidal deposits belonging to underlying NUBX and/or NUDR. The age and extent of this tidal channel is further discussed in section 4.4.1.

Around 1500 m in CS3, NUNAWO and NUNIBA were eroded by more recent activity of the Eems tidal channels. The exact location of this erosion surface is uncertain. It was drawn at this location in accordance with the maximum landward extent of tidal channels in the paleoenvironmental reconstruction (See Panel d in Figure 3.9). In contrast, CS5 shows that NUNAWO and NUNIBA are believed to still be present below the Robbenplaat, Bocht van Watum and Paap directly to the east of the Eemshaven area as tidal channels have never reached deep enough to (fully) erode the NUNAWO and NUNIBA deposits here.

4.3.4 Anthropogenic (NUAAOP)

According to available CPT data and as is visible in the cross section, material used to raise the Eemshaven area at the location of site 2 and 3 consists mostly of sand. Similar to site 1, some (thin) clay layers or lenses may be part of the fill material. Examples can be found in CPT33226, 100441 and 100431.

4.4 Remarks on late-Pleistocene and Holocene stratigraphy

4.4.1 Early-Holocene tidal channel incisions below Eemshaven sites 2 and 3

The newly discovered channel in CS3, CS5 and CS6 was most likely between 200 and 500 m wide and at least 10 m deep based on the elevation difference between the top of

NUNAWO clay and the estimated bottom depth of the channel. Although no dating information is available, it was likely formed during the Atlantic chronozone of the Holocene, immediately after the NUNAWO clays had formed in the early-Holocene salt marshes. When comparing to similar-width tidal channels and inlets in the Wadden Sea area (e.g. Zuidoost Lauwers, Spruit, Pinkegat), 10 - 12 m seems to be a plausible depth for a tidal channel of this width. This suggests that the sea level was around -10 m NAP when this channel formed. Considering the Holocene sea level rise curve (Hijma et al., 2025), this suggests the channel was active around 8 ka, which means it was formed in the early Atlantic chronozone of the Holocene.

A similar channel was found just west of site 2 based on boreholes and CPT profiles. A map indicating the extent of both channels is shown in Figure 4.7.

4.4.2 Distribution and age of NUNAWO clay

CS4 and CS5 show an up to 10 m thick layer of clay in the southeastern tip of the Eemshaven area as well as a few km offshore directly to the east of the Eemshaven. The most likely explanation is that these areas have existed in a supratidal environment of salt marshes for much longer than other parts of the Eemshaven where NUNAWO clays are typically less than 4 m thick. This also agrees best with our knowledge of the paleoenvironmental conditions, although the data suggests that salt marshes and peatlands extended further towards the north and east than the 5500 and 2750 BC reconstructions suggest (Panel a and b in Figure 3.9). Given the Holocene sea level rise curve of Hijma et al., (2025), the salt marsh environment existed until about 7 ka in the southernmost tip of site 3 where NUNAWO clay is found between -4 and -14 m NAP. NUNAWO clay is found between -10 and -14 m NAP below site 2, suggesting it was formed up until around 8 ka. NUNAWO sandy clays and silts at depths between -17 and -20 m NAP below site 1 were formed around 9 ka.

Based on an interpolation of CPT data, the distribution and thickness of NUNAWO clays was mapped in and around the Eemshaven (Figure 4.8). It clearly shows that NUNAWO clays are widespread in the subsurface to the south and in the southeasternmost part of the Eemshaven, indicating the development and preservation of supratidal areas here (salt marshes, salt marsh ridges and peatlands).

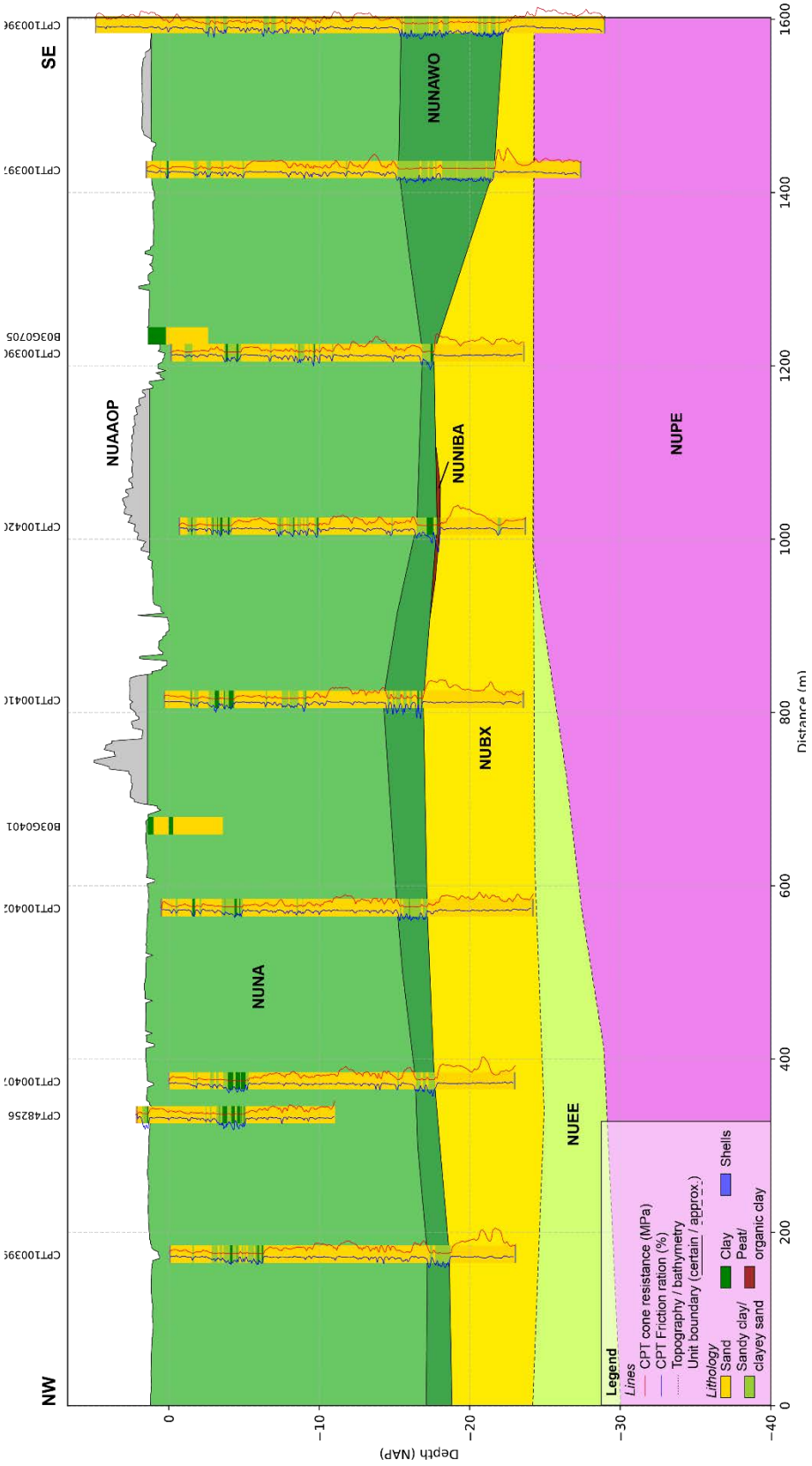

Figure 4.1 CS1: NW - SE cross section of site 1 on the west side of the Eemshaven area. See Figure 4.7 for the location of CS1.

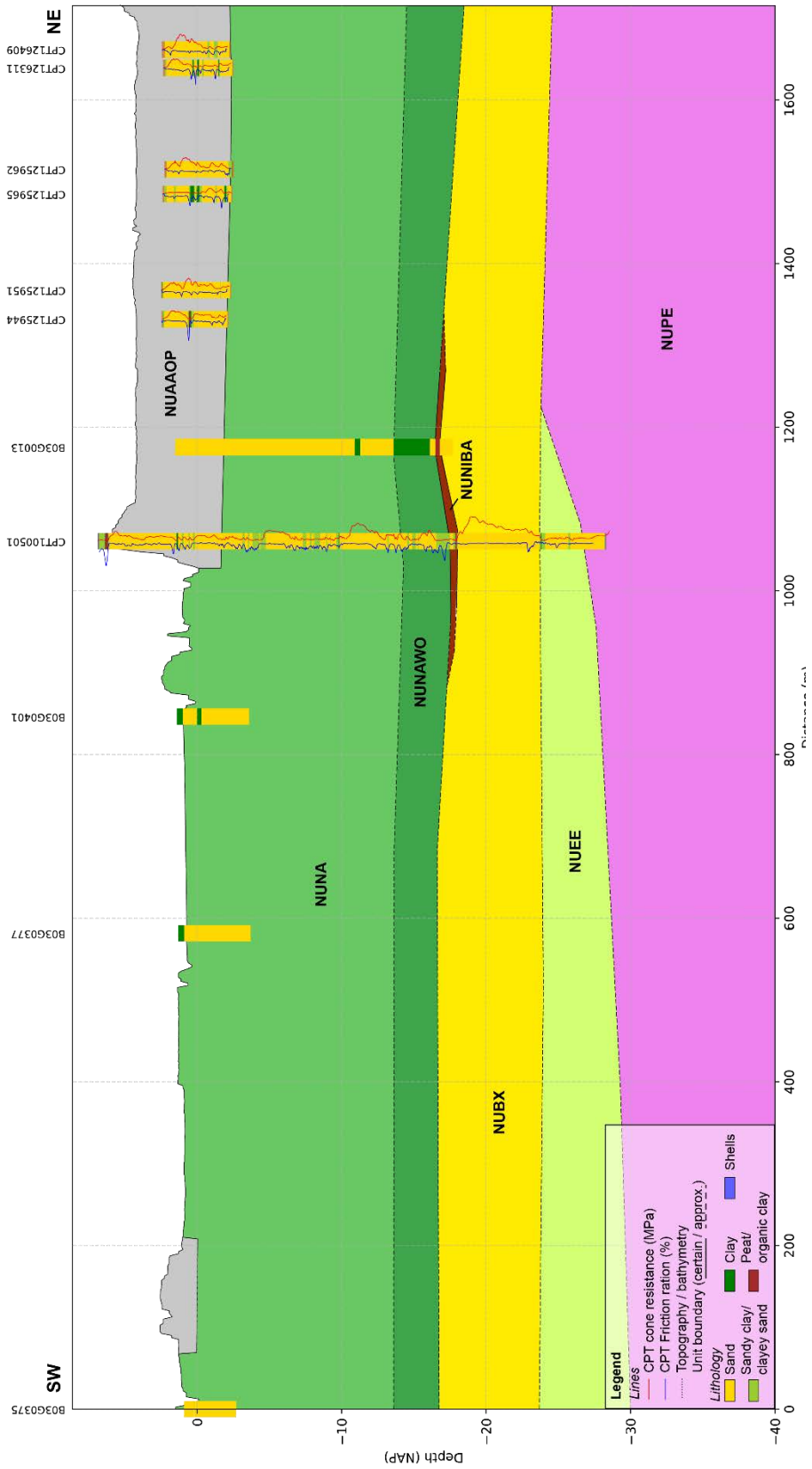

Figure 4.2 CS2: SW – NE cross section of site 1 on the west side of the Eemshaven area. See Figure 4.7 for the location of CS2.

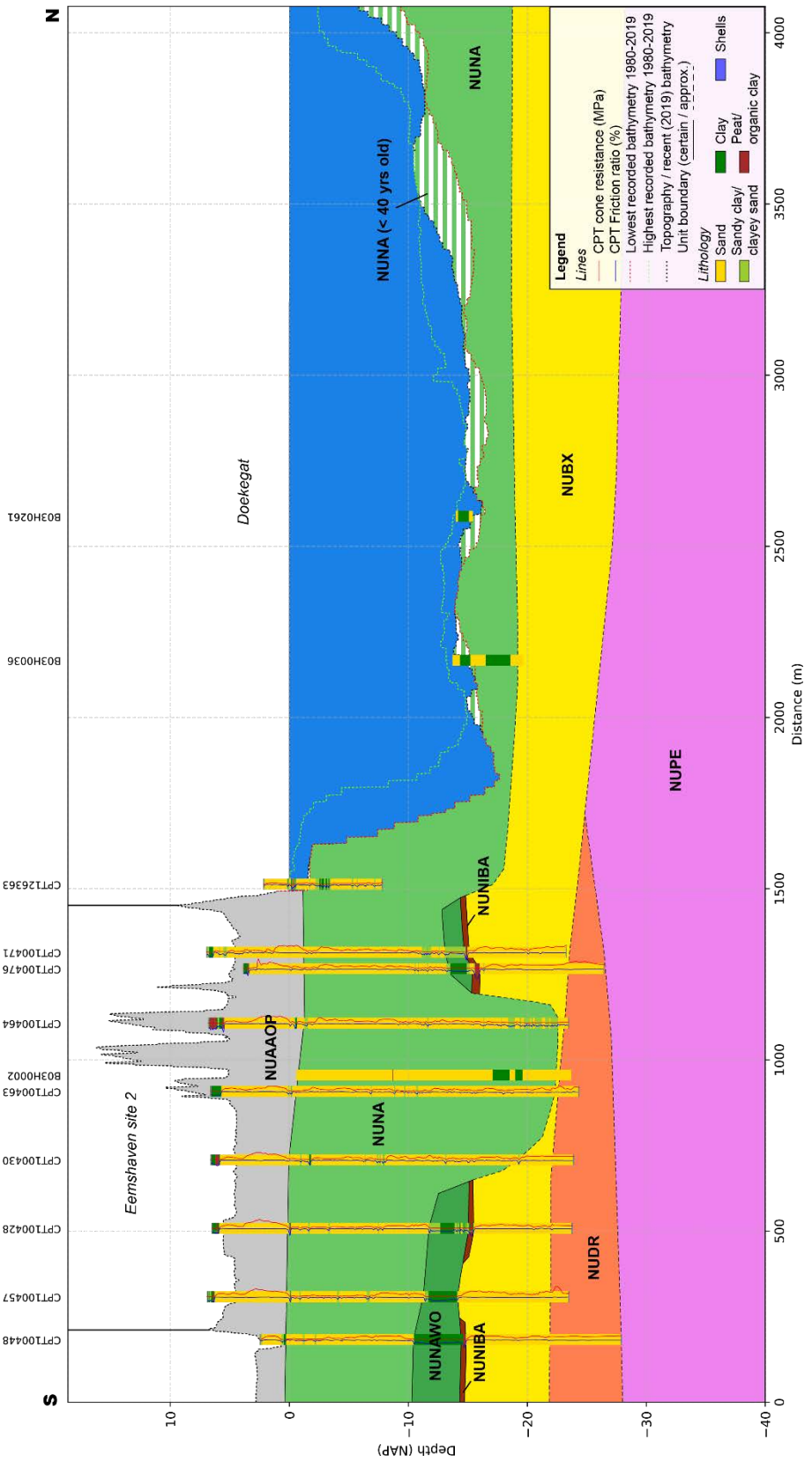

Figure 4.3 CS3: S – N cross section covering site 2 and the Doekegat tidal channel. Note the incised Naaldwijk tidal channel around 1000 m in the profile. See Figure 4.7 for the location of CS3.

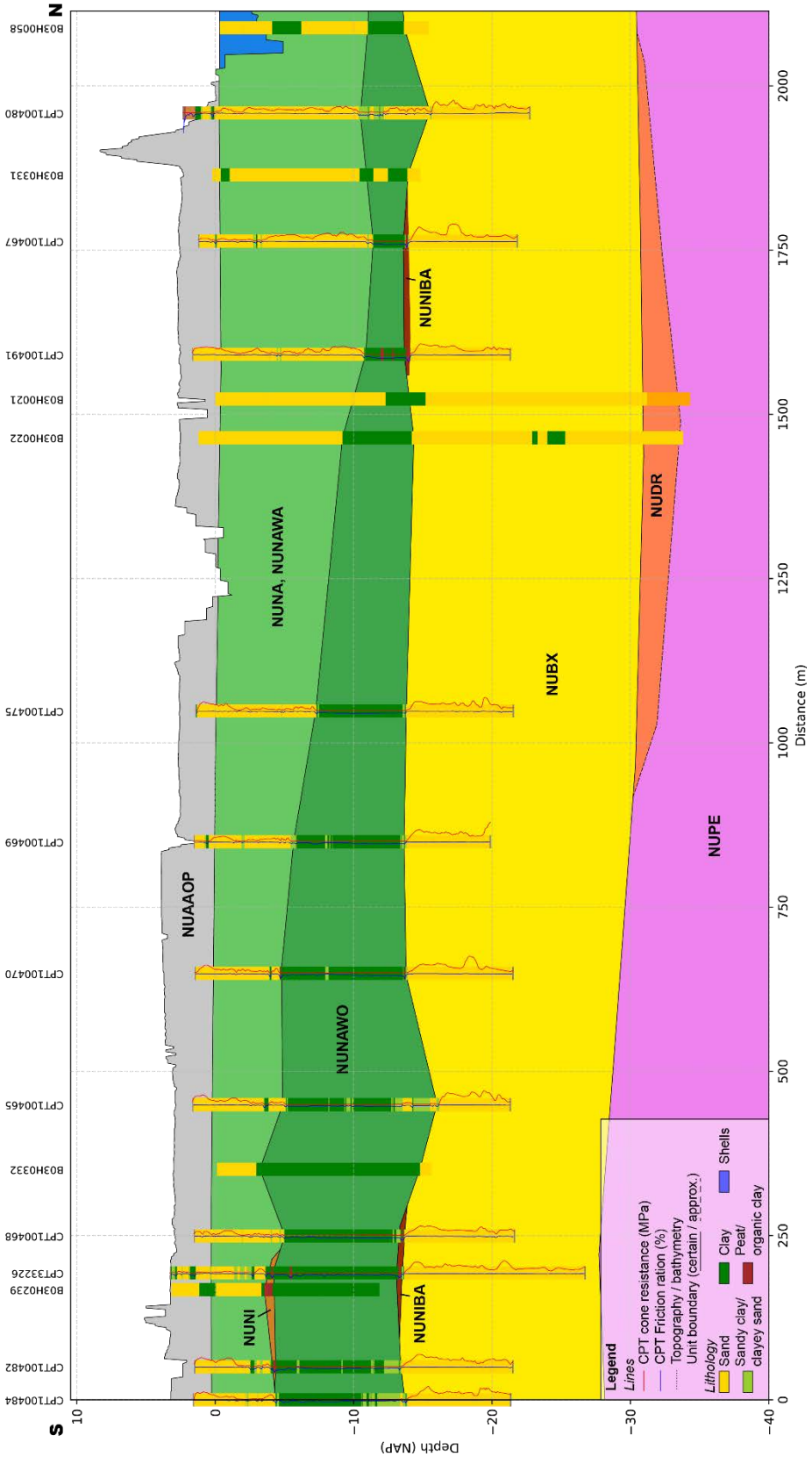

Figure 4.4 CS4: S – N cross section covering Site 3. Note thick NUNAWO clay that decreases in thickness towards the north. See Figure 4.7 for the location of CS4.

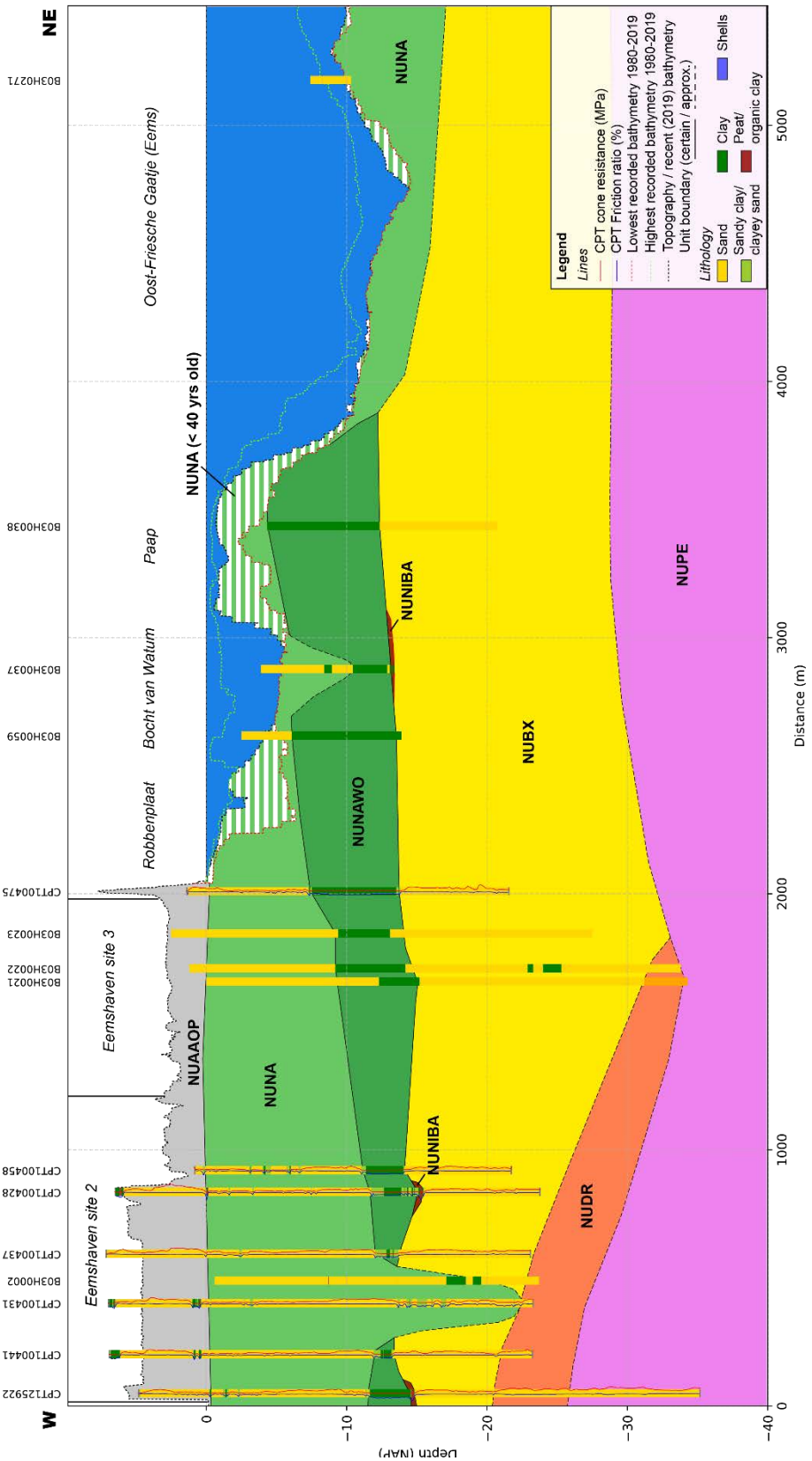

Figure 4.5 CS5: W – E cross section covering site 2, 3 and the immediate offshore area to the east of the Eemshaven. Note the incised Naaldwijk tidal channel in the west and the NUNAWO clay that increases in thickness towards the east. See Figure 4.7 for the location of CS5.

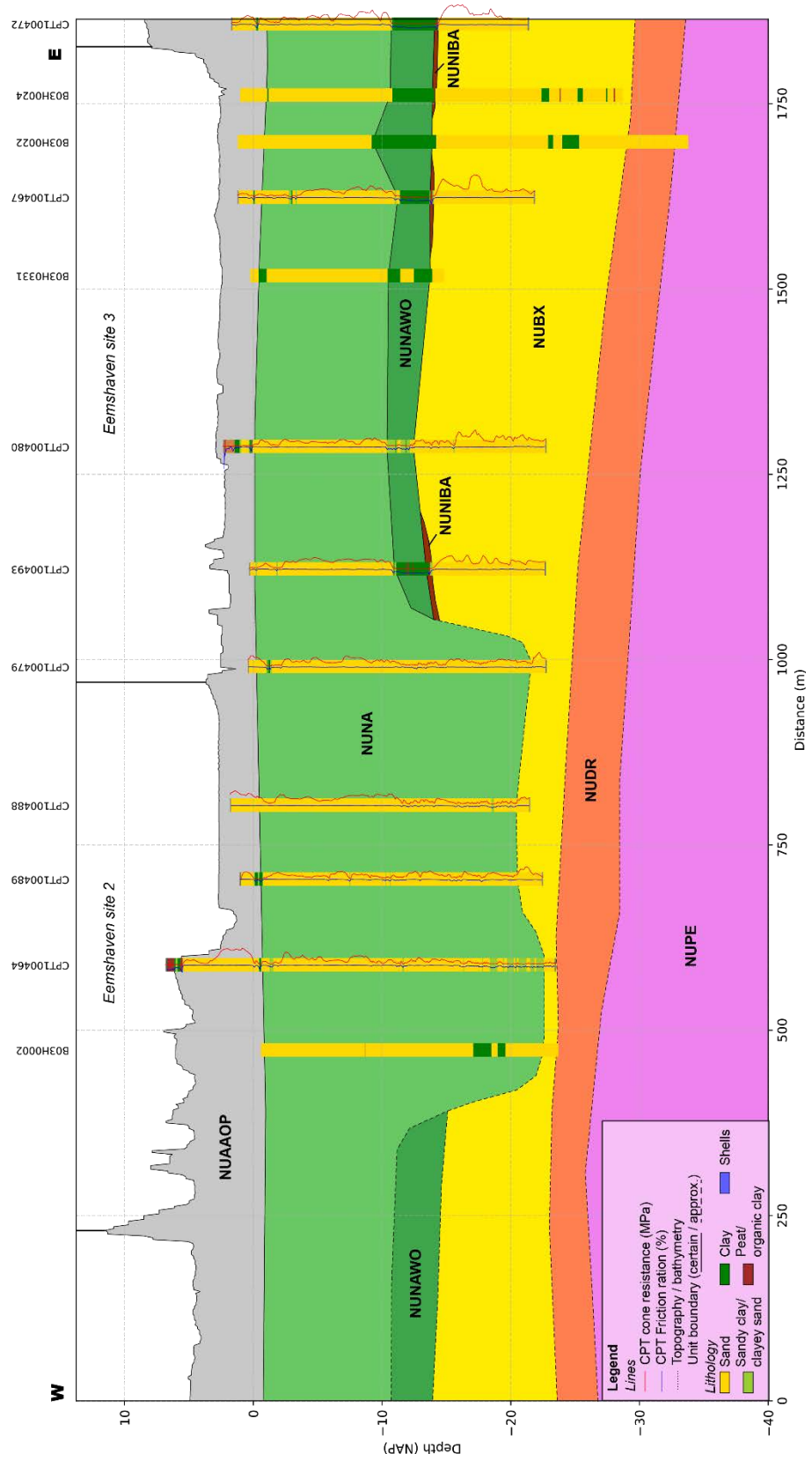

Figure 4.6 CS6: W – E cross section covering both sites 2 and 3. Note the incised Naaldwijk tidal channel. See Figure 4.7 for the location of CS6.

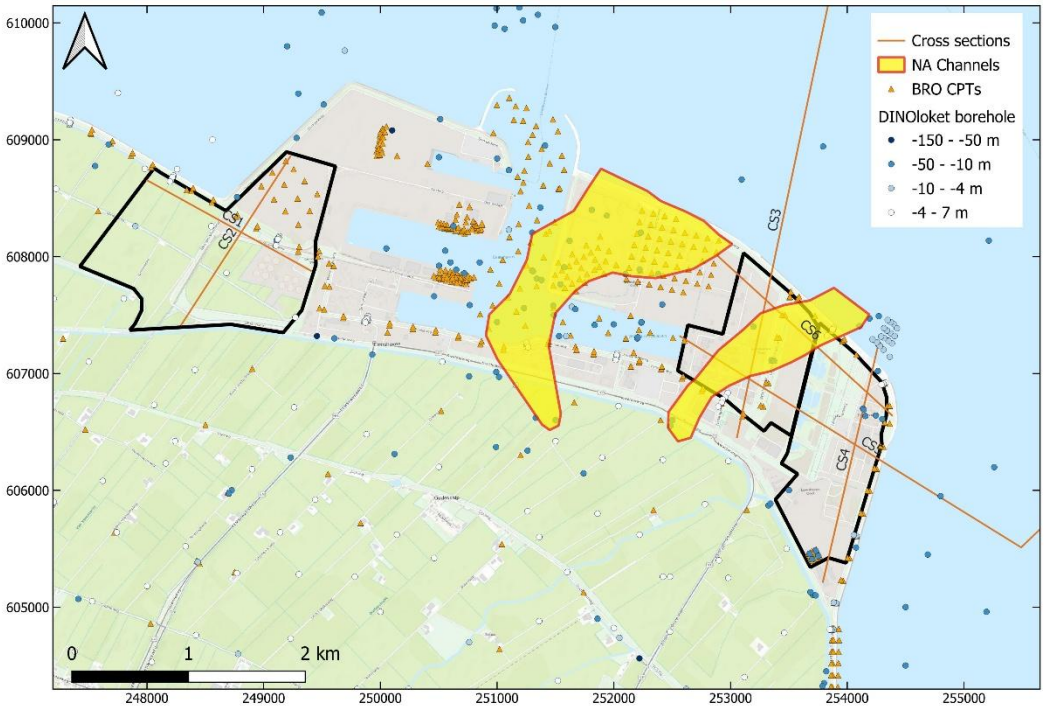

Figure 4.7 Map that shows previously unknown early-Holocene tidal channels. Sandy bed deposits of these channels are generally found between -10 and -20 m NAP. The channels cut into previously deposited early-Holocene clays and basal peat and in many places completely eroded these, thereby cutting into the underlying NUBX and/or NUDR. The channel below site 2 and the northern tip of site 3 is visible in cross sections CS3, 5 and 6 (Figure 4.3, Figure 4.5, Figure 4.6).

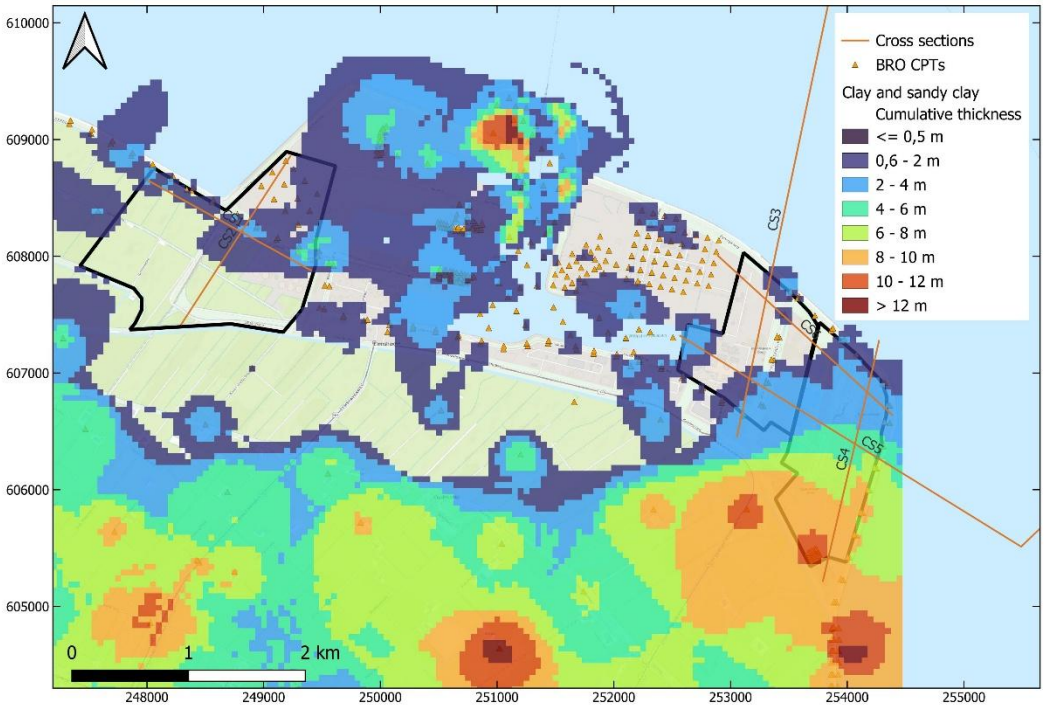

Figure 4.8 Map of the cumulative thickness of Holocene clay layers based on an interpolation of CPT data, clearly showing the up to 10 m thick layer of NUNAWO clay in the southern half of site 3.

5 Geohydrological site characterization

5.1 Introduction

Geohydrological investigations are essential for assessing groundwater conditions in various contexts. They support construction projects by evaluating groundwater levels and pressures that can affect foundations or cause uplift. They help determine the suitability of sites for water extraction and to understand how groundwater moves through the subsurface that might be important for contaminant transport. For spatial planning and permitting, such studies assess the impact of land-use changes on groundwater. Lastly, they are vital in understanding how groundwater influences subsidence, especially in clay or peat soils. The next sections give an overview of data relevant to the above mentioned topics.

5.2 Geohydrological characterization based on REGISII and GeoTOP

The Dutch national geohydrological model REGISII[1] v2.2.3 and the subsurface model GeoTOP v1.6.1 are used to provide a basic overview of the geohydrological conditions at the project area. The cross sections are along the same transects as chosen in the previous chapters, only for the eastern sites a selection is made of two cross sections out of the four shown in given in Figure 2.1. The bottom of the REGIS profiles shown is chosen such that the profiles include what is regarded as the geohydrological base in the National Groundwater Model (LHM, Janssen et al., 2025). In this model, the upper clayey deposits of the Breda formation (NUBRk1) functions as the geohydrological base, i.e. a layer/formation for which it can be safely assumed that water flow is negligible. The depth of the top of this formation is around -240 m NAP at the western site 1 and around -220 m NAP at the eastern sites 2 and 3. The GeoTOP profiles shown are given up to the same depth as used in Chapter 4 (-40 m NAP). Below, the cross sections are discussed per site, although sites 2 and 3 are discussed together.

5.2.1 Site 1 cross sections

In Chapter 4, the cross sections were described up to a depth of -40 m NAP, into the sands of the NUPE formation; between this formation and the geohydrological basis, REGIS distinguishes a limited number of stratigraphical units. At site 1 (Figure 5.1), starting with the oldest formation, we subsequently encounter the complex of the Oosterhout Formation (NUOOc), the second sandy unit of the Oosterhout Formation (NUOOz2), the fourth sandy unit of the Peize-Waalre Formation (NUPZ-Waz4), the Peize complex (NUPZc), the third and second sandy units of the Peize-Waalre Formation (NUPZ-Waz3 and NUPZ-Waz2) and the first sandy unit of the Appelscha Formation (NUAPz1). The north-south and west-east cross section are very similar at the western site.

Figure 5.2 shows cross sections for the shallower subsurface, i.e. the part up to -40 m NAP that overlaps with the cross sections of Chapter 4. This is only done for one of the two cross sections (south-north) because of their strong resemblance. The REGIS schematization largely corresponds with the GeoTOP schematization (middle figure of Figure 5.2) and the descriptions of Chapter 4. For site 1 this entails a sequence (from old to young) of the Peelo Formation, the Eem Formation (wedging out in northeastern direction), Boxtel Formation and the Holocene cover layer. REGIS further distinguishes between lithological units within these formations. Differences are that REGIS does not separately distinguish the anthropogenic layer (NUAAOP), neither does it distinguish between other units (NUNA, NUNAWO, NUNIHO, NUNIBA) of the Holocene. Of these, only NUNA and NUNIBA are observed in the cross section of site 1. As stated in chapter 4, this is a thin layer of basal peat. Peat layers

[1] REGIS = acronym for Regional Geohydrological Information System

can, because of their very low conductivity, form a significant obstruction to flow, but as mentioned in chapter 4 the spatial distribution of NUNIBA is very limited and therefore not very important from a geohydrological perspective.

The distinction of the Wormer stratigraphic unit within the Holocene as given in chapter 4, Figure 4.1 and Figure 4.2, is absent in the Geotop schematization in Figure 5.2. This was newly added to the profiles using CPT records, as described in chapter 4. Geohydrologically this is relevant, as the Wormer unit has a distinctively lower conductivity than most of the rest of the Holocene. Its presence therefore significantly contributes to the resistance of the Holocene layer.

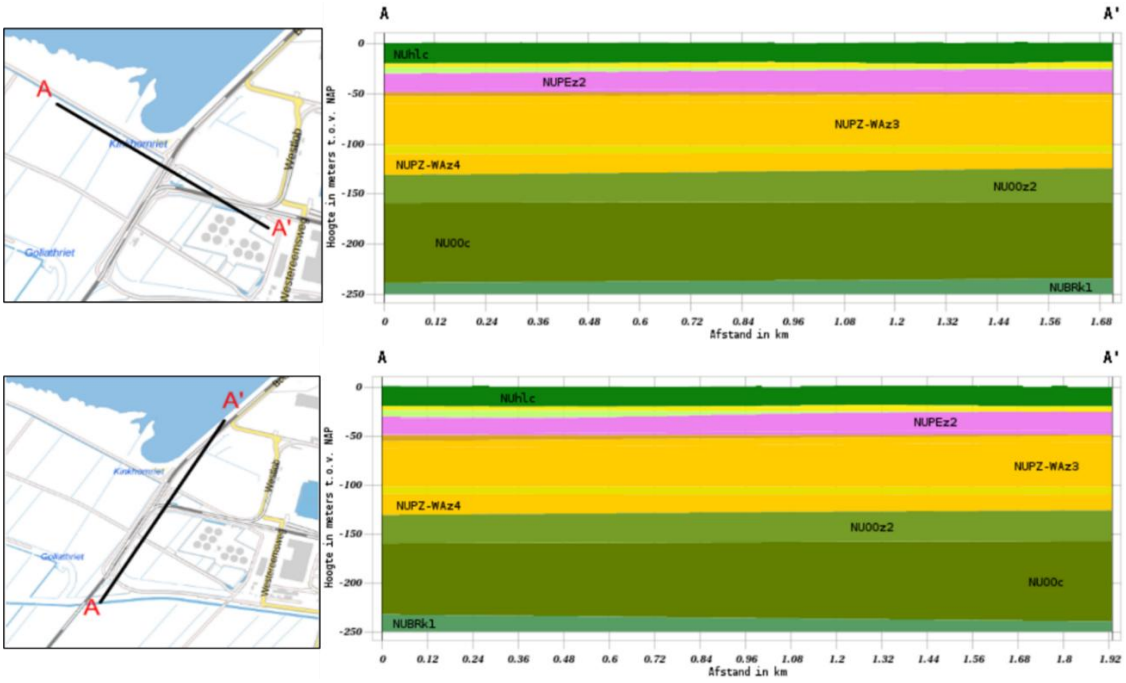

Figure 5.1 Above: Northwest-southeast geohydrological profile based on the model REGISII v2.2.3. Below: Northeast – southwest profile.

GeoTOPs prediction of the most likely lithological occurrences (Figure 5.2, bottom figure) shows a strong dominance of fine sand in the NUEE and NUPE formations. The Holocene formation (NUNA) shows more presence of clay and clayey sands, contributing to the resistance of the cover layer. This is particularly the case in the deeper parts, corresponding to the NUNAWO unit that was distinguished in chapter 4. The NUBX formation shows a strong dominance of medium to coarse sands and gravel, which corresponds with the description in paragraph 4.2.3.

Noteworthy is that, according to REGIS (not shown), the seabed does not incise into the Holocene cover deposits, meaning that there is no direct connection between the sea and the aquifers, probably limiting tidal effects on groundwater levels and pressure heads.

In Table 5.1, the overall geohydrological characterization of site 1, including permeability estimations from REGIS, is given. Generally speaking the system consists of a Holocene cover layer, two aquifer systems and one aquitard. Although, as stated before, in LHM the geohydrological basis of the system is put at the top of the Breda clays, it could probably also have been put at the top of the complex Oosterhout unit here; considering its low vertical conductivities (according to REGIS), this layer will not contribute significantly to flow. If we would consider the top of the complex Oosterhout unit as the geohydrological base, indeed we are left with only one aquitard at the location (NUPZc). This aquitard is considered quite leaky, as REGIS estimates its resistance to be only 100 – 500 days.

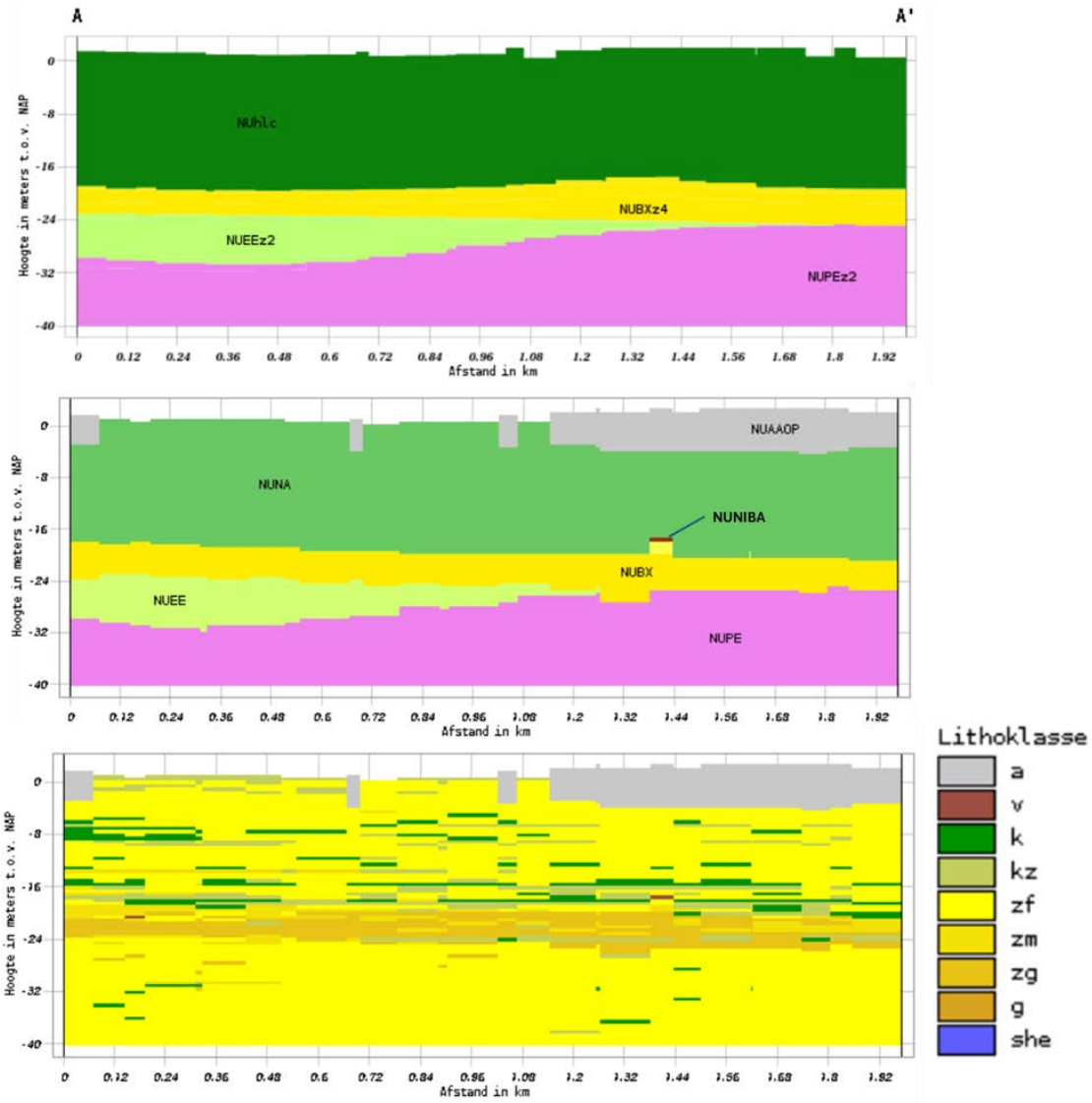

Figure 5.2 South-north cross sections of site 1 up to -40 m NAP. Upper figure: REGIS. Middle figure: GeoTOP, stratigraphical units. Bottom figure: GeoTOP, most likely lithology. Lithoclasses: a = anthropogenic, v = peat, k = clay, kz = clayey sand/sandy clay, zf = fine sand, zm = medium fine sand, zg = coarse sand, g = gravel, she = shells.

Table 5.1 Geohydrological characterization based on REGISII at the center of site 1.

Layer	Geohydrological unit	Dominating Lithologies	Formation name	Top [m NAP]	Bottom [m NAP]	Kh [m/d]	Kv [m/d]
1	Confining layer 1	Sandy clay, middle and fine sand, clay and peat peat	Anthropocene/ Holocene, complex unit	0	-19		
2	Aquifer 1	Sand, gravel, clay	Boxtel	-19	-24	5-10	
		Middle and fine sand	Eem	-24	-27	10-25	
		Middle, course and fine sand	Peelo	-27	-48	10-25	
		Course and middle sand	Appelscha	-48	-52	50-100	
		Middle and course sand	Peize-Waalre	-52	-102	50-100	
3	Aquitard 1	Complex unit, alternation of middle sand, sandy clay, course sand and clay	Peize	-102	-109	5-10	0.01-0.05
5	Aquifer 2	Middle and course sand	Peize-Waalre	-109	-127	25-50	
		Middle and fine sands with shells	Oosterhout	-127	-158	5-10	
6	Aquitard 2	Complex unit, alternation of middle sand, sandy clay, fine sand	Oosterhout	-158	-236	2.5-5	0.005-0.01

5.2.2 Cross sections through sites 2 and 3

Figure 5.3 gives the deeper REGIS cross sections for the east-west profile through sites 2 and 3. Figure 5.4, Figure 5.5 and Figure 5.6 give the shallow REGIS and GeoTOP pcross sections for the east-west profile through sites 2 and 3, the south-north profile through site 2 and the south-north profile through site 3, respectively. Lastly, Table 5.2 gives the overall geohydrological characterization of (the centers of) sites 2 and 3, including permeability estimations from REGIS.

REGIS and GeoTOP cross sections for sites 2 and 3 are given in the REGIS cross sections at sites 2 and 3 (Figure 5.3) are very similar to the description for site 1 when it comes to the part below -40 m NAP (i.e. the parts not covered in Chapter 4). One notable difference is the presence of a Peize clay unit (NUPEk1) within the Peize sand units. This is of potential geohydrological significance, as it constitutes a resistance to flow, although REGIS estimates the resistance to be moderate, in the range of 100 – 500 days here (see also Table 5.2). Another difference is the apparent absence of the Appelscha formation. As this is a sandy layer that, in site 1, is overlaying other sandy layers (thus being part of the same aquifer), its absence in sites 2 and 3 is of little geohydrological significance.

In the shallower parts there are some more differences with site 1. In all profiles, compared to site 1 there is a virtual absence of the Eem (NUEE) formation, and (thin) occurrences of a Drenthe sandy unit (NUDRz3), mainly at site 2. Again, as this Drenthe sandy unit is part of the same aquifer as the underlaying sandy deposit of Peize and the overlaying sandy deposit Boxtel, with comparable hydraulic conductivities (see also Table 5.2) this is of little geohydrological significance.

More important are the differences that are observed in the GeoTOP profiles, particularly at site 3 (Figure 5.6). Here, now also GeoTOP distinguishes a Wormer member in the Holocene

Naaldwijk formation. The cross section of the lithologies prediction of GeoTOP (bottom figure) indicates dominance of silty clays here, corresponding with the observations in paragraph 4.3.3. In chapter 4, Figure 4.8 a map of the occurrence and thickness of the Wormer clays was already presented. In the GeoTOP profile of units the Wormer member wedges out to the north; this is different from the updated profile of chapter 4 (Figure 4.4),in which is was mapped to continue. The lithological prediction of GeoTOP, however, does show a continuation of clayey dominance at the bottom of the Naaldwijk formation. The strong presence of clayey deposits at site 3 results in a relatively high resistance of the Holocene cover layer which is likely to result in higher groundwater levels.

Also for sites 2 and 3 it is observed that the seabed is not in direct connection to the aquifers. This can also be derived from Figure 4.3 and Figure 4.5 in the previous chapter.

The overall geohydrological characterization of the (center of the) sites is given in Table 5.2 . If, again, we take the top of the Oosterhout formation as the actual geohydrological basis here (instead of the top of the Breda clay as does LHM), we have (according to REGIS) a system of a Holocene cover layer with below that three aquifers and two aquitards. The Holocene cover layer will have substantial resistance where its cumulative clay layer thickness (Figure 4.8) is multiple meters. The NUPEk2 aquitard has quite low vertical conductivity values according to REGIS, resulting in a resistance of thousands of days, depending on the thickness. The second aquitard, formed by the Peize complex, has a much lower resistance of 100 – 500 days.

Unfortunately there is no publicly available pumping test data available (e.g. in DINOloket) for the Eemshaven or its surroundings to obtain more certainty around transmissivities and resistances of the various subsurface layers.

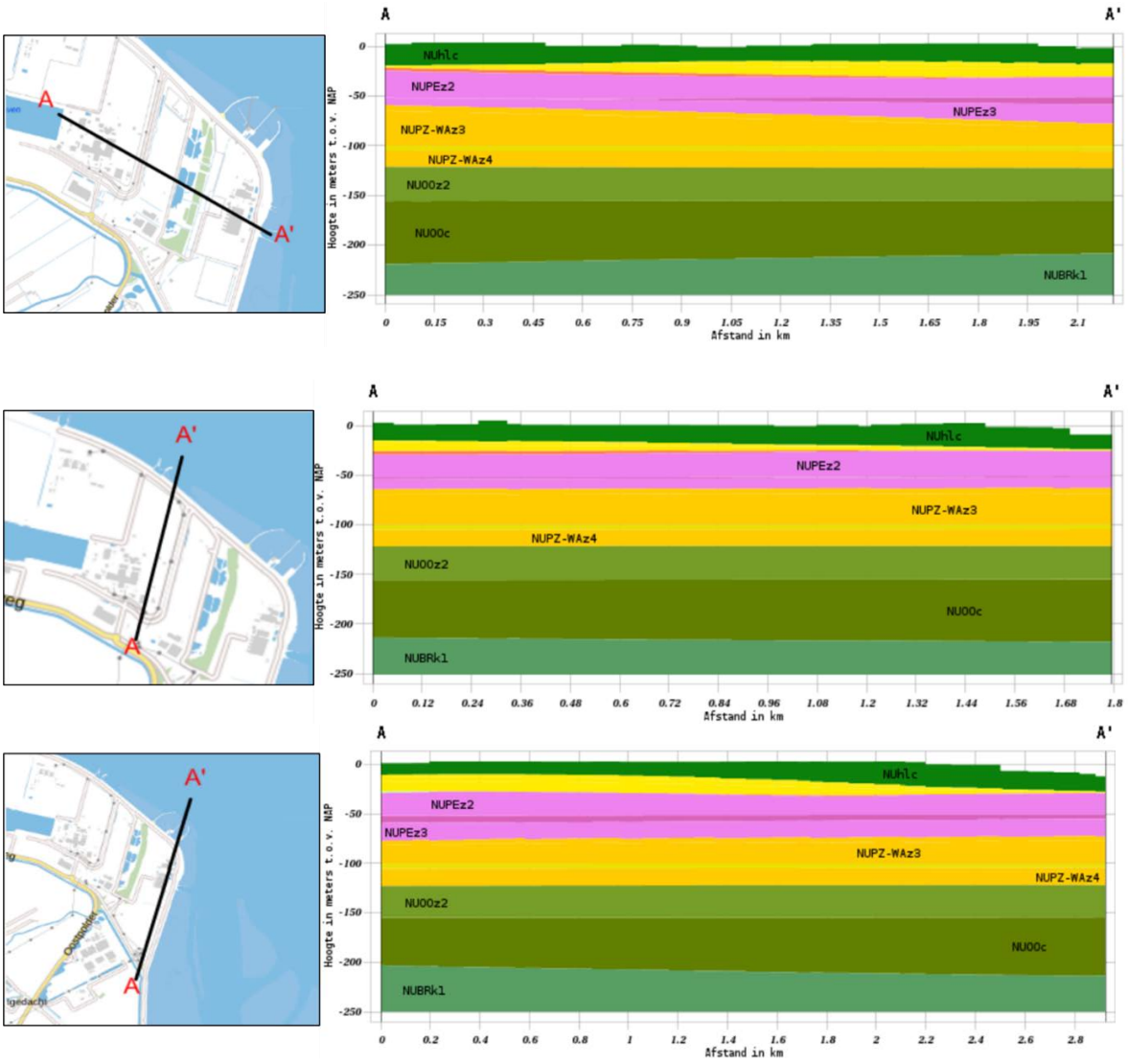

Figure 5.3 Northwest-southeast geohydrological profile along sites 2 and 3 based on the model REGISII v2.2.3.

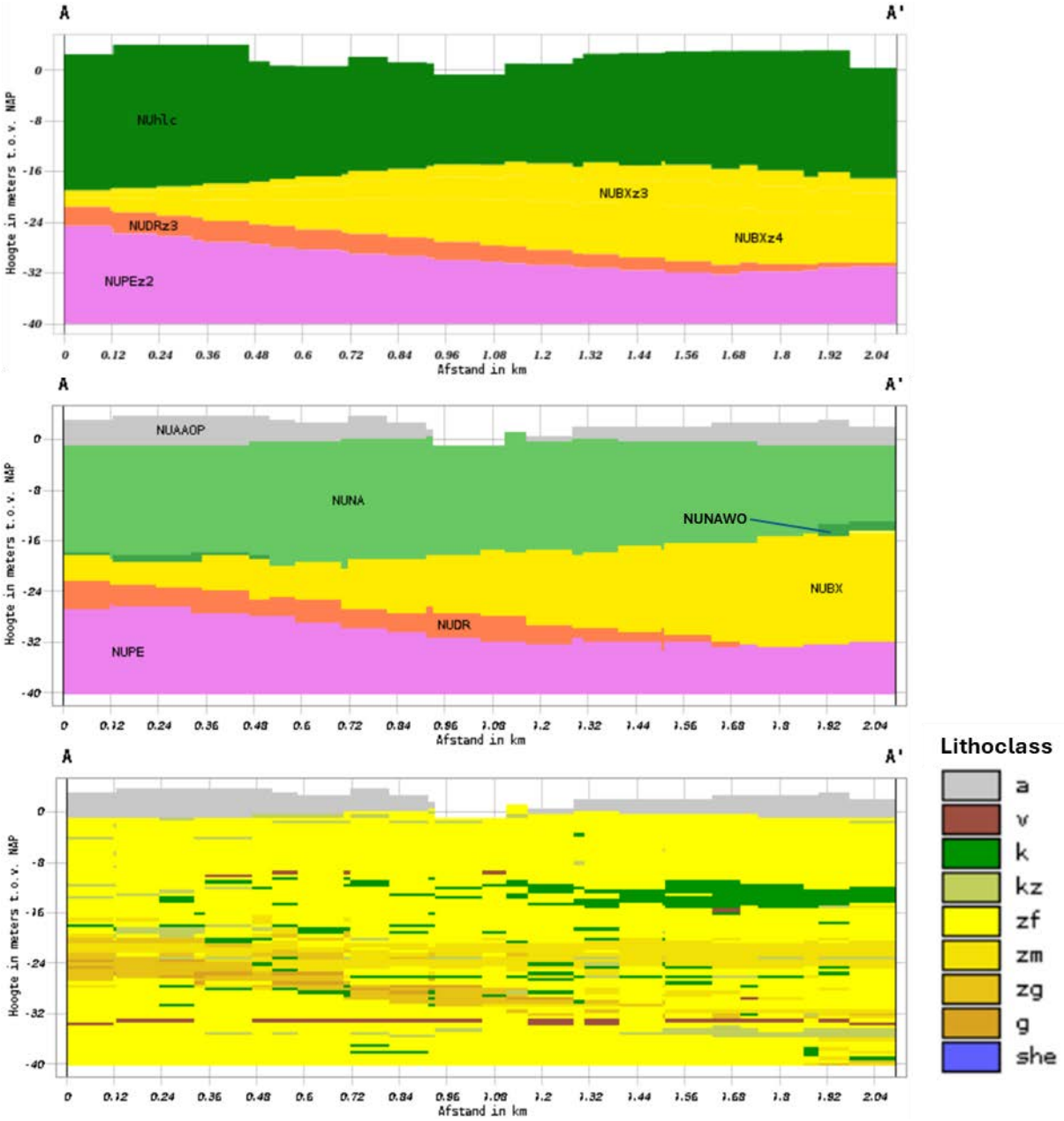

Figure 5.4 West-east cross sections through sites 2-3 up to -40 m NAP. Upper figure: REGIS. Middle figure: GeoTOP, stratigraphical units. Bottom figure: GeoTOP, most likely lithology. Lithoclasses: a = anthropogenic, v = peat, k = clay, kz = clayey sand/sandy clay, zf = fine sand, zm = medium fine sand, zg = coarse sand, g = gravel, she = shells. For location of cross section see upper plot of Figure 5.3.

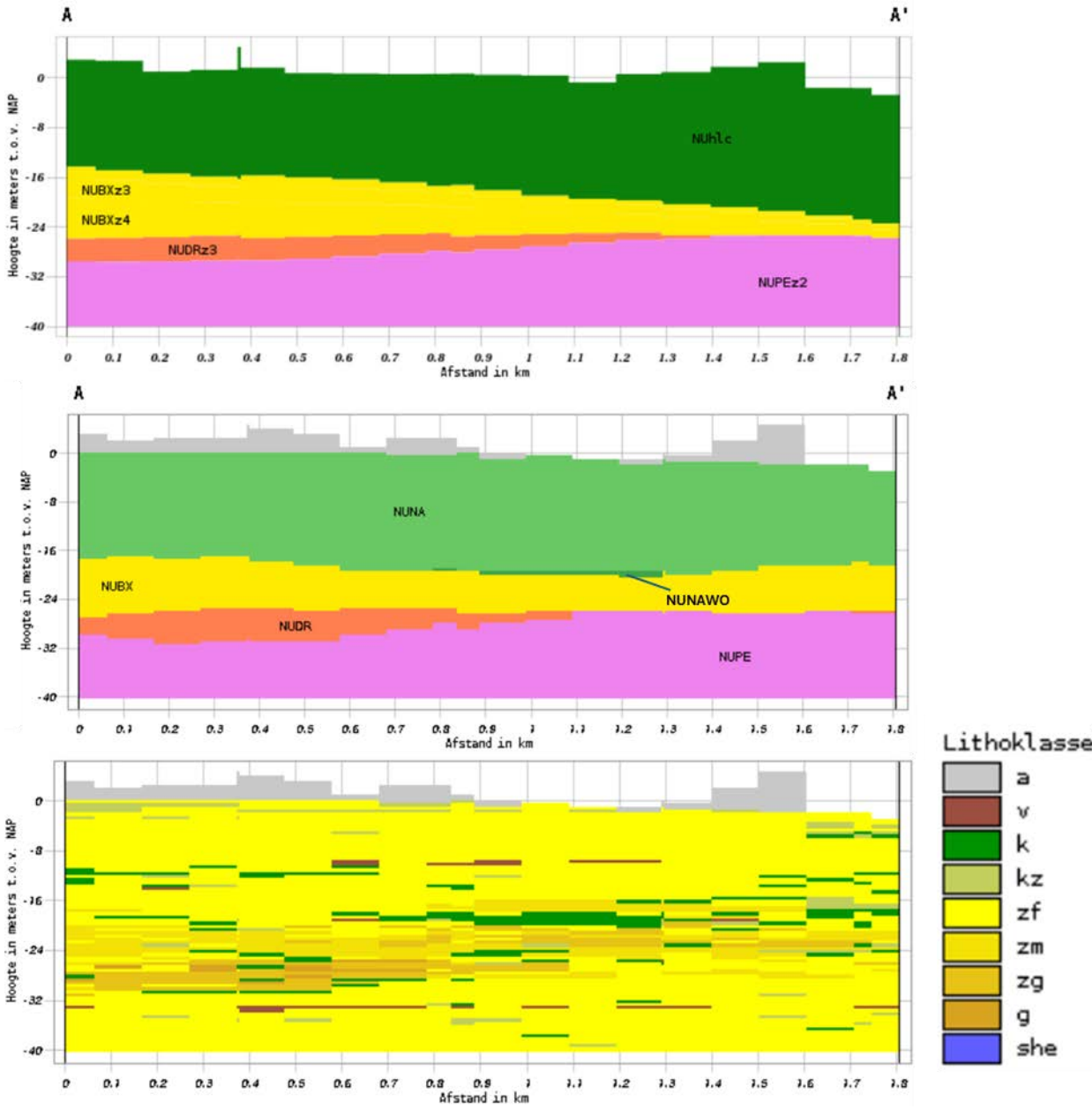

Figure 5.5 *South-north cross sections of site 2 up to -40 m NAP. Upper figure: REGIS. Middle figure: GeoTOP, stratigraphical units. Bottom figure: GeoTOP, most likely lithology. Lithoclasses: a = anthropogenic, v = peat, k = clay, kz = clayey sand/sandy clay, zf = fine sand, zm = medium fine sand, zg = coarse sand, g = gravel, she = shells. For location of cross section see middle plot of Figure 5.3.*

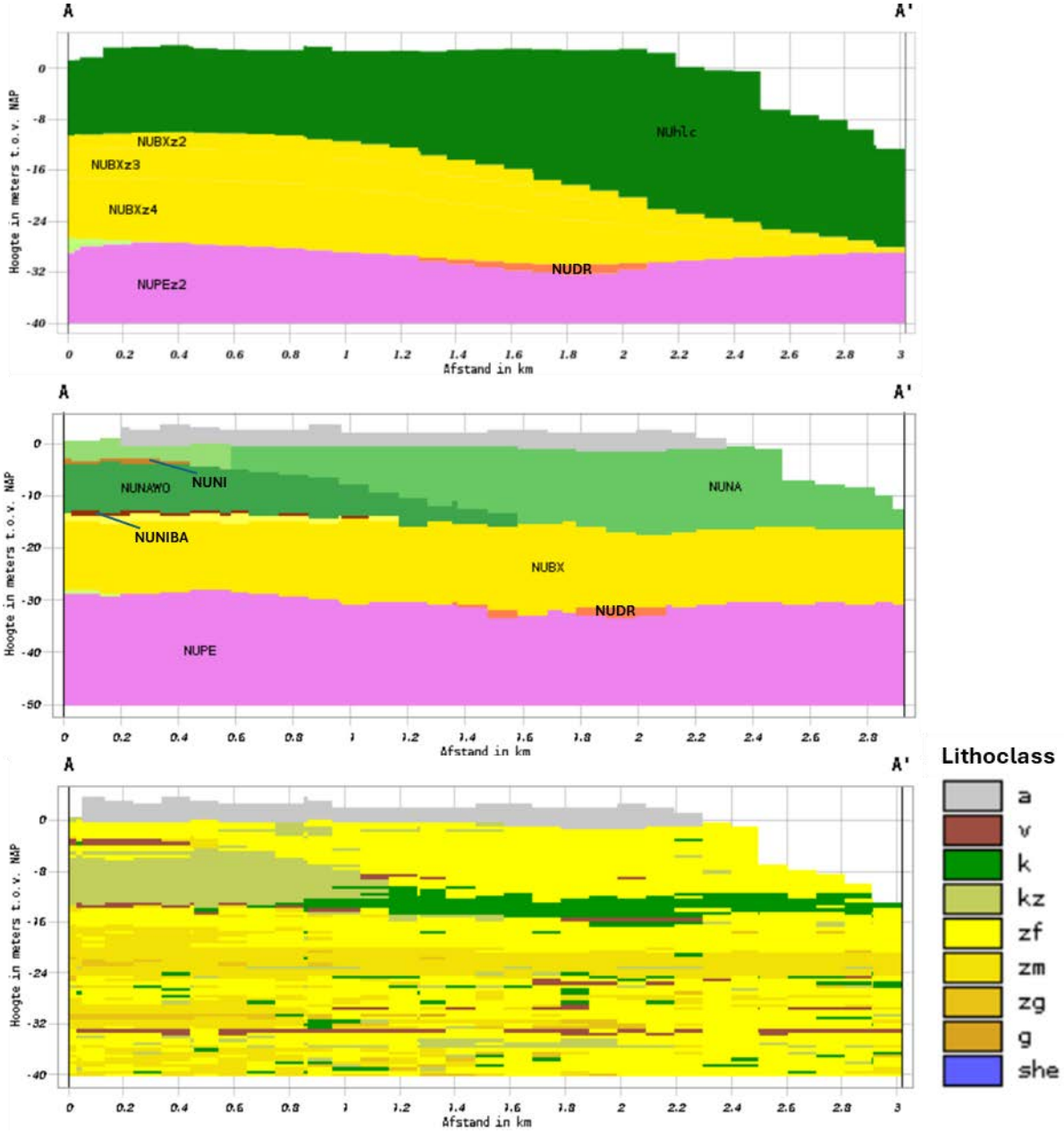

Figure 5.6 South-north cross sections of site 3 up to -40 m NAP. Upper figure: REGIS. Middle figure: GeoTOP, stratigraphical units. Bottom figure: GeoTOP, most likely lithology. Lithoclasses: a = anthropogenic, v = peat, k = clay, kz = clayey sand/sandy clay, zf = fine sand, zm = medium fine sand, zg = coarse sand, g = gravel, she = shells. For location of cross section see lower plot of Figure 5.3.

Table 5.2 Geohydrological characterization based on REGISII at the center of sites 2 and 3. Only the top and bottoms of the layers differ between both sites; they are indicated as {top site 2} / {top site 3} and {bot site 2} / {bot site 3}.

Layer	Geohydrological unit	Dominating Lithologies	Formation name	Top [m NAP]	Bottom [m NAP]	Kh [m/d]	Kv [m/d]
1	Confining layer 1	Sandy clay, middle and fine sand, clay and peat peat	Anthropocene/ Holocene, complex unit	1 / 3	-17 / -13		
2	Aquifer 1	Sand, gravel, clay	Boxtel	-17 / -13	-25 / -30	5-10	
		Coarse and middle sand	Drente	-25 / -30	-28 / -31	25-50	
		Middle, course and fine sand	Peelo	-28 / -31	-52	10-25	
3	Aquitard 1	Sandy clay, clay, fine sand	Peelo	-52 / -51	-53 / -57	5-10	0.0005 – 0.001
4	Aquifer 2	Middle, course and fine sand	Peelo	-53 / -57	-64 / -73	5-10	
		Middle and course sand	Peize-Waalre	-64 / -73	-100 / -100	25-100	
6	Aquitard 2	Complex unit, alternation of middle sand, sandy clay, course sand and clay	Peize	-100 / -100	-105 / -105	5-10	0.01-0.05
7	Aquifer 3	Middle and course sand	Peize-Waalre	-105 / -105	-122 / -122	25-50	
		Middle and fine sands with shells	Oosterhout	-122 / -122	-155 / -155	5-10	
6	Aquitard 3	Complex unit, alternation of middle sand, sandy clay, fine sand	Oosterhout	-155 / -155	-216 / -209	2.5-5	0.005-0.01

5.3 Groundwater extraction

For information on groundwater extractions at or near the sites, both Dinoloket (www.dinoloket.nl) and the website www.wkotool.nl were advised. Dinoloket reports two extractions for dewatering purposes, see Figure 5.7 One of them already ended, the other one starts in April 2025. No information on extraction rates is known.

Www.wkotool.nl reports more groundwater extractions (Figure 5.8). It is not clear for what purpose they were installed, but most likely these are also for (temporary) dewatering as other purposes are generally not allowed in the Eemshaven.

There are no drinking water or industrial production extractions nearby.

Figure 5.7 Overview of extractions for dewatering in the Eemshaven according to DINOLoket (www.dinoloket.nl).

Figure 5.8 Locations of groundwater extractions according to wkotool.nl.

5.4 Groundwater level monitoring and regional groundwater flow situation

Public available information on measured piezometric levels is available through www.DINOloket.nl and https://www.grondwatertools.nl/gwsinbeeld/. The monitoring wells in the neighborhood with relatively recent observations are given in Figure 5.9. No piezometric data are available from the project sites. The closest monitoring well located to any of the sites is well B03G0105, located at approximately 200m east of the border of site 1. The other wells are all more than 1200m away from the sites and may represent a very different geohydrological situation than on the project sites. The most recent hydraulic head data for the measurements in B03G0105 are from 2020. Also the other monitoring wells do not provide more recent data.

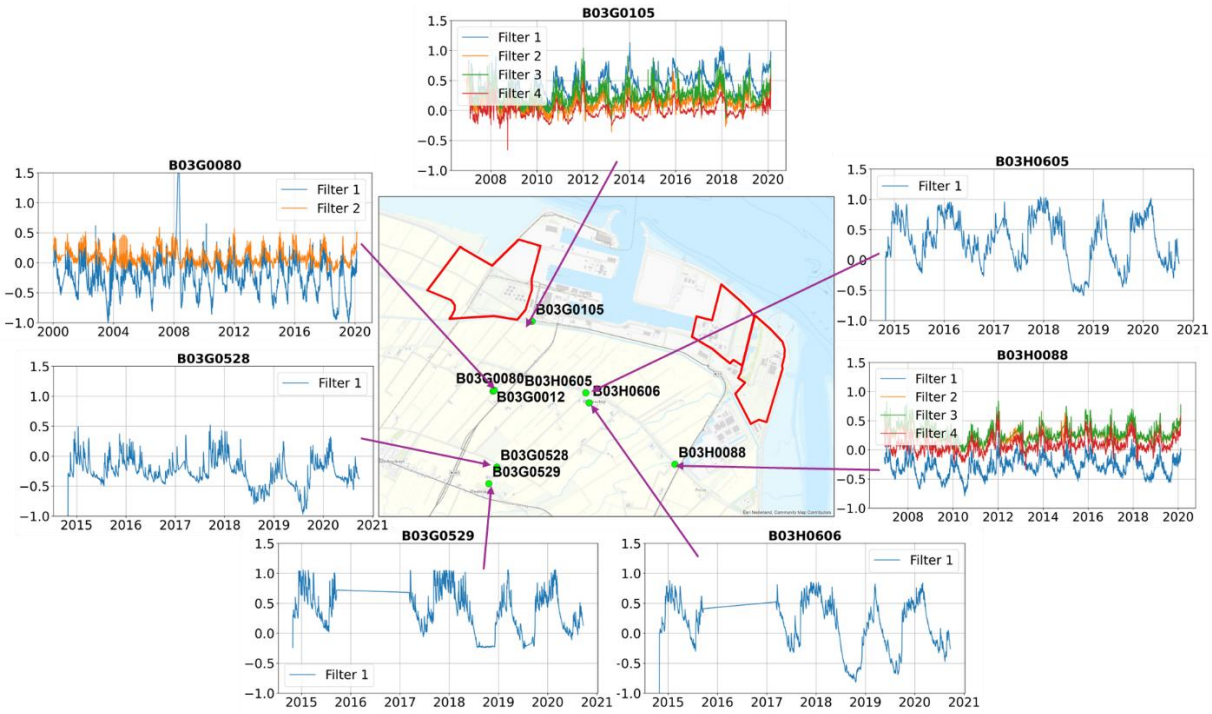

Figure 5.9 Locations of the monitoring wells near the Eemshaven sites. Graphs show groundwater heads on the y-axis in m NAP as a function of time on the x-axis.

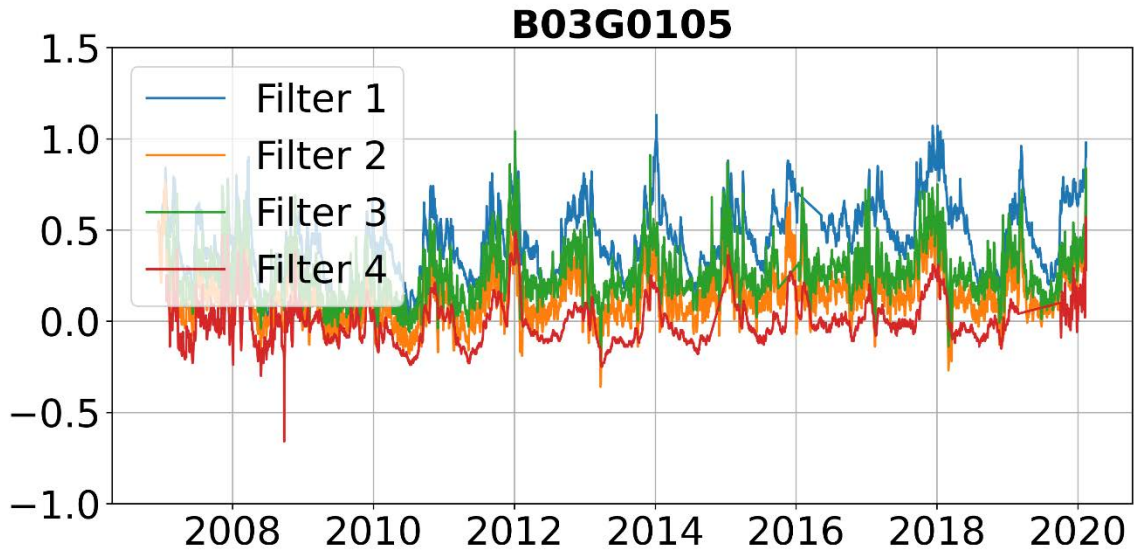

Figure 5.10 Measurement time series of the four piezometric filters of well B03G105. Graphs show groundwater heads on the y-axis in m NAP as a function of time on the x-axis.

Figure 5.10 shows the monitoring results of B03G0105 in more detail. The monitoring location has four filters at different depths; see Table 5.3. Measured heads in filter 1 are higher than those in filter 2, suggesting infiltration takes place from the Holocene cover to the underlying Boxtel sands. Surprisingly, the heads in the Peize-Waalre sands (filter 3) are a bit higher than those in the Boxtel sands (filter 2), suggesting there is upward seepage. In the REGIS model, both layers belong to the same aquifer, so not much of a head difference was expected. In the borehole description of the well, however, a low-permeable layer is described as part of the Urk Formation, Tynje member (URTY), which is not found in REGIS at this location. It is not known what causes the upward seepage here at this depth. Unknown

groundwater abstractions could play a role, as well as salinity differences between the two filters.

B03G0105 is very close (28 m) to the Binnenbermsloot/Oostpolderbermkanaal, which is kept at a stage of -0.69 m NAP (which is also the year-round target water level for the surface water in the Oostpolder area south of the Eemshaven). This is lower than the groundwater levels all year round, meaning that at this location groundwater is always discharging into the surface water. At the three Eemshaven sites, groundwater discharge will for a large part be towards the sea. Due to the proximity in the south, however, of the Oostpolder with its lower managed water levels, from the southern parts of the sites also groundwater discharge towards the Oostpolderbermkanaal and Oostpolder can be expected.

Most relevant for the site evaluation are the groundwater levels, more than the deeper heads. The groundwater level is best represented by the measurements of the upper filter, but even this filter is positioned quite deep, at the bottom of the NAWA formation. Its measurements therefore do not exactly reflect the phreatic head, but are lower than that, as there is resistance between the phreatic level and the filter. In the next section it is evaluated whether an existing groundwater model can help get an idea of the groundwater levels occurring at the sites.

Table 5.3 Metadata of monitoring well B03G0105.

Well	RD-X [m]	RD-Y [m]	Filter	Top filter [m NAP]	Bottom filter [m NAP]	Layer
B03G0105	249455	607320	1	-11.89	-13.89	Bottom of NAWA
			2	-19.89	-21.89	Boxtel sand
			3	-58.89	-60.89	Peize-Waalre
			4	-106.89	-108.89	Peize-Waalre

5.5 Modelled groundwater situation

5.5.1 Introduction

As discussed above, the groundwater levels at the project sites are not well represented by existing measurements. As an addition, predicted groundwater levels can be derived from the Dutch Geohydrological Model (LHM) that simulates daily groundwater levels. The model resolution has a computation resolution of 250 x 250 meters, and it therefore serves to simulate regional conditions rather than local ones. Nevertheless, the LHM should be suitable to give insights in regional geohydrological conditions. The LHM describes the subsurface in eight layers in which the lithology of GeoTOP has been incorporated, see Figure 5.11. The model incorporates the effect of the low permeable lithologies as low permeability values between two subsequent model layers. Where these layers are absent, the permeability is higher.

Although the LHM has not specifically been calibrated and validated for the Eemshaven sites, it should be suitable to derive an idea of the larger scale, regional flow patterns from.

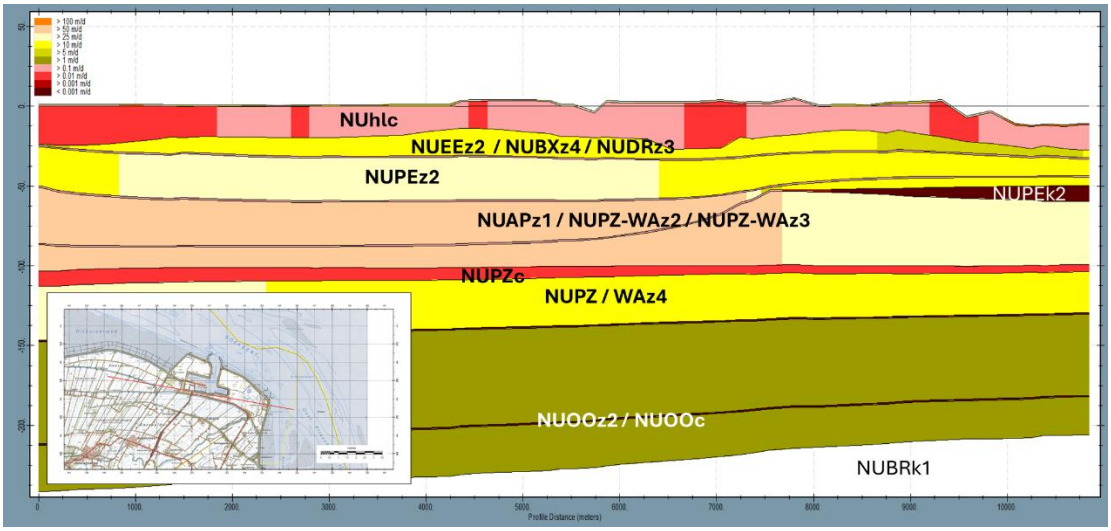

Figure 5.11 Cross section over the Eemshaven through the LHM showing the 8 model layers. It also indicates where the groundwater level (black line) is approximately positioned. The color scale represents hydraulic conductivities, from high (light yellow) to low (dark red). For the aquifers, the color scale reflects the horizontal conductivity (Kh) values, for the aquitard the vertical (Kv).

Figure 5.12 compares the groundwater level as calculated by the LHM at the location of well B03H060 to the monitoring results of the upper filter of that well. In LHM, the groundwater level generally fluctuates between 0.5 and -0.75 m NAP, dropping further in very dry summers. The monitoring results are higher, and as explained in the previous section the true phreatic levels are expected to be even higher than the measured heads at this depth. So, the LHM is off here quite a bit (0.5 – 0.75 m at least). It should be kept in mind, however, that the comparison entails one between a point value and a value that is representative for an area of 250x250 m. This could be part of the explanation. The dynamics of the measured time series (= difference between highest and lowest groundwater levels) are reasonably reproduced by the LHM at this location, albeit that the dynamics are a bit larger in LHM than in the observations.

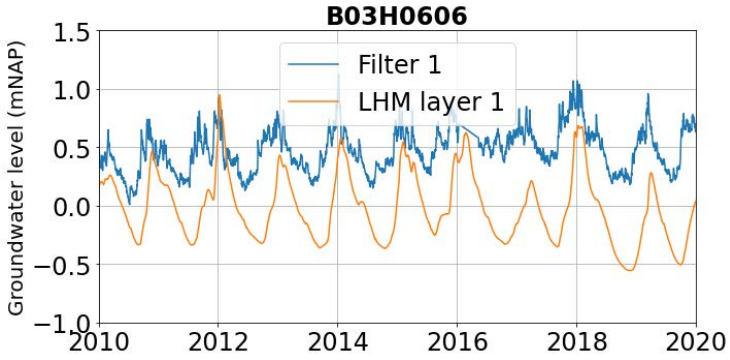

Figure 5.12 Comparison modelling results the LHM of the monitoring results of the upper filter of B03H0606.

Figure 5.13 compares the LHM results for the centres of the three sites together with the LHM result for the measurement location B03G0105. It shows that the groundwater levels at site 1 are comparable to that of the measurement location. The groundwater levels at the centres of sites 2 and 3 are similar to each other, but are higher than on site 1, particularly the levels in the winter. which is most likely due to the fact that site 1 is closer to dewatering features (ditches, agricultural drainage) and also has significantly lower surface elevations, see the horizontal lines in Figure 5.13 and also Figure 5.14.

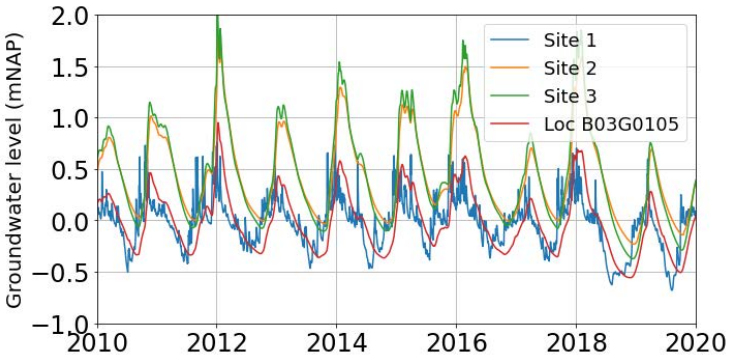

Figure 5.13 Comparison of groundwater levels calculated by the LHM for four locations: the centers of sites 1, 2 and 3 and the location of monitoring well B03G0105.

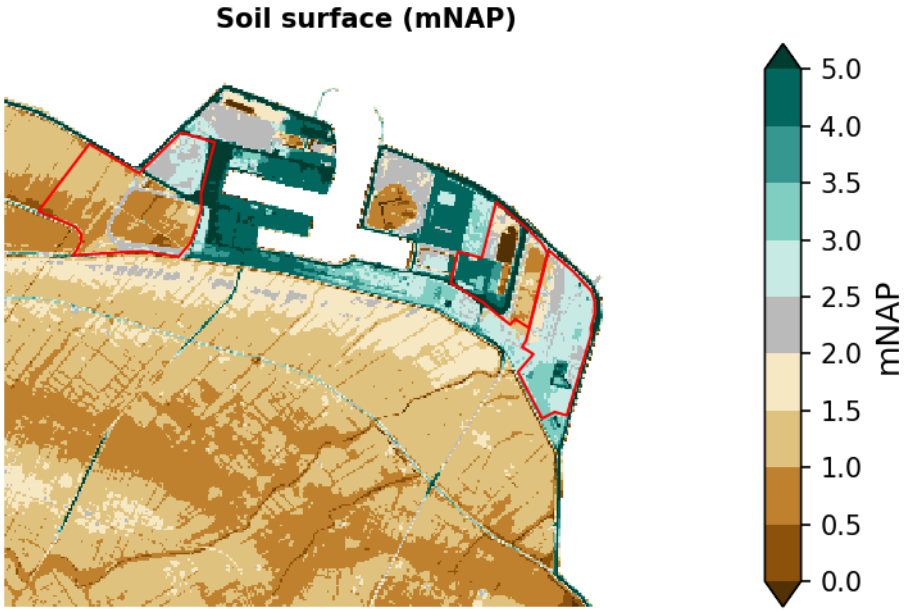

Figure 5.14 Soil surface elevation at and around the project sites (source: AHN2).

With the LHM also 2D characterizations of the groundwater levels were produced. These are given in Figure 5.16. It shows the calculated mean groundwater level over time (2010-2020) of the area, both in m NAP and meters below soil surface. Site 2 shows a large variation in groundwater level depth, with relatively deep levels in the south-west part and shallow levels in the northern part. This is directly related to the variations in soil surface level. Also site 1 has a clear division in a part with deeper and shallower groundwater levels because of this. On average, modelled groundwater levels are deepest at site 3.

Absolute groundwater levels (in m NAP) are lowest at site 1 and highest at site 3. Particularly in the east – southeast part of site 3 the groundwater levels are relatively high; this is due to higher resistance of Holocene layer here, because of the presence of the clayey Wormer member as discussed in sections 4.4.2 and 5.2.2. A visualization of the resistance of the Holocene cover layer in LHM is given in Figure 5.16. Indeed it shows an elevated resistance in the zone with higher groundwater levels.

Besides the mean groundwater levels, Figure 5.15 (bottom figures) also gives the calculated mean highest (GHG) and mean lowest (GLG) groundwater levels over the period 2010-2020. These are defined as the average of the three highest resp. lowest groundwater levels of every year. Particularly the GHG is relevant, as it related to inundation risk. At site 3, the

GHG remains well below 1 m.b.s.l.. At site 1, however, there are areas where the calculated GHG is shallower than 0.5 m.b.s.l, with most of the terrain having a GHG between 0.5 and 1 m.b.s.l. At site 2 the variation is largest, again due to the large variations in soil surface level.

It is recalled here that the LHM calculated lower groundwater levels than observed at the measurement location B03G0105. If this is extrapolated to the rest of the domain, this would mean higher groundwater levels than shown in Figure 5.15, and consequently also a higher induced inundation risk. Of course, from one measurement location the model performance in the rest of the domain cannot be reliably inferred. The observed mismatch does however illustrate that the LHM results are uncertain and the presented results should be considered indicative and illustrative and not more than that. A more localized modelling approach, fed with local data and calibrated and validated on a decent set of on-site piezometric measurements is necessary to be able to obtain more reliable modelling results.

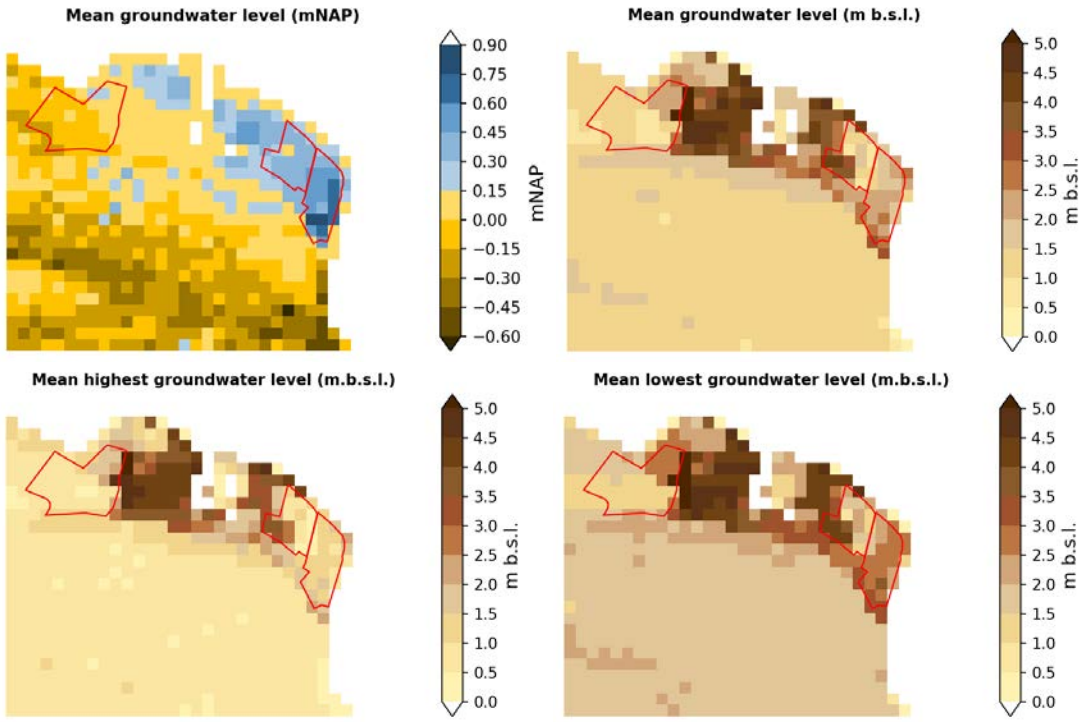

Figure 5.15 Calculated groundwater levels by the LHM over the period 2010-2020. M.b.s.l = meters below soil surface level.

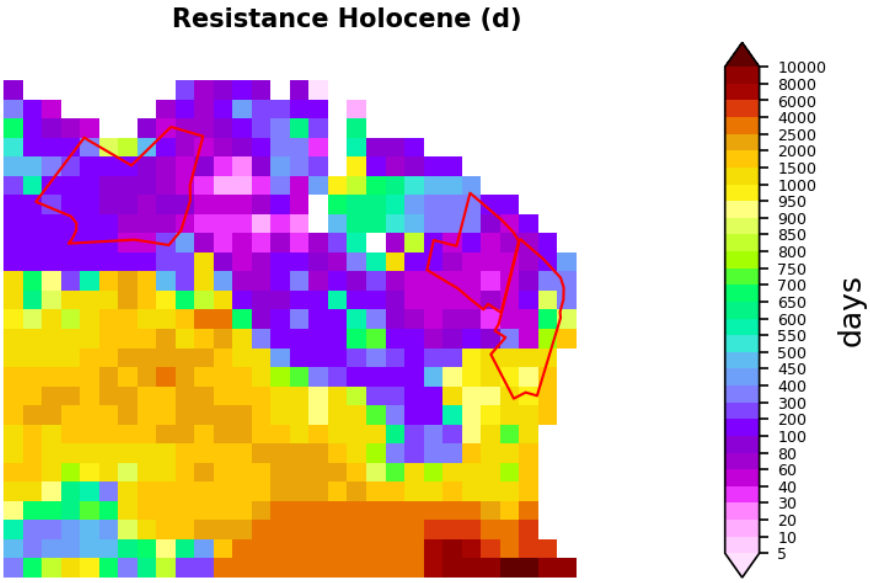

Figure 5.16 Resistance of the Holocene layer in LHM 4.3.3.

The fact that no groundwater monitoring wells are present at the potential project sites makes makes the geohydrological evaluation and model results of the sites uncertain. It is advisable to develop and execute a monitoring plan, preferably consisting of multiple monitoring wells per site with filters at different depths, to capture both horizontal and vertical gradients. Monitoring should continue for at least one year to capture seasonal effects. High frequency monitoring would be advisable for at least a short period to capture tidal effects.

5.6 Simulated salt concentrations

The presence of salt in the subsurface can accelerate corrosion of steel and concrete structures and may alter soil properties, leading to stability issues and reduced durability of foundations.

The Eemshaven sites are located near salty seawater. Salt water has a higher density than fresh water and therefore affects groundwater flow. Delsman et al. (2020) constructed a nationwide three-dimensional distribution of chloride concentration in the Dutch groundwater. For the Eemshaven area, this distribution relies heavily on analytical measurements (groundwater samples) and Vertical Electrical Soundings (VES) from quite far away, as no data were available from the area itself. This makes that the 3D chloride distribution is in principle quite uncertain here. The distribution suggests a completely saline subsurface (not shown). For a large part this makes sense, as the Eemshaven was built on land that was reclaimed from the sea. However, since the construction of the harbour fresh rainwater has been infiltrating which causes freshening of the upper groundwater (formation of a freshwater lens). Therefore at least to some depth fresh to brackish groundwater is expected.

The 3D chloride distribution was used as initial condition for a nationwide density-dependent groundwater flow and transport model (LHM-fresh-salt, Delsman et al. (2020). With this model the change of salt/chloride concentrations with time can be simulated. When evaluating the results of this model it was found that on the Eemshaven sites, starting from the completely saline initial conditions, some freshening of the upper groundwater indeed takes place but this fresher top layer quickly reaches an equilibrium (a ‘steady state’) and does not grow anymore. This is shown in Figure 5.17, which gives the result of LHM-fresh-salt after a 20 year simulation time. Simulating longer did not significantly change these profiles anymore. This shows that, in the model, the fresh groundwater recharge is discharged in a relatively shallow fashion, via shallow discharge routes. This is due to a

combination of short discharge routes (the sea is close) and the presence of substantial vertical resistance to flow. In theory this behaviour could also have been caused by very limited groundwater recharge, for example as a result of a large fraction of built-up or paved areas. In the model however, this is not the case; the estimated recharge values are 0.6 – 0.7 mm/d on average, which is not particularly low. Also from aerial photos it is apparent that much of the land on the sites is left open. This, of course, could change in the future, further limiting the potential of the freshwater lenses to grow.

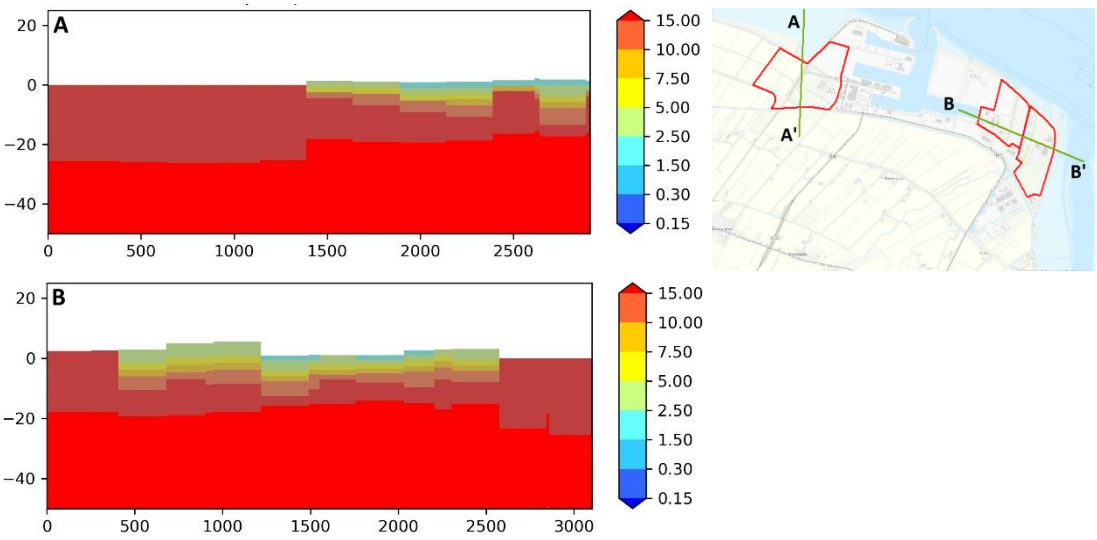

Figure 5.17 Left: cross sections of the model result of LHM-fresh-salt after 20 years simulation time, starting from a completely saline initial condition. Right: the location of the cross sections.

6 Geotechnical parameters

6.1 Geotechnical cross sections

6.1.1 Used CPTs

For the geotechnical analysis, soil properties are derived for the geological cross sections CS1, CS3 and CS4, describing each site. Section 6.1.2 to 6.1.4 describe the three subareas and section 6.1.5 provides an overview of the representative cross sections. Figure 6.1 highlights the ground level and final penetration depth of the CPTs used for the three cross sections.

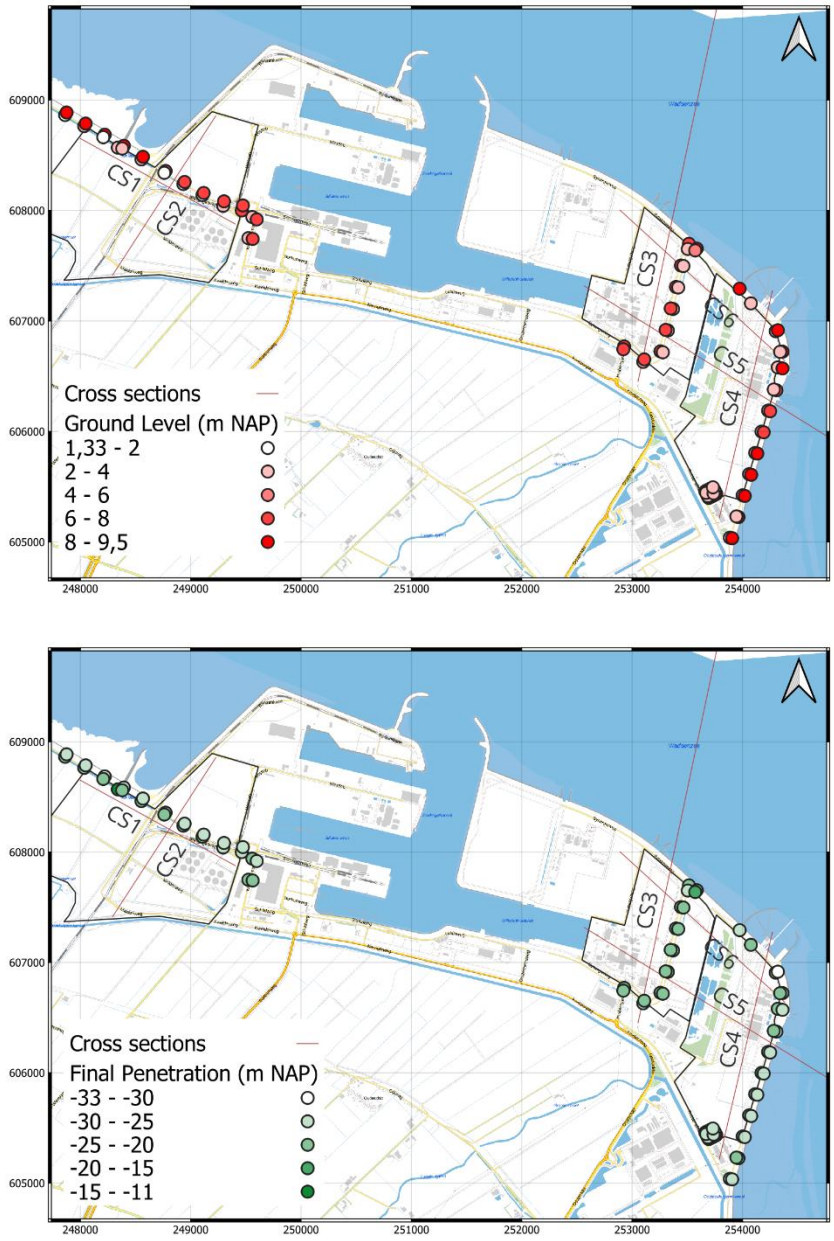

Figure 6.1 The ground level (top) and final penetration depth (bottom) of CPT's used for the geotechnical cross sections CS1, CS3 and CS4.

The soil classification in Section 6.1.2 to section 6.1.4 is based on the classification by Robertson (1990), which has been adjusted by Fugro to the Dutch conditions. The classification for the Eemshaven uses the non-normalized classification including changes proposed by Lengkeek (2024) for organic soils. The lithologies are determined separately for each CPT in 20 cm depth interval based on cone resistance and friction ratio. The automatic procedure then divides the CPTs in intervals with a length of 25 m along the cross section. Within each interval the lithologies over depth are grouped and a distribution of the present lithologies at each depth within each 25 m interval is computed. The profile is coloured according to these percentages. The subareas are described in further detail in the following paragraphs. The used CPTs may be further from the cross section in the perpendicular direction, and the cross section therefore provides an overview of the geotechnical properties of the area.

6.1.2 CS1 Site 1

Figure 6.2 present the geotechnical cross section for CS1. Figure 6.3 and Figure 6.4 A contour plot of the cone resistance of the closest CPT to the cross section line for CS1. highlight the cone resistance of the CPTs closest to the cross sectional line. The contour plots are created by assigning the values of the closest CPTs at their position along the cross section and interpolating in between the CPTs. Figure 6.3 and Figure 6.4 A contour plot of the cone resistance of the closest CPT to the cross section line for CS1.
provide an indication of the resistance of each layer, and indicate stronger and weaker zones. These plots also provide an overview of the local variation within layers.

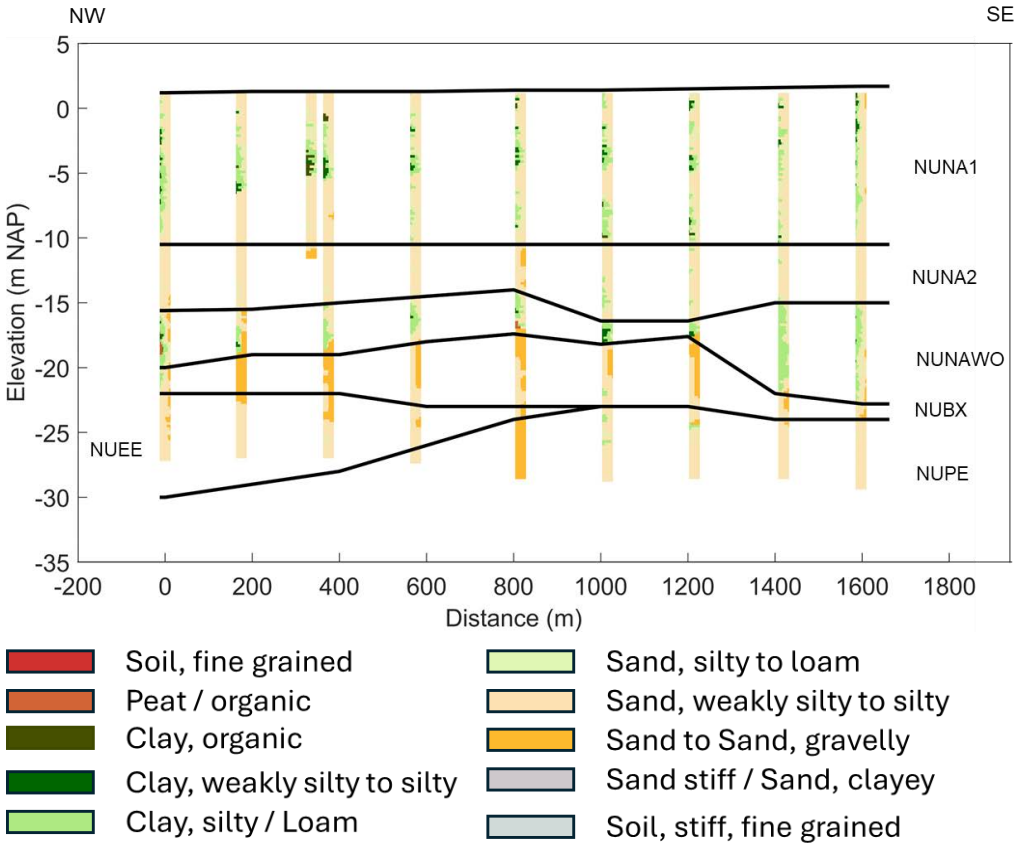

Figure 6.2 *The geotechnical lithological classification of CS1 according to automatic CPT classification. The black lines provide interpreted layer boundaries.*

CS1 has a top Holocene layer consisting mainly of sand with two clayey intervals. These fine-grained intervals are not consistent over the area in thickness and number. The cone resistance in this top is low in the fine-grained layers and roughly 10 MPa in the sand

intervals. At the bottom of the NUNA formation a stronger sand layer is present (NUNA2), which can contain thin clay or silt layers, reducing the cone resistance locally. An additional distinction of the fine material in NUNA1 may also be possible, but additional investigation is necessary as significant variation exists. The NUNAWO layer consists of sandy clay. Below the layer there are local peat patches at. This peat layer (the NUNIBA layer) is not included as a separate layer in the geotechnical profile due to the limited thickness and high variance in presence. Further investigation is required to map its presence in the area. The NUNAWO layer can contain thin sand layers. This locally causes an increase in the measured cone resistance of the clay. No thin layer correction on the measured cone resistance has been applied. Therefore the used cone resistance of the sandy layers within this unit may be underestimated and the cone resistance of the clay a little overestimated. The NUBX layer is a medium to coarse sand layer with cone resistances varying between 10 and 30 MPa.

The NUEE layer is not encountered in the closest CPTs, but is present on further CPTs. This indicates that it is a sand layer with cone resistance between 10 and 20 MPa. The NUPE layer consists of sands with a similar cone resistances as the NUEE layer, and may on contain very stiff clay (potclay), but this has not been observed in the CPTs and is unlikely considering the geological history.

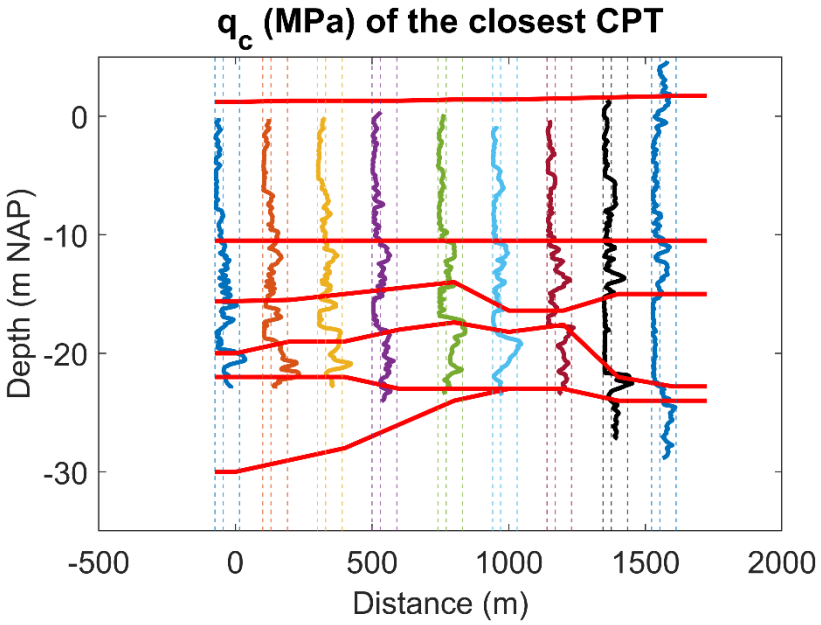

Figure 6.3 The cone resistance of the closest CPT to the cross section line for CS1. For each CPT the dotted lines indicate a cone resistance of 0, 10 and 30 MPa.

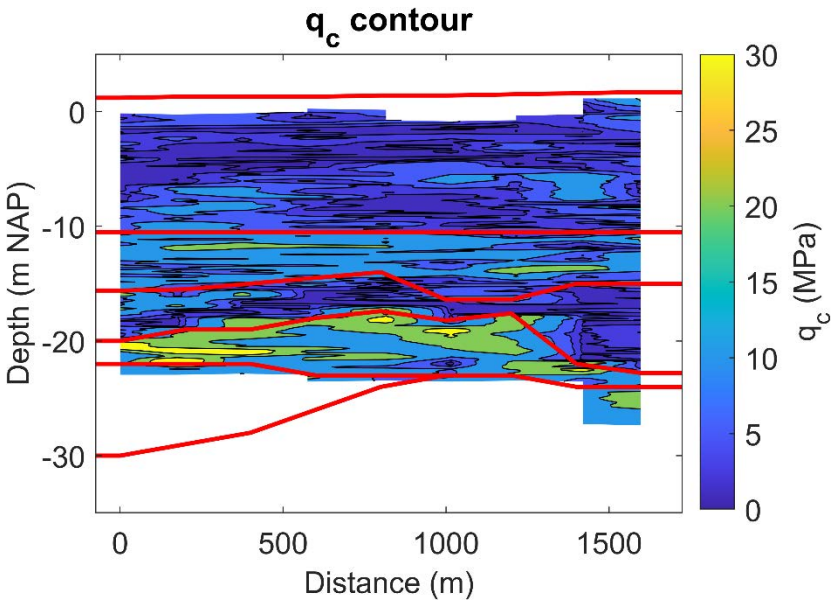

Figure 6.4 A contour plot of the cone resistance of the closest CPT to the cross section line for CS1.

6.1.3 CS3 Site 2

Figure 6.5 presents the detailed view of the cross sectional layering of CS3, and Figure 6.6 and Figure 6.7 highlight the cone resistance of the CPTs closest to cross section line. The land has been raised with sand. This is the NUAAOP layer in the cross section. The cone resistance in this layer is high, mostly exceeding 30 MPa, especially for the shallow depth. The cone resistance in the NUNA layer varies significantly, between 0 and 30 MPa. This clearly indicates the thin clay or silt layers, which makes the unit difficult to classify. The NUNAWO unit consists mainly of (organic) clays. The cone resistance in the NUNAWO layer is very low, and the layer is discontinuous due to the NUNA tidal channel.

The Boxtel (NUBX) and Drenthe (NUDR) formations are difficult to distinguish due to their similar cone resistance and similar classification. The cone resistance of these layers is between 10 and 30 MPa. No CPTs reach the NUPE layer, but their properties are expected to be similar to CS1. Further soil investigation into these deeper layers is advised.

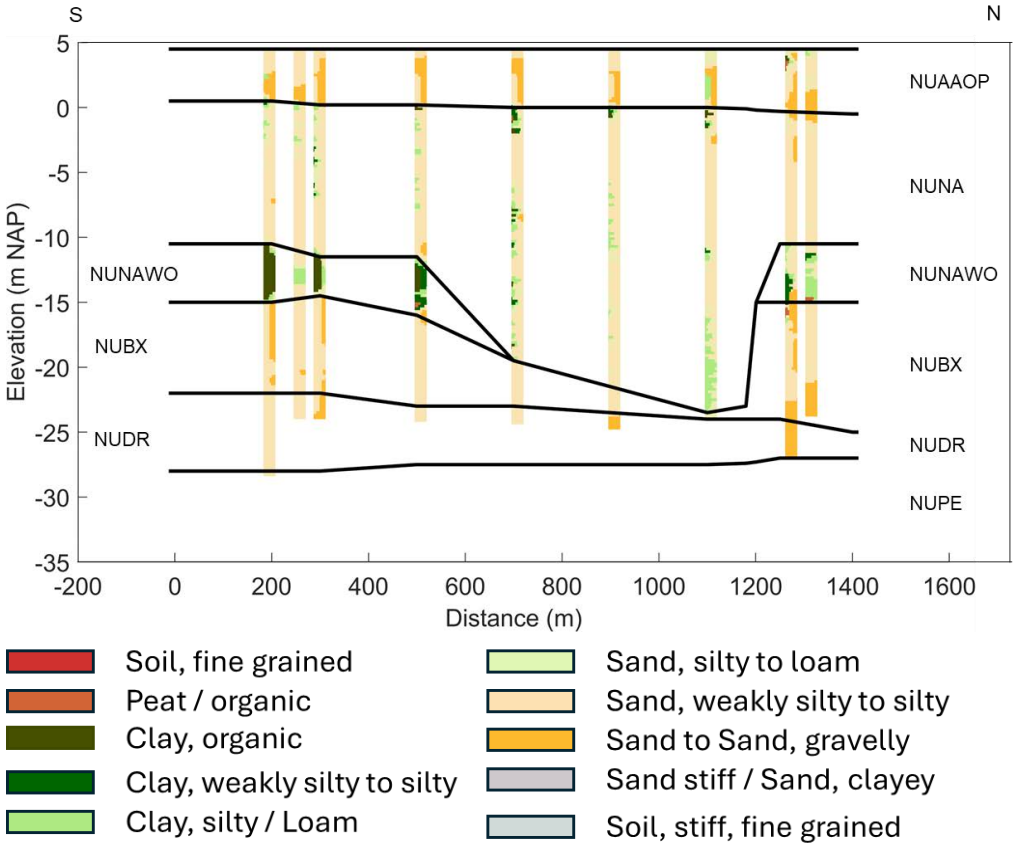

Figure 6.5 The geotechnical soil classification of CS3 according to automatic CPT classification. The black lines provide interpreted layer boundaries.

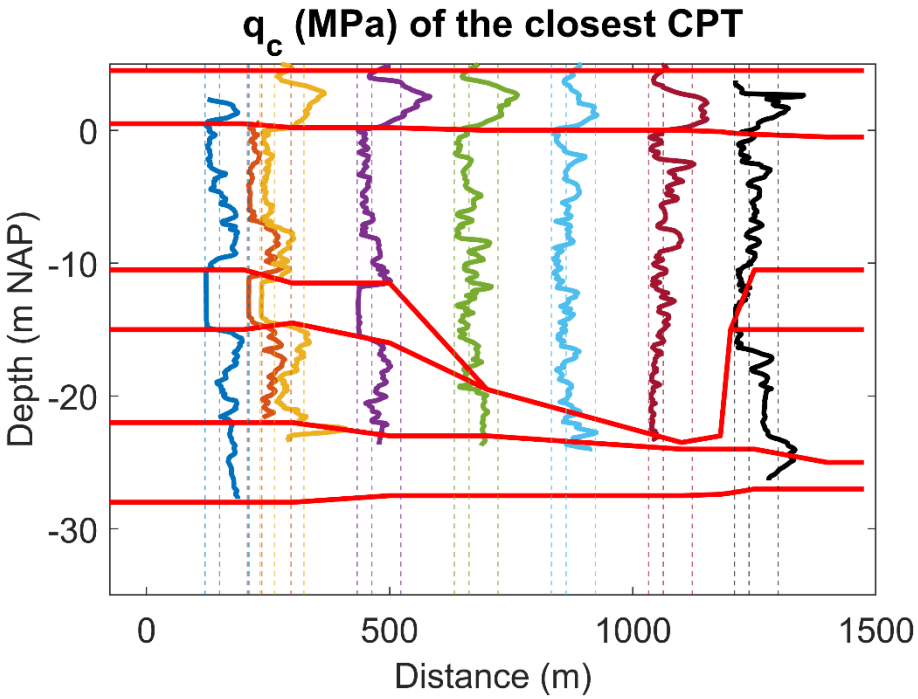

Figure 6.6 The cone resistance of the closest CPT to the cross section line CS3. For each CPT the dotted lines indicate a cone resistance of 0, 10 and 30 MPa.

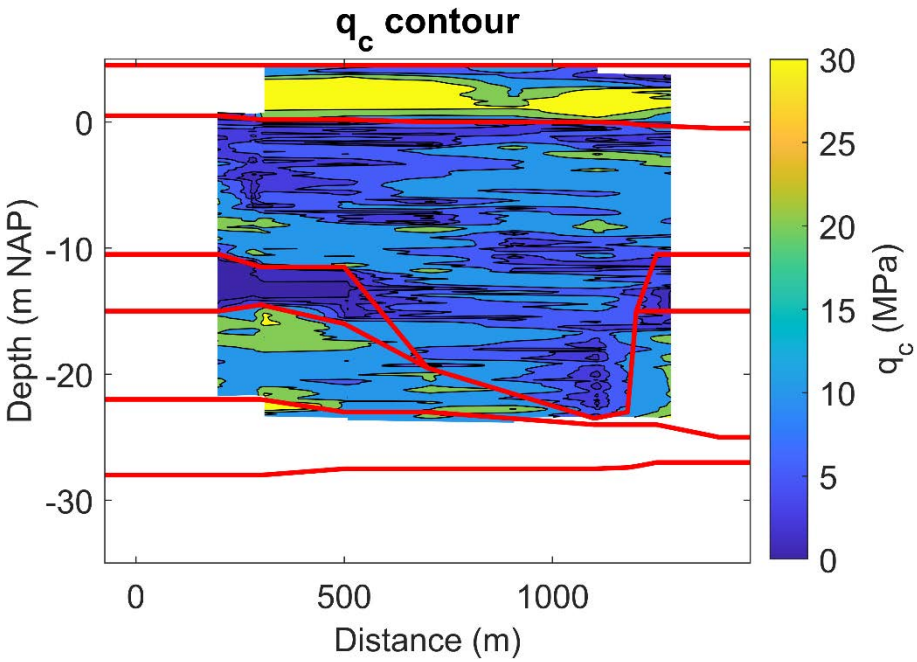

Figure 6.7 A contour plot of the cone resistance of the closest CPT to the cross section line CS3.

6.1.4 CS4 Site 3

Figure 6.8 presents the detailed view of the cross sectional layering of CS4, and Figure 6.9 and Figure 6.10 highlight the cone resistance of the CPTs closest to the cross sectional line. The NUAAOP layer is similar to CS3 with a lower ground level. A single CPT on the external slope of the dyke highlights a fine grained content in this layer, and is not representative for this layer. The cone resistance in the NUNA layer again varies significantly between 0 and 30 MPa. This clearly indicates the thin clay or silt layers, which makes the layer difficult to classify. The fine grained NUNAWO layer is almost 10 meters thick at the south side of CS4, and has a very low cone resistance, indicating (organic) clays. The NUBX layer is a medium to coarse sand layer with cone resistances varying usually between 10 and 30 MPa. Locally, the cone resistance shows peaks up to 50 MPa. The NUDR and NUPE formation are deeper at this location and are not represented in the CPTs.

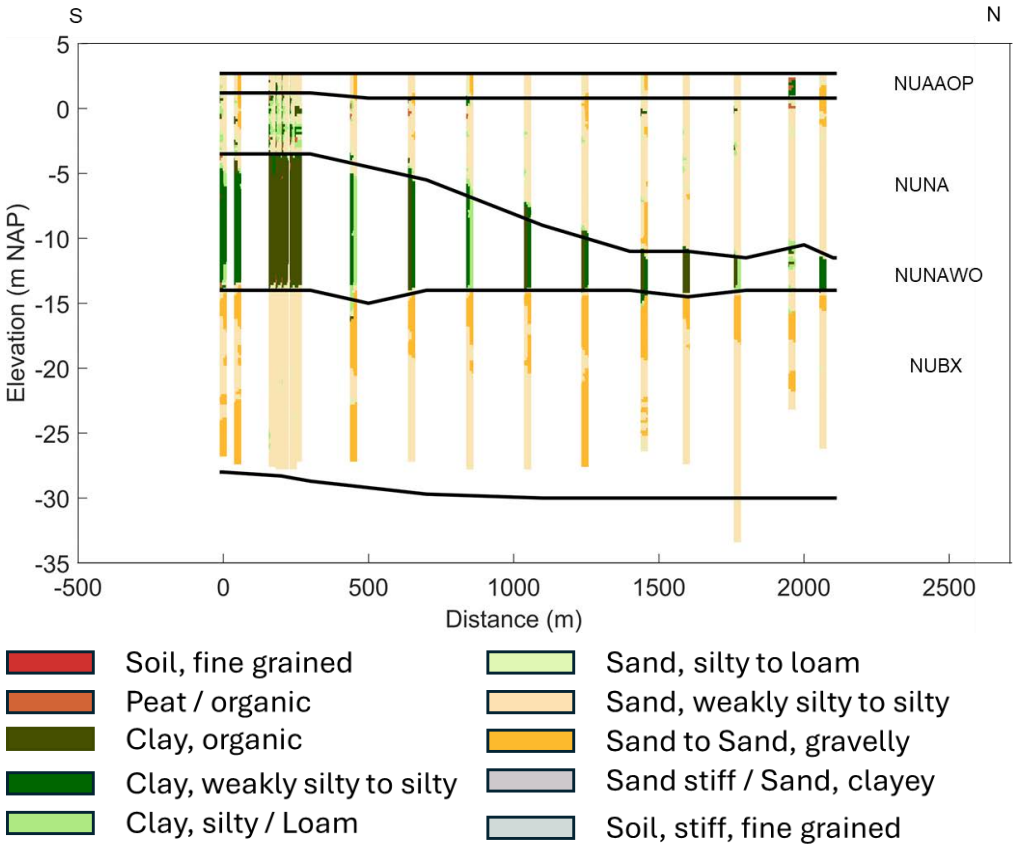

Figure 6.8 The geotechnical soil classification of CS4 according to automatic CPT classification. The black lines provide interpreted layer boundaries.

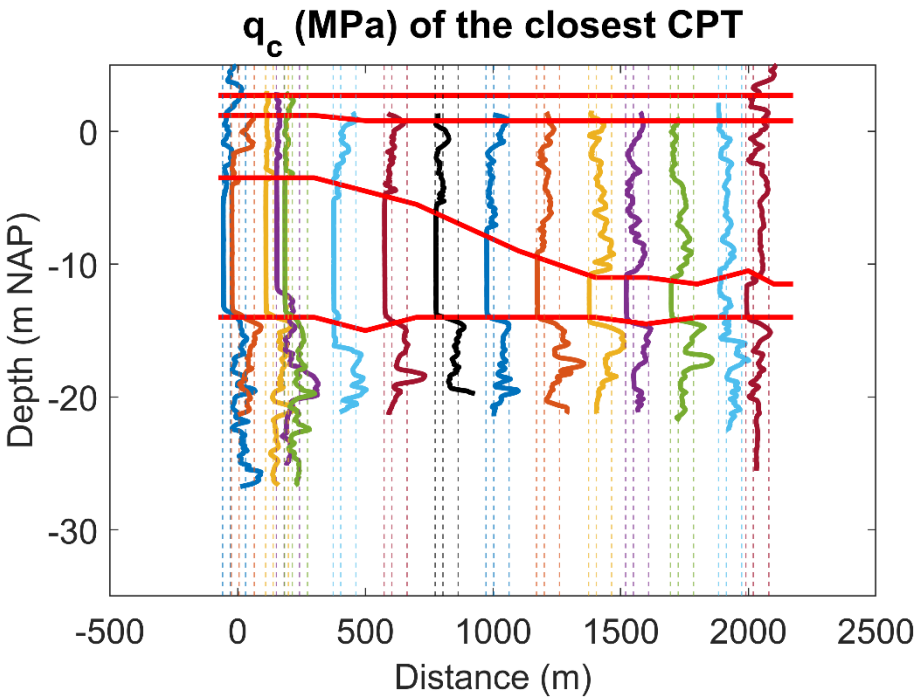

Figure 6.9 The cone resistance of the closest CPT to the cross section line CS4. For each CPT the dotted lines indicate a cone resistance of 0, 10 and 30 MPa.

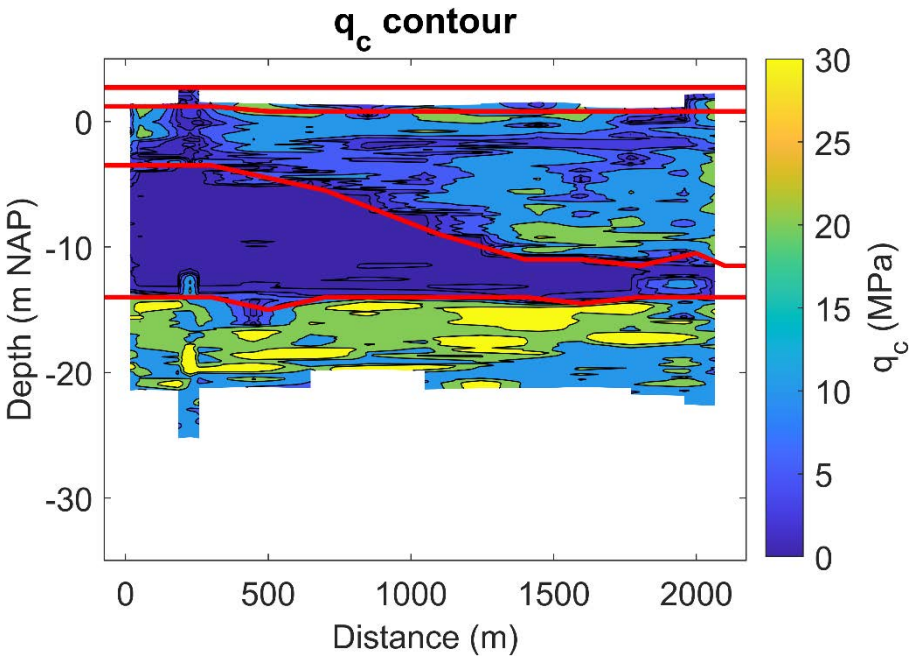

Figure 6.10 A contour plot of the cone resistance of the closest CPT to the cross section line for Subarea 3.

6.1.5 Representative cross sections

Figure 6.11, 6.12 and Figure 6.13 provide schematic representations of the cross sections, providing an indication of the different layers, which can be used in the current design phase. Note that the layer boundaries of the land fill are vague, and that the organic layer may be absent in specific locations. This must be further quantified in later stages of the design process. The used layer boundaries have been provided in Appendix B.

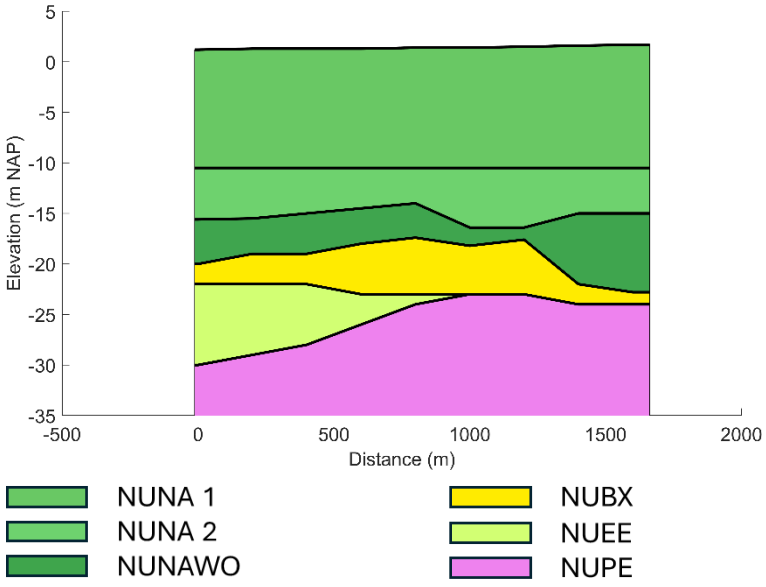

Figure 6.11 Representative geotechnical cross section for Site 1 (CS1).

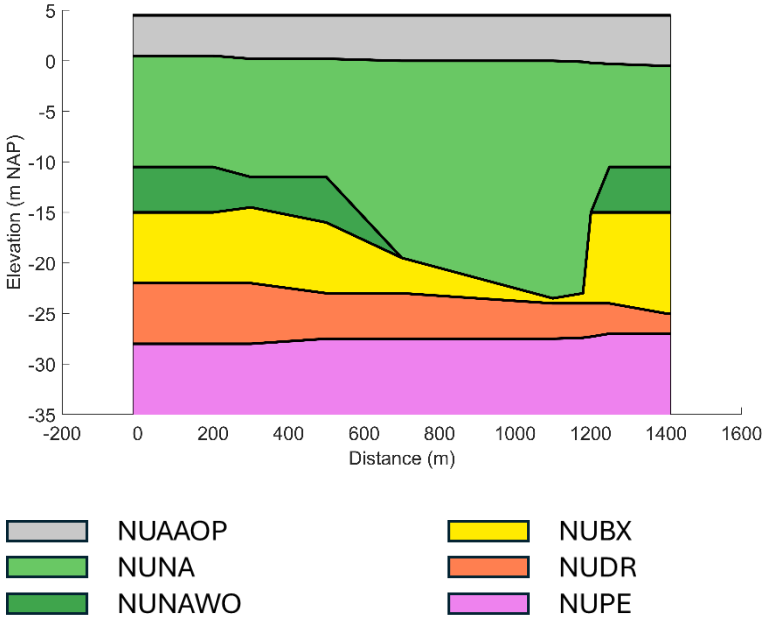

6.12 Representative geotechnical cross section for Site 2 (CS3)

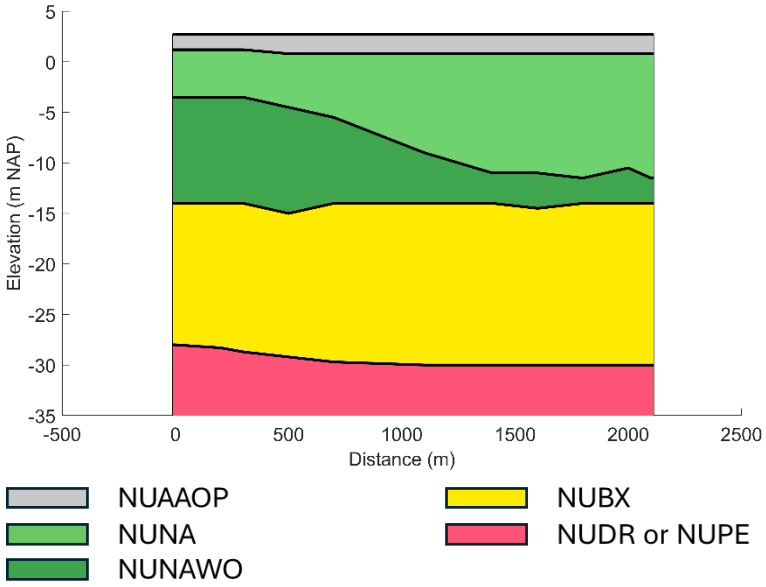

Figure 6.13 Representative geotechnical cross section for Site 3 (CS4). Note that a distinction between NUDR and NUPE is not made due similarities in expected properties and lack of data to distinguish their location.

6.2 Selection of soil parameters

6.2.1 Unit weight

The unit weight of the soil layers is determined based on a Netherlands-specific correlation between the cone resistance and the unit weight (Lengkeek et al., 2018). The unit weight is presented for the closest CPTs, which is in good agreement with the average unit weight over the CPTs per group.

Figure 6.14 to Figure 6.16 present the unit weight of sites 1, 2 and 3. Note that the groundwater level is assumed to be at 0.0 m NAP at site 1, 0.4 m NAP at site 0.4 and 0.5 m NAP at site 3, resulting in a lower unit weight above the water level. The saturated unit weight

of the sand in the NUAAOP layers is between 20-21 kN/m^3. Above the ground water level it is approximated to 18.5-19.0 kN/m^3.

The saturated unit weight of the sand in the NUNA layers varies significantly due to the presence of the fine layers. The sand is estimated to have a unit weight between 19.5 and 20.5 kN/m^3. The fine unit weight of the fine layers is estimated to be between 15.5 and 17.5 kN/m^3. It is assumed that the intermediate results are caused by the interference between the fine and sand layers. The variation in the NUNA 2 layer of CS1 and the NUNA layer of CS3 is smaller with a unit weight ranging between 19.5 and 20.5 kN/m^3.

The unit weight of the clay layers in the NUNAWO formation is between 14.0 and 15.0 kN/m^3 in CS3 and CS4. In CS1 the unit weight is higher at approximately 16 to 17 kN/m^3. However, it is possible that this is caused due to interference with small sand layers, and it is suggested to assume a similar unit weight as CS3 and CS4 for the clay (between 14.0 and 15.0 kN/m^3) until further investigation. The thin sand layers cannot be classified based on the CPTs. For this initial investigation the same properties of the NUNA sand layers are assumed.

The sand layers below the NUNAWO formation have a consistent unit weight between 19.5 and 20.5 kN/m^3. Potentially, some clay may be present in these deeper layers for which the unit weights are assumed to be between 16-18 kN/m^3.

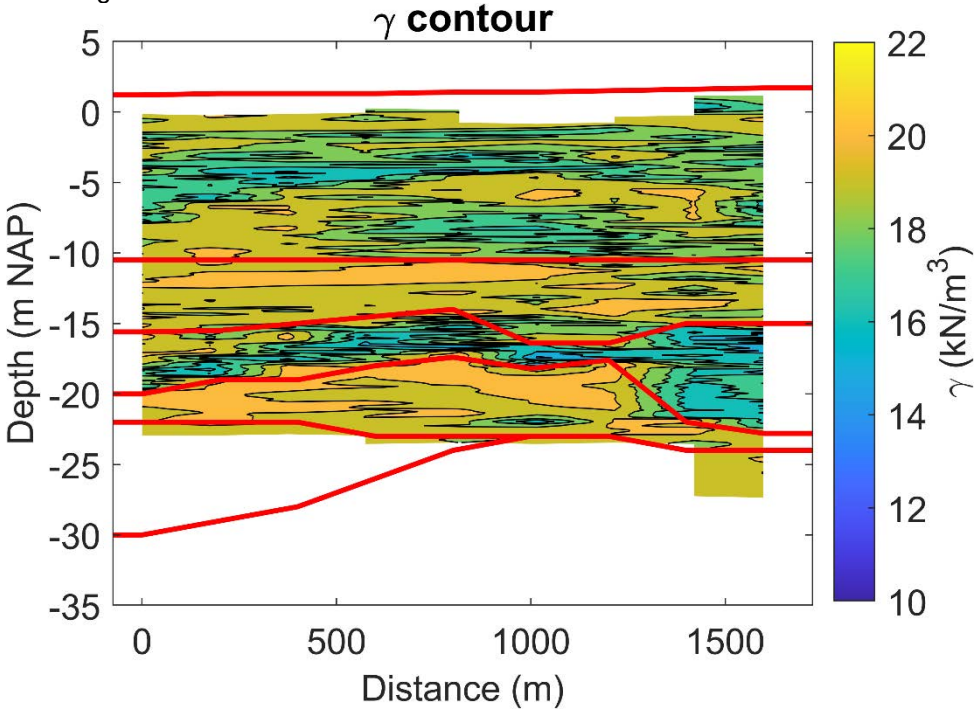

Figure 6.14 Contours of the estimated unit weight according to Lengkeek et al. (2018) based on the closest CPT to the cross section line CS1.

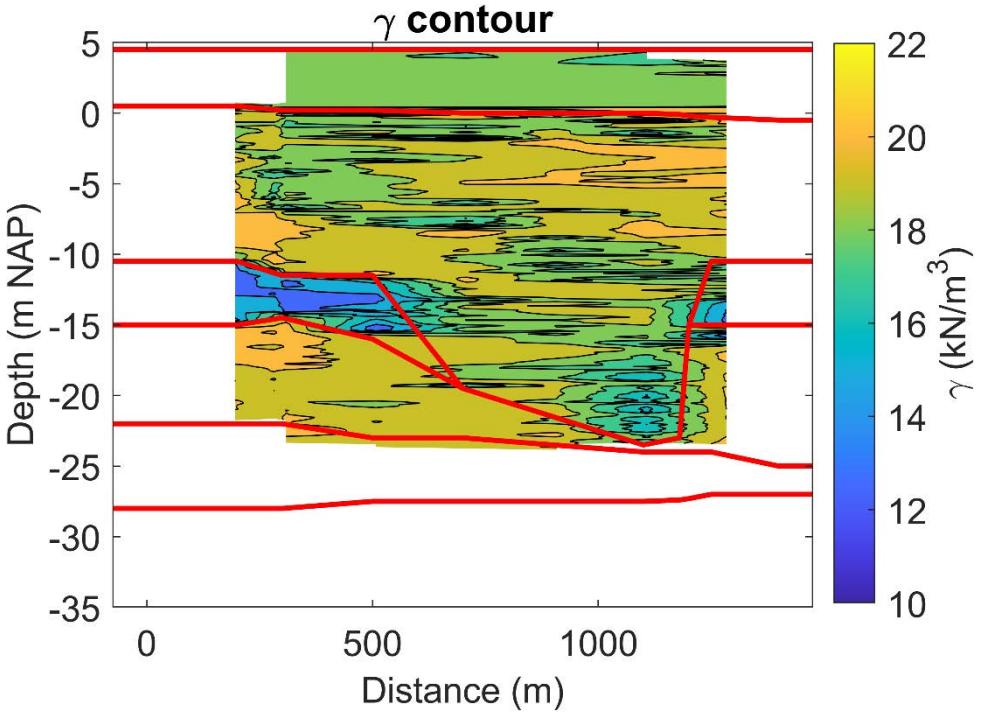

Figure 6.15 Contours of the estimated unit weight according to Lengkeek et al. (2018) based on the closest CPT to the cross section line CS3.

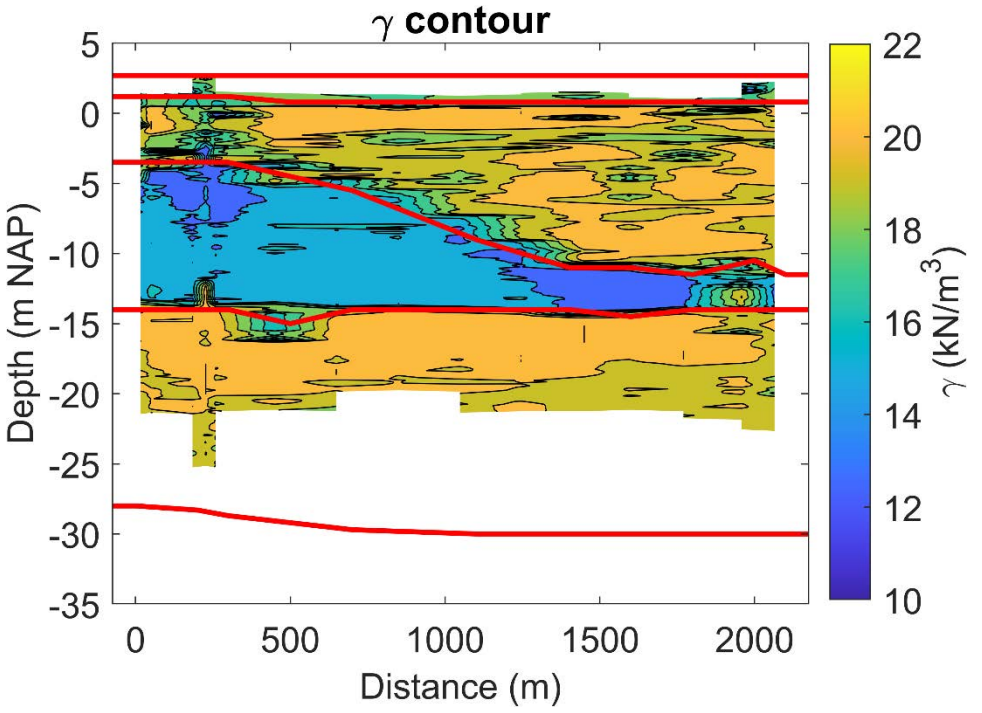

Figure 6.16 Contours of the estimated unit weight according to Lengkeek et al. (2018) based on the closest CPT to the cross section line CS4.

6.2.2 Minimum/maximum unit weight

The minimum and maximum unit weight have not been derived from CPT data. Laboratory testing on soil samples will be required to estimate these properties.

6.2.3 Relative density sand layers

The relative density of the sand layers is assessed using the correlation of Lunne and Christoffersen (1983). This correlation was not designed for landfills, and further investigation might therefore be required. Figure 6.17 to Figure 6.19 highlight the correlation results for sites 1, 2 and 3, and they are summarized in section 6.4. Due to the influence of local thin layers for each area, the average relative density per group is presented. It should be noted that for the cone resistance no thin layer correction or any other correction for layer boundaries is applied. This results in a conservative estimate of the relative density.

The anthropogenic NUAAOP layer at site 2 is very dense with the correlation computing an RE = 0.9 to RE = 1.0 close to CS3. At site 1 the NUAAOP layer is loose to medium dense, and may contain clay and silt layers. NUAAOP layer of site 3 is expected to be similar to site 2, i.e. dense. The relative density of the NUNA layers is generally loose (RE = 0.3) to medium dense (RE = 0.7) with locally denser sands (RE > 0.8). The accuracy of the correlation is questionable, especially in the sections with thin clay layers. The relative density of thin sand layers in the NUNAWO cannot be approximated. Based on the limited data within this layer is assumed to be medium dense (RE = 0.5).

The NUBX layer consists mostly of medium dense material (RE = 0.5 to RE = 0.7), with locally dense zones of RE > 0.8. In site 3 the NUBX layer contains a denser section (RE = 0.7 to RE = 0.9) between NAP -15 m and NAP -20 m. The limited data for the NUEE and NUPE layers indicate a loose (RE = 0.3) to medium dense (RE = 0.5) material, and the limited data for the NUDR layer indicates a medium dense (RE = 0.6) sand.

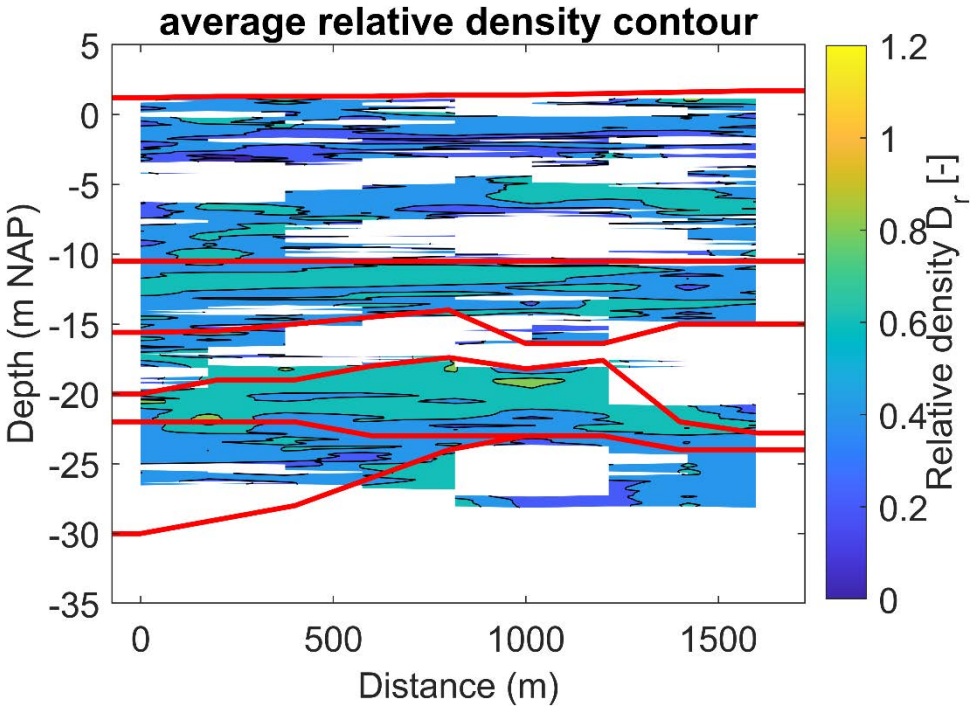

Figure 6.17 Contours of the estimated average relative density according to Lunne & Christoffersen (1983) based on all CPTs near the cross section line CS1. The red lines provide interpreted layer boundaries.

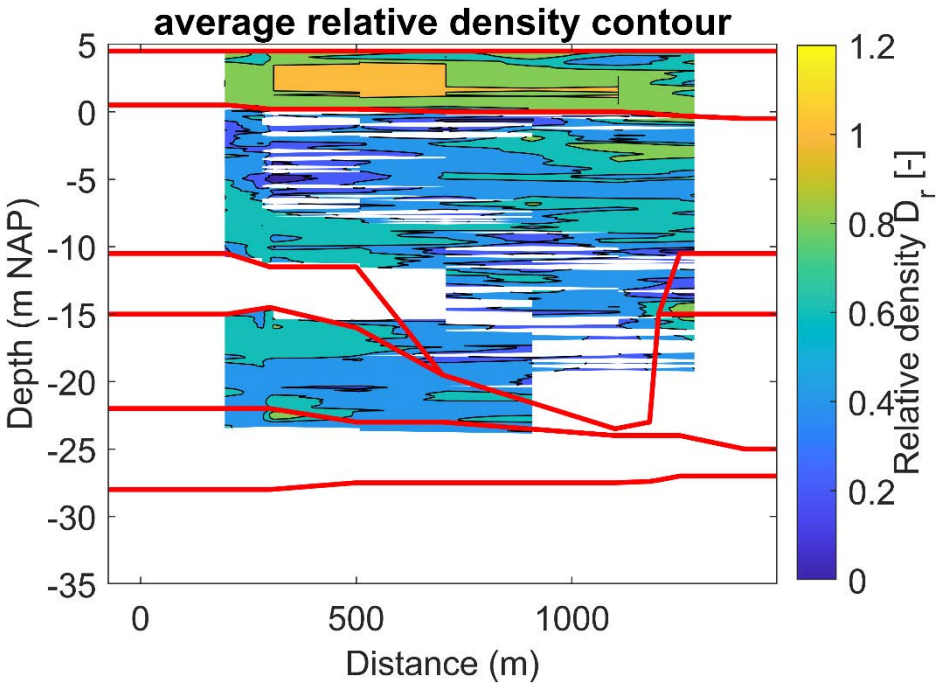

Figure 6.18 Contours of the estimated average relative density according to Lunne & Christoffersen (1983) based on all CPTs near the cross section line CS3. The red lines provide interpreted layer boundaries.

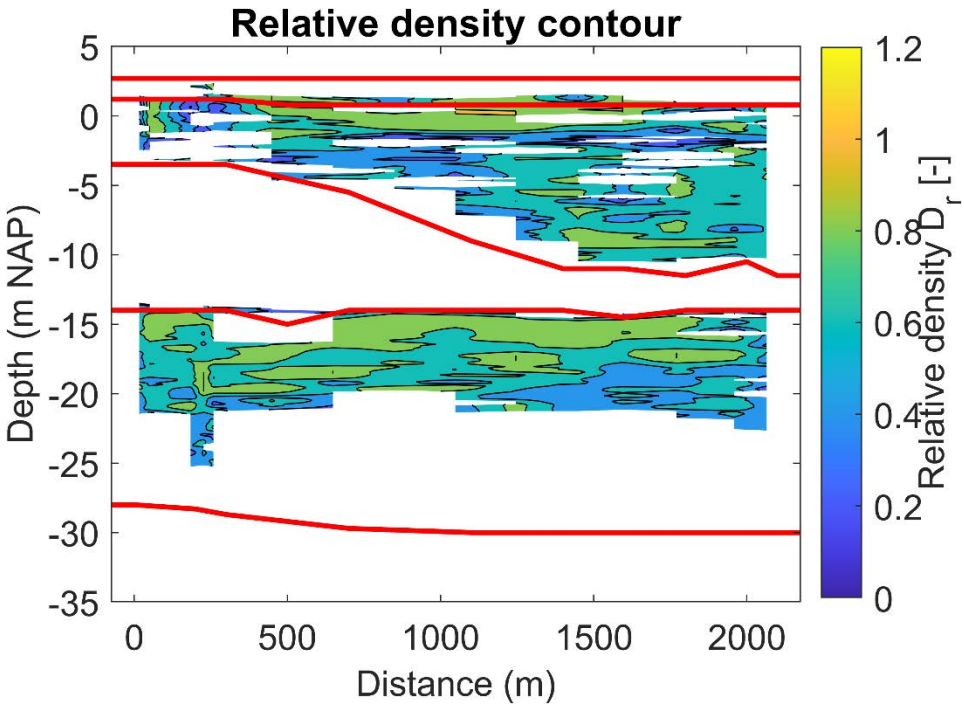

Figure 6.19 Contours of the estimated average relative density according to Lunne & Christoffersen (1983) based on all CPTs near the cross section line for Subarea 3. The red lines provide interpreted layer boundaries.

6.2.4 Strength parameters

6.2.4.1 Friction angle ϕ

The friction angle has been estimated based on the normalized cone resistance and an interpolation on Table 2.b of NEN9997. The data used for the interpolation is provided in Appendix B. These estimates presented here must be confirmed with element testing.

The friction angle in the denser NUAAOP layer at site 2 and site 3 is between 36° and 40°. This may be caused by an overestimation of the normalized cone resistance at the low effective stress. The assumed friction angle is therefore 36° for this layer. The friction angle in the looser NUAAOP layer at site 1 is estimated to be between 30° and 32°. The sand in the NUNA layer is estimated to have a friction angle between 31° and 33°, which drops to between 27.5° and 29.0° in the finer grained material. Due to the small layers the friction angle may be overestimated for this fine grained material. Further investigation is required. In the organic clayey NUNAWO layer the friction angle decreases to 15°. The NUNAWO layer also contains some non-organic zones for which the friction angle is estimated to be between 27.5° and 29.0° (strong sandy).

The sand in the lower NUBX, NUDR, NUEE and NUPE layer is estimated to have also have a friction angle between 31° and 33°, with local dense patches with a friction angle of 36°.

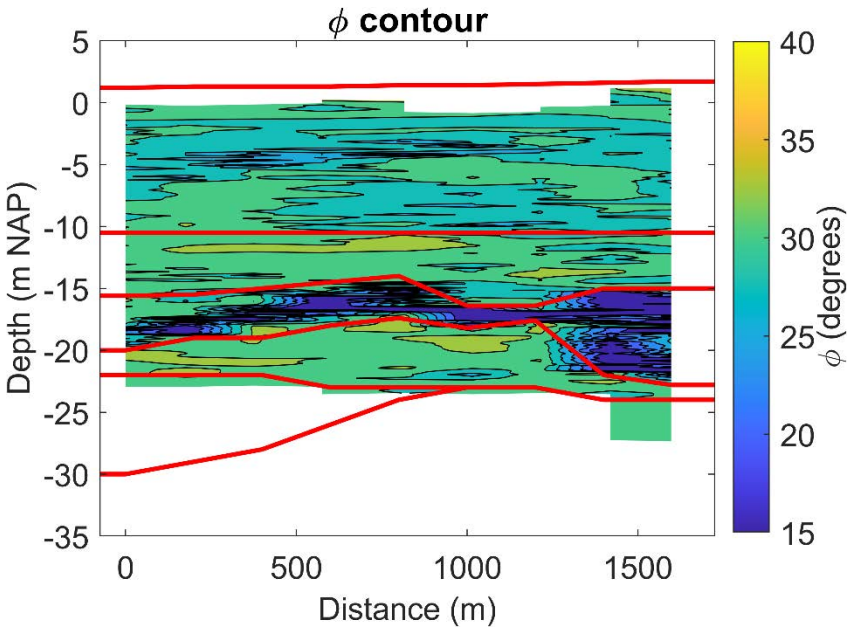

Figure 6.20 Contours of the estimated ϕ according to an interpolation of NEN-9997 based on the closest CPTs near the cross section line CS1.

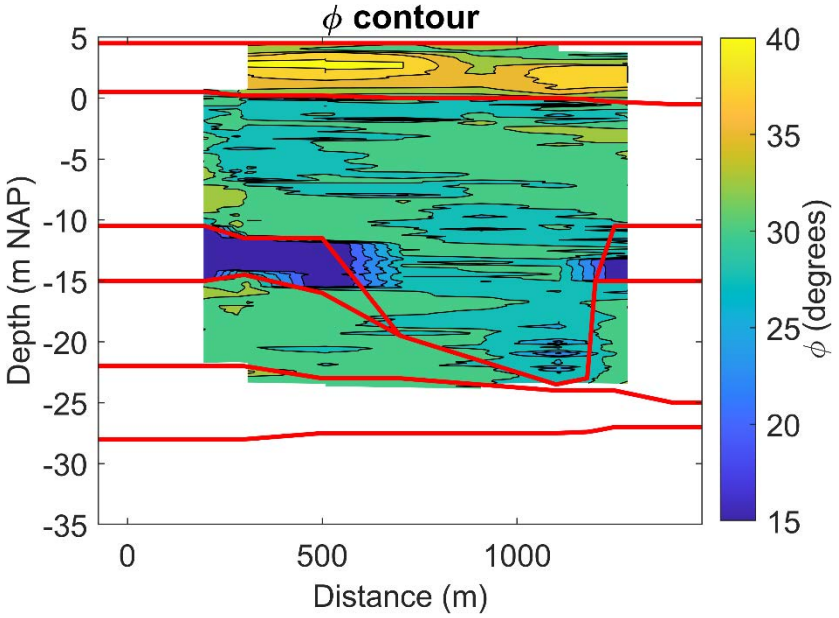

Figure 6.21 Contours of the estimated ϕ according to an interpolation of NEN-9997 based on the closest CPTs near the cross section line CS3.

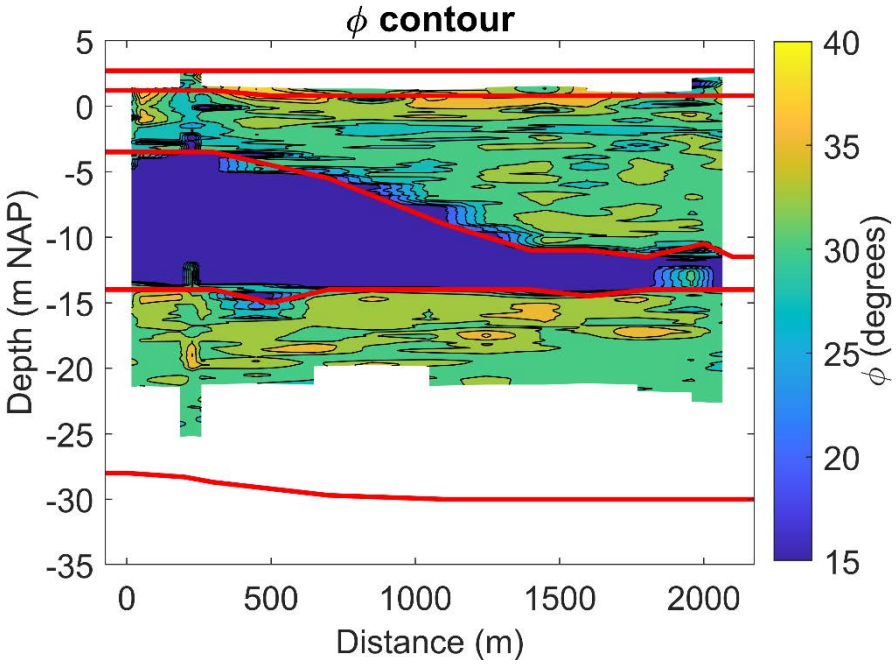

Figure 6.22 Contours of the estimated ϕ according to an interpolation of NEN-9997 based on the closest CPTs near the cross section line CS4.

6.2.4.2 Cohesion c

Interpolation on the NEN9997 table does not provide a consistent effective cohesion. Therefore the following estimates are suggested:

- Sand/silt layers: c = 0 kPa.
- Clay (strong sandy) zones: c = 1 kPa.
- Peat/organic clay: c = 1 kPa.

6.2.5 Stiffness parameters

The stiffness of granular materials found in the subsurface varies with the confining stress level and thus with the depth of the material. An efficient way to account for this variation of stiffness with depth within an otherwise uniform soil formation is by relating the stiffness

parameter (E) to a reference stiffness (E_{ref}) at an effective confining stress (σ_c') that is equal to a reference stress (p_{ref}), typically taken as 100 kPa (atmospheric pressure). This models the stiffness as a stress dependent parameter. The relation between stiffness and effective confining soil stress is for cohesionless soil:

$$E = E_{ref} \cdot \left(\frac{\sigma_c'}{p_{ref}} \right)^m$$

With:

- E stiffness [kN/m^2].
- E_{ref} stiffness at reference stress level p_{ref} [kN/m^2].
- p_{ref} reference stress level, commonly p_{ref} = 100 kPa is used.
- m power defining the change of E with changing σ_c' [-], commonly m = 2/3 is used.

As an initial estimate the E_{100} has again been determined from interpolation (using Appendix B which is based on the NEN-9997 Table 2.B). Fixed suggestions for 'm' are provided in NEN-9997, and m =2/3 is used here. The results for the three cross sections are provided in Figure 6.23 to Figure 6.25 and summarized here.

The reference stiffness in the natural sand layers is estimated to be between 30 and 50 MPa, with local loose and dense zones with a reference stiffness of respectively 15 and 70 MPa. Especially the NUBX layer is stiffer with an reference stiffness between 30 and 70 MPa. The thin clay and silt layers are estimated to have The NUAAOP layer is stiff with a reference stiffness exceeding 70 MPa (up to 110 MPa). The clay of the NUNAWO layer is estimated to have a reference stiffness between 1 and 2 MPa, corresponding to a moderately stiff organic clay.

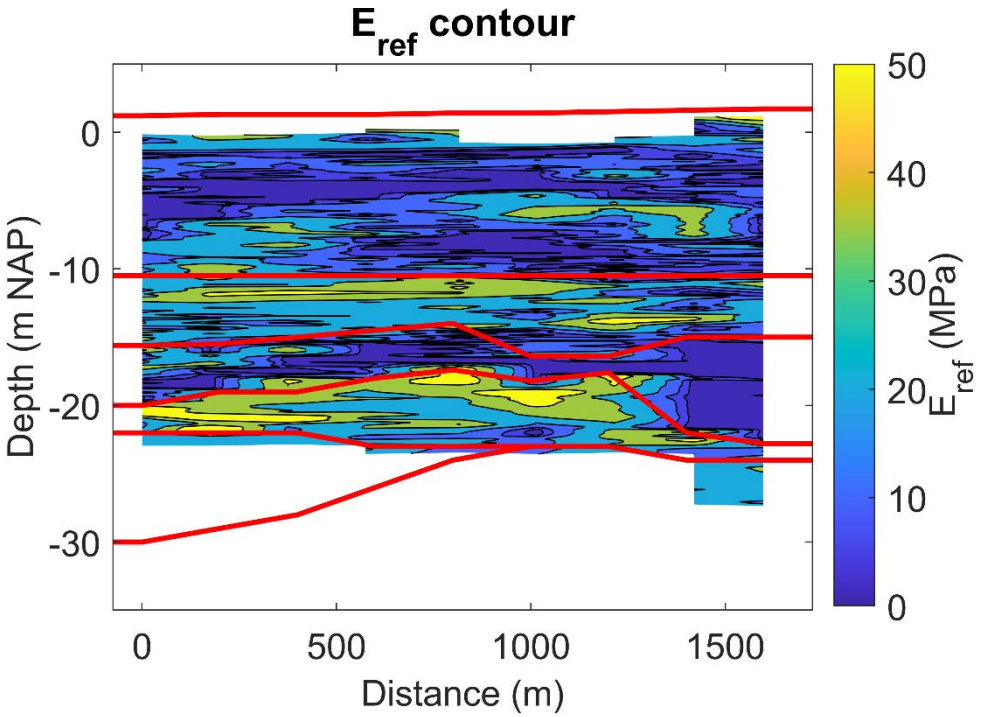

Figure 6.23 Contours of the estimated E_{100} according to an interpolation of NEN-9997 based on the closest CPTs near the cross section line CS1.

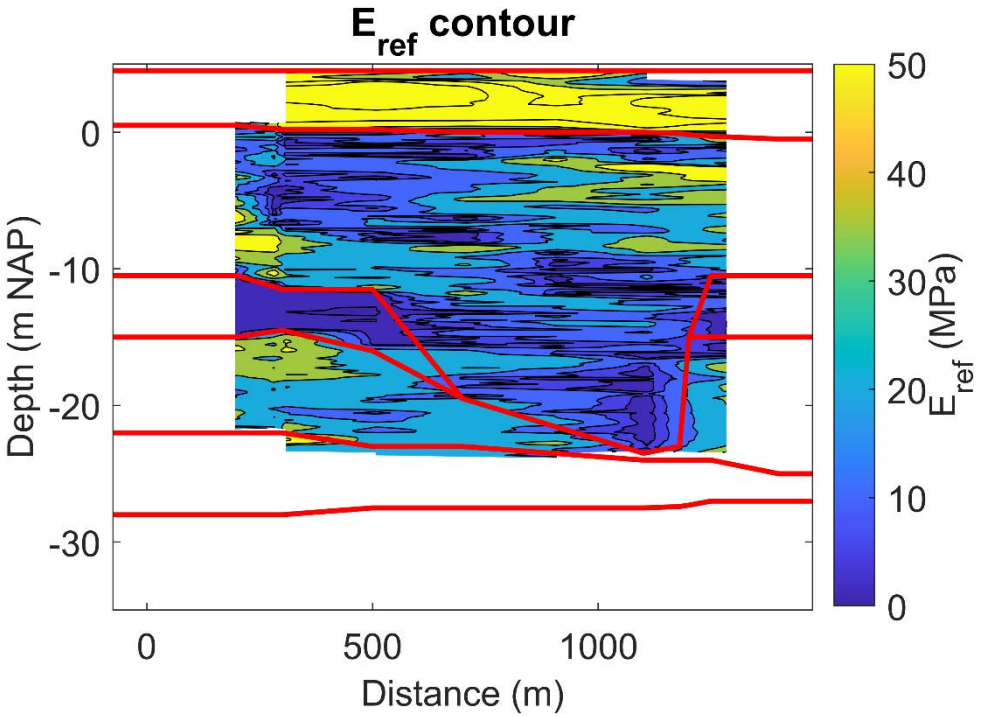

Figure 6.24 Contours of the estimated E_{100} according to an interpolation of NEN-9997 based on the closest CPTs near the cross section line CS2.

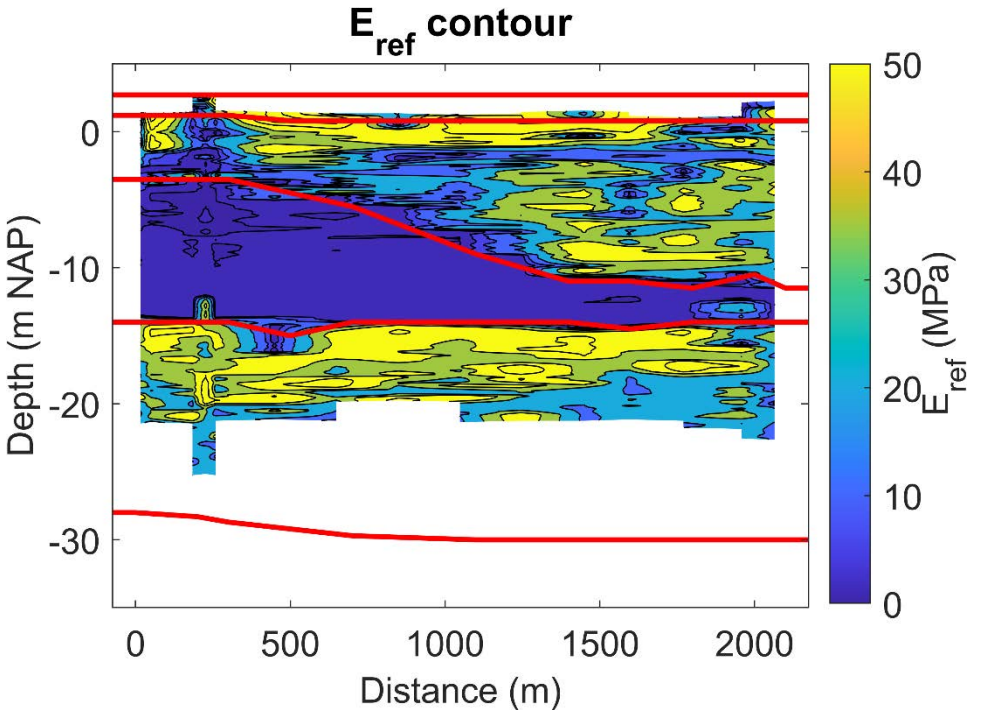

Figure 6.25 Contours of the estimated E_{100} according to an interpolation of NEN-9997 based on the closest CPTs near the cross section line CS3.

6.3 Settlement parameters

The settlement parameters are based on Dutch experience based on table 2.b of NEN 9997, the Dutch version of EC7. Again the results have been interpolated based on the normalized cone resistance. The settlement parameters are shown in this section, and summarized in the geotechnical parameters in Section 6.4.

6.3.1 Site 1 (CS1)

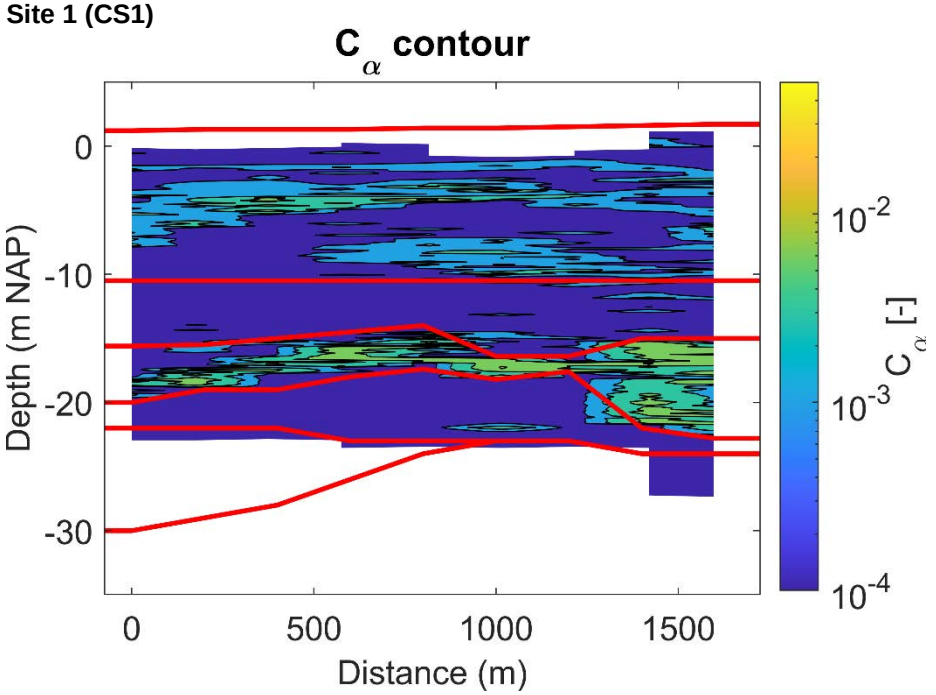

Figure 6.26 Contours of the estimated C_α according to an interpolation of NEN-9997 based on the closest CPTs near the cross section line CS1. Note that in the sand layer $C_\alpha = 0$.

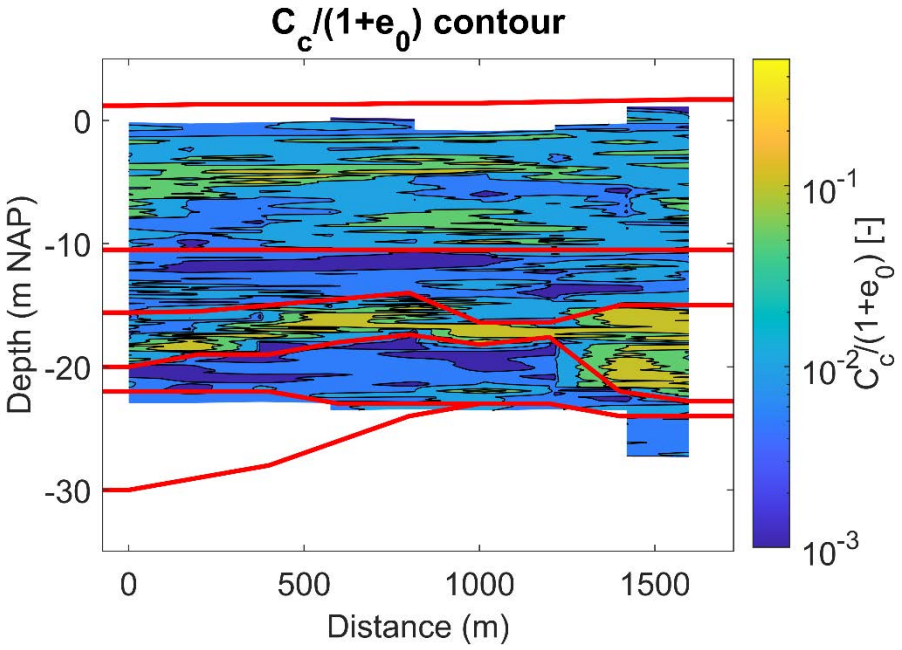

Figure 6.27 Contours of the estimated $C_c/(1+e_0)$ according to an interpolation of NEN-9997 based on the closest CPTs near the cross section line CS1.

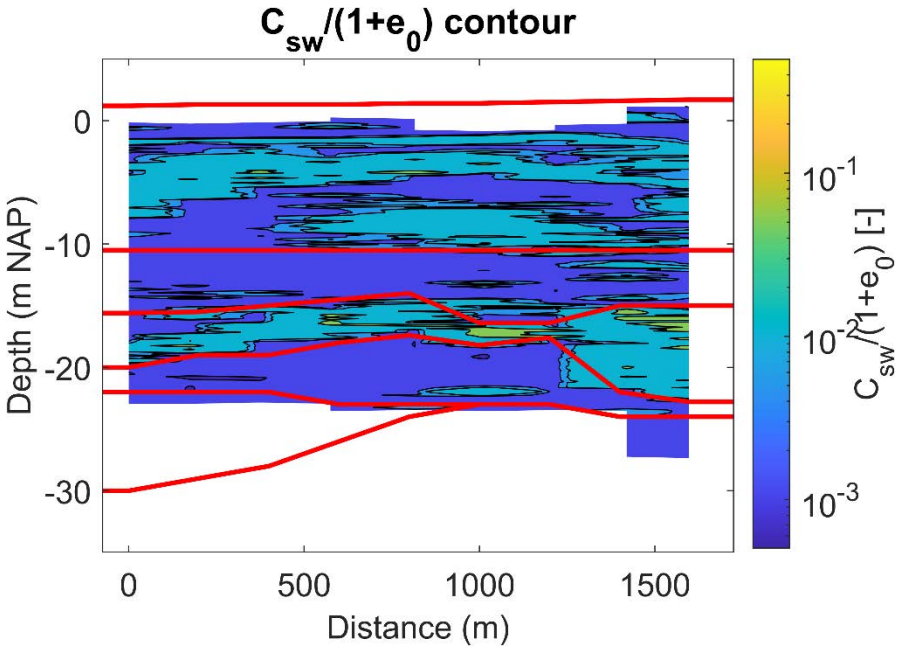

Figure 6.28 Contours of the estimated $C_{sw}/(1+e_0)$ according to an interpolation of NEN-9997 based on the closest CPTs near the cross section line CS1.

6.3.2 Site 2 (CS3)

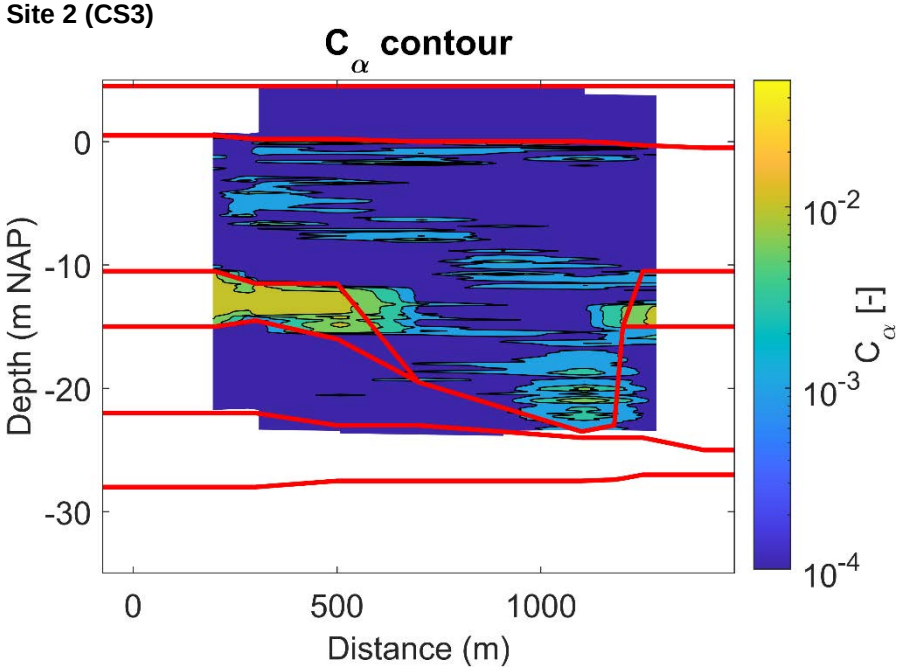

Figure 6.29 Contours of the estimated C_α according to an interpolation of NEN-9997 based on the closest CPTs near the cross section line CS3. Note that in the sand layer $C_\alpha = 0$.

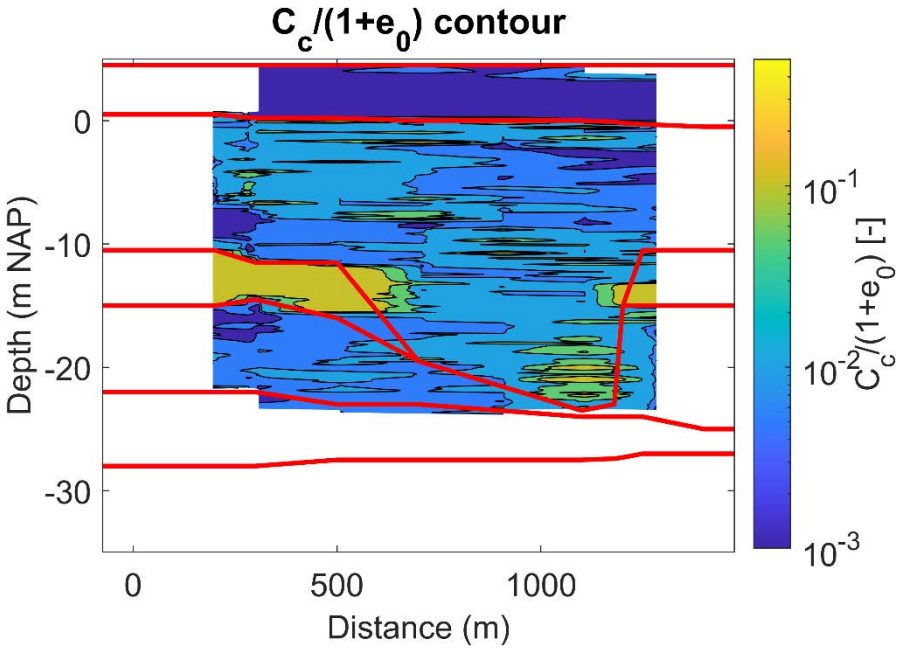

Figure 6.30 Contours of the estimated $C_c/(1+e_0)$ according to an interpolation of NEN-9997 based on the closest CPTs near the cross section line CS3.

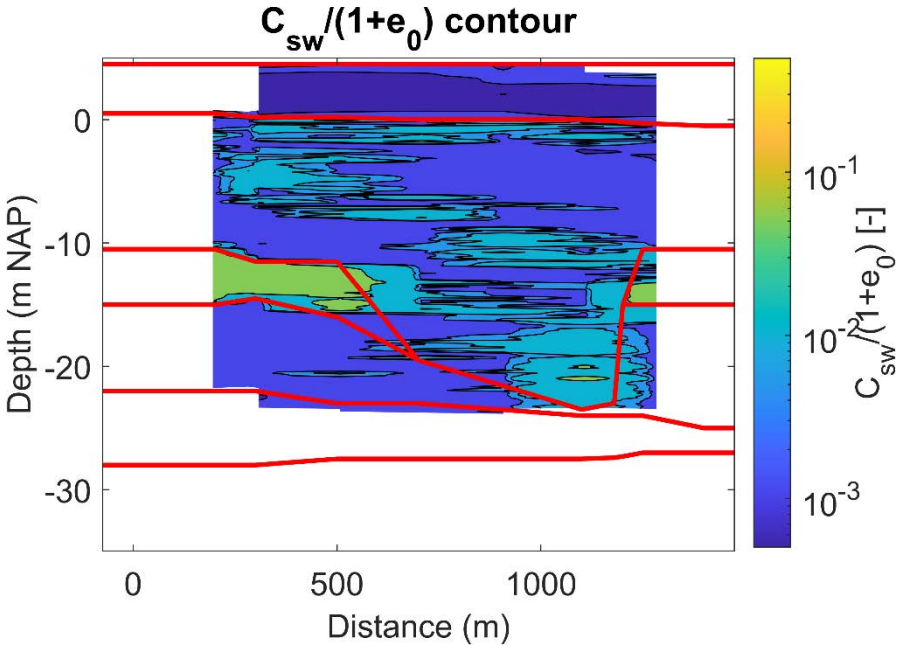

Figure 6.31 Contours of the estimated $C_{sw}/(1+e_0)$ according to an interpolation of NEN-9997 based on the closest CPTs near the cross section line CS3.

6.3.3 Site 3 (CS4)

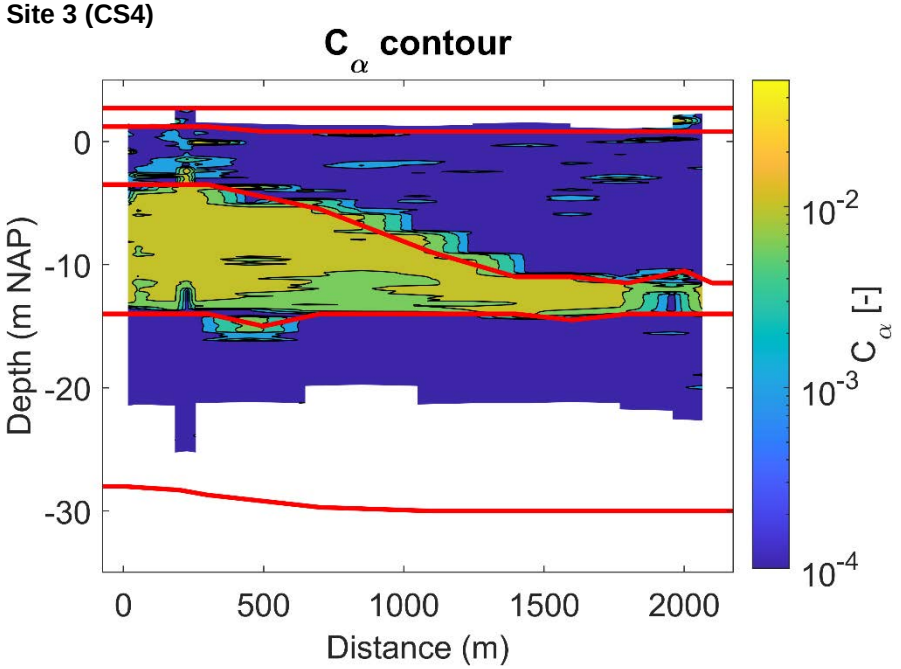

Figure 6.32 Contours of the estimated C_α according to an interpolation of NEN-9997 based on the closest CPTs near the cross section line CS4. Note that in the sand layer C_α = 0.

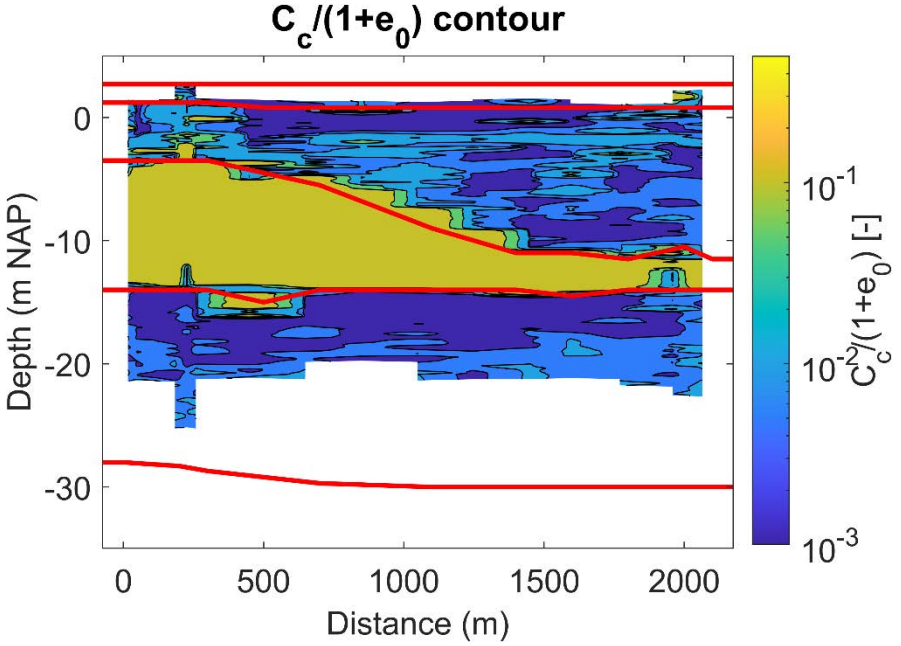

Figure 6.33 Contours of the estimated $C_c/(1+e_0)$ according to an interpolation of NEN-9997 based on the closest CPTs near the cross section line CS4.

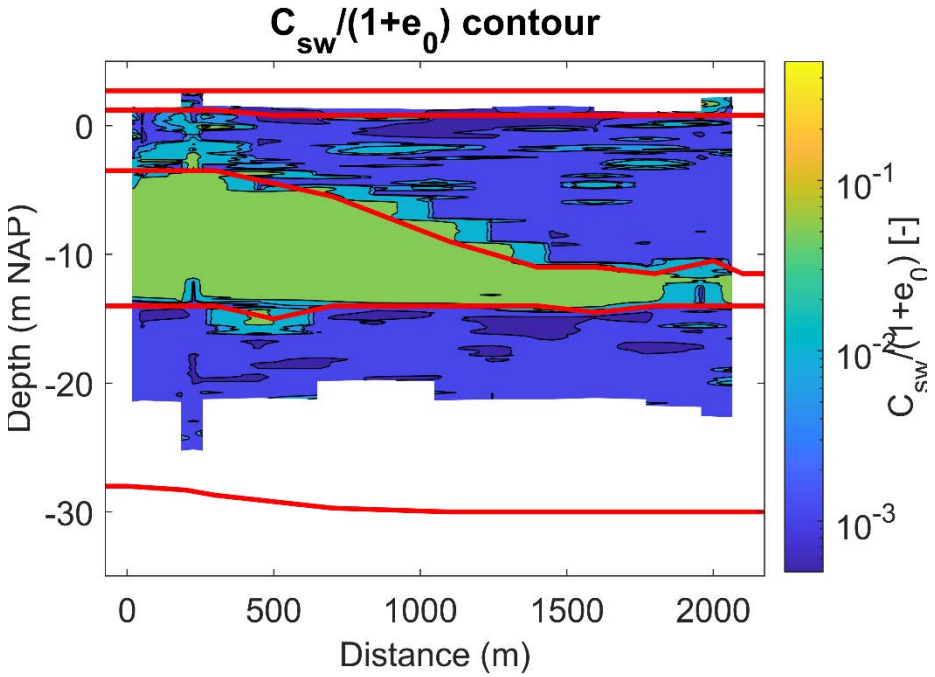

Figure 6.34 Contours of the estimated $C_{sw}/(1+e_0)$ according to an interpolation of NEN-9997 based on the closest CPTs near the cross section line CS4.

6.4 Summary of geotechnical parameters

6.4.1 Selected soil profiles

Section 6.1.5 provides a schematic representations of the sites. A summary of the material properties for these representations is provided in Table 6.1 to Table 6.3. Note that significant variation is present in the layers, especially regarding thin clay and sand layers in the various formation, as was highlighted in the previous sections. The NUNAWO layer is not continuously present in site 2, due to the tidal channels. This has not been included in the tables, and should be further investigated in the design stage.

Table 6.1 Summary of the material properties for site 1.

layer	Top of layer	Relative density	Unit weight	Strength parameters		Stifness	Settlement parameters		
	m + NAP		γ kN/m^3	c kPa	ϕ degr	E100 MPa	$C_c/(1+e_0)$	$C_{sw}/(1+e_0)$	C_a
NUAAOP (sand)*	4.2	Loose – medium dense	17 – 19.0 (moist) 19 - 21 (wet)	0	30 – 32	15-30	0.0075 – 0.0115	0.0025-0.0038	0
NUNA 1 (sand)	1.7 – 1.2	Loose – medium dense	19.5 – 20.5 (wet)	0	31 – 33	30 – 50	0.0075 – 0.0115	0.0025-0.0038	0
NUNA 1 (clay)	1.7 – 1.2		15.5 – 17.5	1	27 – 29	1 – 15	0.05 – 0.25	0.01-0.075	0.001 – 0.012
NUNA 2 (sand)	-10.5	Medium dense	19.5 – 20.5	0	33	30 – 50	0.0038 – 0.0075	0.0013 - 0.0025	0
NUNAWO (clay)	-14.0 – -16.4		14 – 15	1	15	2 – 3	0.09 – 0.15	0.03 - 0.05	0.004 – 0.007
NUNAWO (thin sand layers)	-14.0 – -16.4	Medium dense	19.5 – 20.5	1	27 – 29	15 – 30	0.0038 – 0.0075	0.0013 - 0.003	0
NUBX (sand)	-17.4 – -22.8	Medium dense – dense	19.5 – 20.5	0	31 – 33	30 – 70	0.0025 – 0.0038	0.001-0.0013	0
NUEE (sand)	-22.0 – -23.0	Loose – medium dense	19.5 - 20.5	0	31 – 33	30 – 50	0.0038 – 0.0075	0.0013-0.003	0
NUPE (sand)	-23.0 – -30.0	Loose – medium dense	19.5 - 20.5	0	31 – 33	30 – 50	0.0038 – 0.0075	0.0013-0.003	0

**The NUAAOP layer is absent in the southern part of site 1*

Table 6.2 Summary of the material properties for site 2.

layer	Top of layer m + NAP	Relative density	Unit weight	Strength parameters		Stifness	Settlement parameters		
			γ kN/m^3	c kPa	ϕ degr	E100 MPa	$C_c/(1+e_0)$	$C_{sw}/(1+e_0)$	C_a
NUAAOP (sand)	4.5	Dense	18.5 – 19.0 (moist) 20 - 21 (wet)	0	36	70 – 110	0.0015 – 0.0023	0.0005 – 0.0008	0
NUNA (sand)	0.5 – -0.5	Loose – medium dense	19.5 – 20.5	0	31 – 33	30-50	0.0075 – 0.0115	0.0025-0.0038	0
NUNA (clay)	0.5 – -0.5		15.5 – 17.5	1	27 – 29	1 – 15	0.05 – 0.25	0.01-0.075	0.001 – 0.012
NUNAWO (clay)	-10.5 – 11.5		14 – 15	1	15	1 – 2	0.15 – 0.25	0.05-0.075	0.01 – 0.012
NUNAWO (thin sand layers)	-10.5 – 11.5	Medium dense	19.5 – 20.5	1	27 – 29	15 – 30	0.0038 – 0.0075	0.0013 - 0.003	0
NUBX (sand)	-14.5 – -24	Medium dense – dense	19.5 – 20.5	0	31 – 33	30 – 70	0.0025 – 0.0038	0.001-0.0013	0
NUDR (sand)	-22 – -25	Medium dense	19.5 – 20.5	0	31 – 33	30 – 50	0.0030 – 0.0050	0.001-0.0016	0
NUPE (sand)	-27 – -28	Loose – medium dense	19.5 – 20.5	0	31 – 33	30 – 50	0.0038 – 0.0075	0.0013-0.003	0

Table 6.3 Summary of the material properties for site 3.

layer	Top of layer m + NAP	Relative density	Unit weight	Strength parameters		Stifness	Settlement parameters		
			γ kN/m^3	c kPa	ϕ degr	E100 MPa	$C_c/(1+e_0)$	$C_{sw}/(1+e_0)$	C_a
NUNAAOP (sand)	2.7	Dense	16 - 20 (moist) 19 - 21 (wet)	0	36	70 – 110	0.0015 – 0.0023	0.0005 – 0.0008	0
NUNA (sand)	0.8 – 1.2	Loose – medium dense	19.5 – 20.5	0	31 – 33	30-50	0.0075 – 0.0115	0.0025-0.0038	0
NUNA (clay) (presence limited)	0.8 – 1.2		15.5 – 17.5	1	27 – 29	1 – 15	0.05 – 0.25	0.01-0.075	0.001 – 0.012
NUNAWO (clay)	-3.5 – -10.0		14 – 15	1	15	1 – 2	0.15 – 0.25	0.05-0.075	0.01 – 0.012
NUNAWO (thin sand layers)	-3.5 – -10.0	Medium dense	19.5 – 20.5	1	27 – 29	15 – 30	0.0038 – 0.0075	0.0013 - 0.003	0
NUBX (sand)	-14 – -15	Medium dense – dense	19.5 – 20.5	0	31 – 33	30 – 70	0.0025 – 0.0038	0.001-0.0013	0
NUDR/NUPE (sand)	-28 – -30	Loose – medium dense	19.5 – 20.5	0	31 – 33	30 – 50	0.0038 – 0.0075	0.0013-0.003	0

6.4.2 Attention points

With the exception of the NUNAAOP, subsurface conditions are similar for all subareas. The NUNAAOP layer is dense at site 2 and 3 and loose to medium dense at site 1, while the natural layers below consist mainly of loose to medium dense sands. The NUNAWO clay layer varies significantly in thickness, and can be absent in site 2 and the northern part of site 3. Additionally, the Eemshaven area is known for soil profiles with layers consisting of alternating sand and silt/clay layers at centimeter scale. These layers can be distinguished based on a low cone resistance, low variable friction ratio and high water pressures (when measured). These layers are difficult to classify based on CPT data.

The parameters derived here are based on CPT data using correlations and Dutch standards. Additional laboratory testing on local material has not yet been performed. Since most of the CPTs do not reach deeper than -25 m NAP, geotechnical information is scarce for the deeper parts. Further investigation at larger depths is required before more detailed design phases are started. Also, laboratory testing on soil samples is required for future design phases.

Due to the presence of loose sand, densification of the NUNA layer may be required before construction. Additionally, due to the thin clay or sand layers/lenses and the inconsistent thickness of the NUNAWO layer uneven settlements may be expected.

The region is known for static liquefaction of the external slopes of the foreshore. This is accounted for in regular evaluations of the flood defenses and, if needed, mitigating actions are taken. It may need re-evaluation for low likelihood events for a NPP. A stiff overconsolidated clay layer (“Potklei”) is present in the region, and is possibly encountered in the NUPE layer. This stiff clay layer may have a high horizontal soil stress. A denser CPT grid can determine the likelihood of encountering this clay layer within the region.

7 Subsidence, settlements and bearing capacity

This section gives an overview of the observed and potential causes of subsidence as well as settlement under load which may occur at the surface of the Eemshaven area.

7.1 Local causes of subsidence

Subsidence in this area can be broken down into a number of components:
1. Regional subsidence due to gas production from the Groningen gas field.

Subsidence due to gas production is significant in Groningen. This is due to the decline in reservoir pressure, which caused the rocks to compact and settle. The maximum total subsidence since the start of gas extraction some 60 years ago is estimated to be 0.46 m at the centre of the gas field (NAM, 2020; VEN B.V, 2020). Around the Eemshaven area this is in the order of 0.15 - 0.2 m.

A related effect is the depletion of pore pressure in aquifers surrounding the Groningen field, which contributes to additional surface subsidence. This is due to the compaction of the aquifers themselves (TNO & Deltares, 2022).

Gas production officially ceased in 2024 and subsidence rates are expected to decrease as the subsurface stabilizes. However, it is unknown how quick exactly subsidence rates will decline. Subsidence is expected to continue into the foreseeable future and is closely monitored by the government body that monitors mining activity (Staatstoezicht op de Mijnen, SodM). An extra 4-5 cm of subsidence is to be expected by 2080 (NAM, 2020).

2. Compaction of peat and clay layers

Due to their relatively high compressibility, peat and clay layers are rather susceptible to compaction. This applies in particular to relatively young (Holocene) clays and peats at shallow depth. Therefore, relatively small pore pressure reductions due to groundwater extraction or water table lowering can cause compaction (compression of the soil skeleton and loss or pore space) and land subsidence (STOWA, 2020). The same applies to small increases in overburden weight by sedimentation or by construction (landfill, buildings, infrastructure). Note that subsidence due to construction is often referred to as settlement, and may involve large loads (weight additions). Irrespective of the cause of compaction, the induced compaction and subsidence can be rather persistent, decreasing slowly over decades due to the slow dewatering of the compacting layers (consolidation) and soil creep. Apart from the presence of soft-soil layers (peat, clay), the recent historic development of the Eemhaven sites, notably reclamation from the sea and construction, therefore strongly determines the current subsidence condition associated with this subsidence component. Soft-soil layers (peat, clay) can be present in the Holocene formations of Naaldwijk and Nieuwkoop. Subsidence effects are expected to be stronger at the location of site 3 due to the thicker NUNAWO clay and possibly NUNI peat layers.

3. Decomposition of organic material

Under waterlogged conditions, organic soils such as peat are relatively stable. However, when organic soils are exposed to oxygen (aeration), microbial communities (bacteria, archaea, and fungi) break down the organic material. This process is often referred to as peat oxidation (STOWA, 2020). This decomposition results in the loss of organic matter, which is a critical component of the soil's structure and volume. As the organic material is decomposed, the volume of the soil decreases (directly by material loss and indirectly as the soil loses its ability to support the overlying load and compacts). This volumetric loss contributes to

subsidence. In the Eemshaven area, there is almost no possibility for peat oxidation as all the known peat layers are below the mean lowest groundwater level.

4. Glacio-isostatic adjustment (GIA)
GIA is a collective term that describes the dynamic response of the lithosphere-mantle system to mass changes on ice-age timescales. At the time of the last glacial maximum, the Eemshaven area had been uplifted due to the forebulge effect of the Weichselian ice sheet to the north. As the ice sheet began to melt during deglaciation, its weight was removed and the Earth's crust started to rebound. The forebulge in turn began to collapse as the ice mass decreased, leading to subsidence in most of the Netherlands and northern-Germany (Wallinga et al., 2004). The effect is still ongoing and is associated with subsidence rates of about 5 cm per century (Hijma & Kooi, 2018).

5. Tectonics and natural compaction of deep sedimentary layers
Tectonic effects are related to faulting and folding in the crust and cooling of the lithosphere, whereas compaction refers to the compression and porosity reduction of (deeper) sedimentary layers. In the Eemshaven area, these background effects constitute a subsidence rate of about 0.02 - 0.03 m/kyr (Hijma et al., 2025).

7.2 Measurements & models

The European Ground Motion Service (EGMS (copernicus.eu)) and the Bodemdalingskaart 2.0 (Bodemdalingskaart 2.0 (skygeo.com)) both show ground motion data on a local, national and continental scale with millimeter accuracy. They are derived from Sentinel-1 radar images at full resolution, on which a multi-temporal interferometric analysis (InSAR) is done. These data include both natural and anthropogenic ground motion.

Figure 7.1 shows the total ground motion for the north of Groningen and the Eemshaven area. Subsidence rates are typically 3.5 to 6 mm/year. Ground motion is relatively uniform in the area. Some local differences may be explained by differences in settlement of the landfill material and structures.

On a regional scale, ground motion in the area is dominated by subsidence due to gas extraction from the Groningen gas field. At least 3 mm/yr is explained by subsidence due to gas extraction from the Groningen gas field when using the figures reported by the NAM of 0.15 - 0.20 m since the start of production (NAM, 2020). Another 0.5 mm can be explained by GIA, which leaves up to 3 mm/year of subsidence that could be linked to other processes, such as compaction of peat and clay layers in the shallow subsurface. Note that at some locations ground motion measurements are related to human activities such as construction and moving objects on the location. Positive values of ground motion (uplift) and larger negative values consisting large steps in the InSAR time series are usually related to these types of human activities.

The *Climate Impact Atlas* (2023) shows subsidence scenarios – projections into the future - for different IPCC and water management scenarios. The subsidence includes contributions by peat oxidation, compaction of Holocene soft-soil layers due to water management (no construction effects), and mining (gas extraction and salt mining). Subsidence scenario ‘low’ is associated with IPCC scenario GL (limited climatic warming of 1 ºC in 2050 and 1.5 ºC in 2085), and water level fixation. This scenario is associated with relatively limited subsidence by peat oxidation and soft-soil compaction. Scenario ‘high’ is related to the IPCC WH scenario (larger climatic warming of 2 ºC in 2050 and 3.5 ºC in 2085), and water level indexation (water level periodically lowered in concert with soft-soil land subsidence). The conditions in this scenario lead to enhanced soft-soil subsidence relative to the ‘low’ scenario.

The subsidence scenarios indicate that in the Eemshaven area, up to 2050 and 2100, subsidence is expected to be limited: in the range of 3-10 cm (Figure 7.2). The maps do not allow discerning spatial differences of subsidence within this range. Moreover, since the aggregate subsidence is shown, the maps also do not provide information on the relative contribution of gas extraction and soft-soil subsidence in the prognoses.

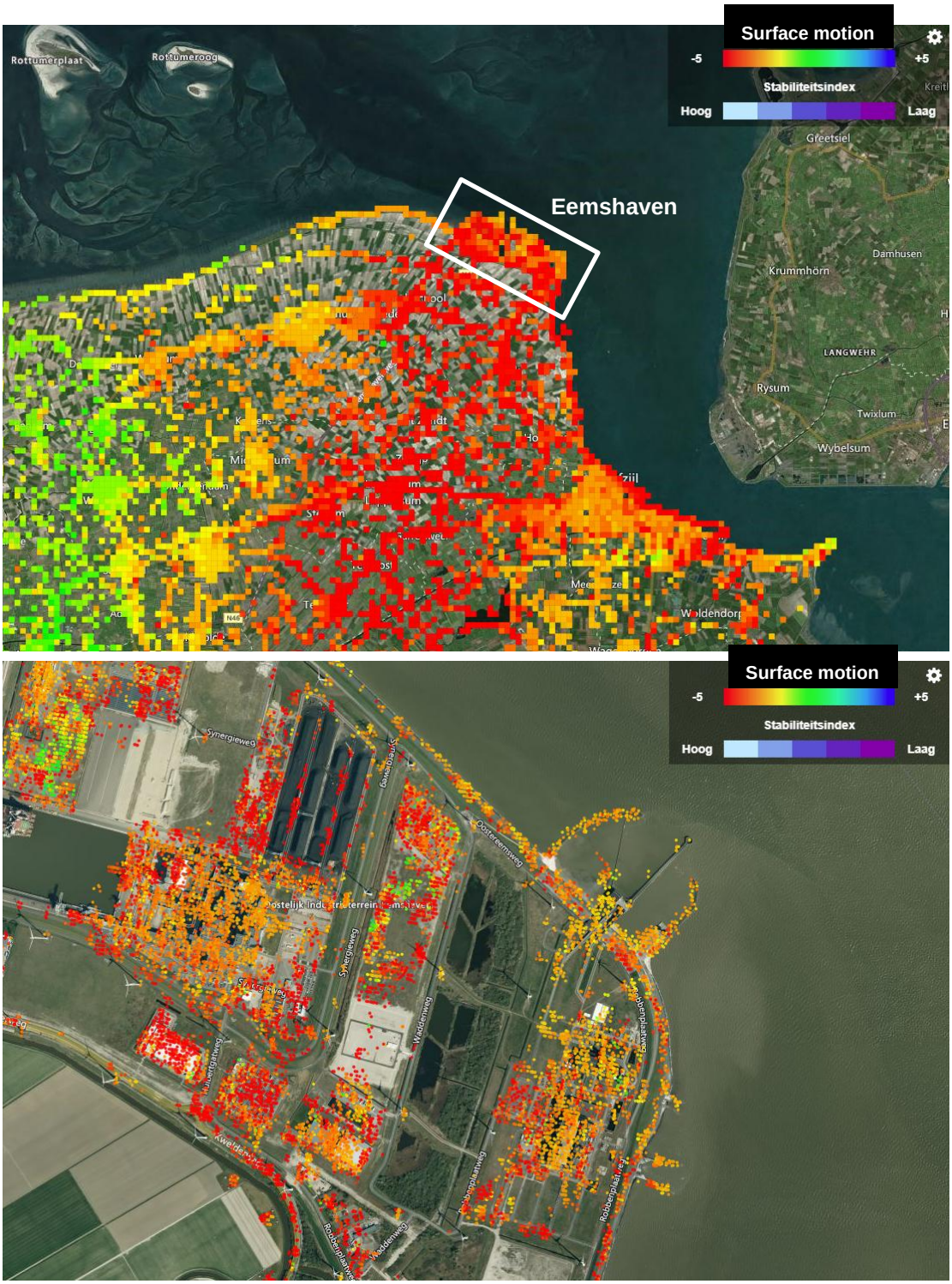

Figure 7.1 Magnitude of ground motion for the period October 2017 to October 2022 shown on the regional scale in the upper image and the local scale of sites 2 and 3 in the lower image (Bodemdalingskaart 2.0). The Eemshaven area subsides at a rate of 3.5 to 6 mm.

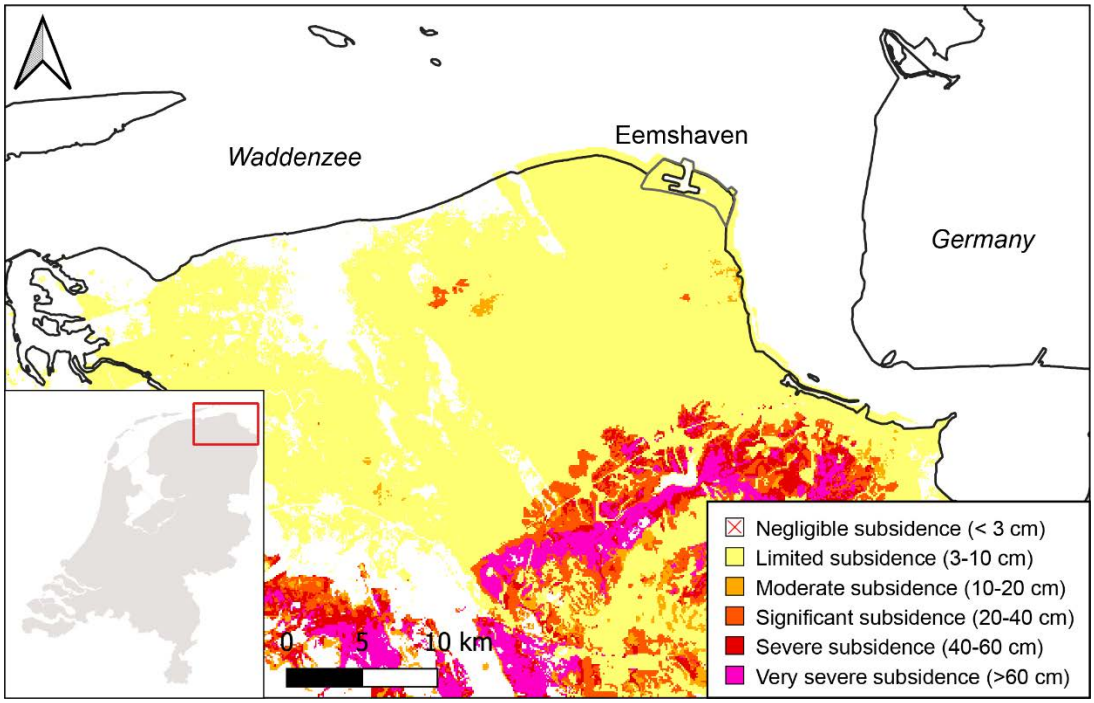

Figure 7.2 Map of the predicted subsidence in the Groningen Region for the period 2020-2100 for scenario 'low' (after Climate Impact Atlas, 2021). The predicted subsidence for the Eemshaven area and surrounding region is in range of 3 to 10 cm.

7.3 Settlements

This section provides a first assessment of the potential settlement of the building at the three sites in the Eemshaven. The objective of the settlement calculations is to get a first estimate (order of magnitude) of the settlements to be expected when building a power plant at the envisaged locations.

7.3.1 Building dimensions

The final building dimensions will be determined by the vendors. For the first estimate of the settlement and bearing capacity the following building dimensions are used:

- Length: 100 m.
- Width: 60 m.
- Basement depth: 15 m below ground level.

The load at foundation level was provided by the client as 690 kPa. This is equivalent to roughly 27.5 m of solid reinforced concrete.

Additionally, it is assumed that the local ground level will be raised from the current ground level to a platform height of NAP + 8 m before building construction starts. Raising will be done with well compacted sand.

According to the information provided, the building will be founded on a shallow foundation, i.e. no piled foundation is used. Installation of piles is considered by one or more vendors. However, these piles will not be used as a direct foundation, but with the objective to enhance strength and stiffness of the subsurface. The top of these piles will be below the foundation level of the reactor building. The building will not rest directly on these piles. For the present analyses the presence of these piles will be ignored.

7.3.2 Locations

At the Eemshaven location three sites are considered. Site 1 is located at the western part of the industrial area, partly located at the industrial area and partly in the polder. Present ground level of the industrial part is at NAP + 4.4m and for the polder area at NAP + 1.0 m.

Site 2 and 3 are located at the eastern part of the industrial area. Present ground level for site 2 is partly at NAP + 4.4 m and partly at NAP + 2.5 m. Present ground level for site 3 is at NAP + 2.5 m.

The top layer at the industrial area consists of anthropogenic sand. Below this the subsoil consists of a sandy layer with interbedded clay. This layer may be partly a tidal deposit with laminated sand-silt/clay layers. Between NAP - 10 m and NAP and NAP – 14.5 m a layer (NUNAWO) consisting of clay is present. This layer is partly missing at site 2. Below NAP – 14.5 m the subsoil consists mainly of sand. At site 2 and 3 potclay is present, at a depth between approximately NAP – 53 m and NAP – 59 m.

At the considered locations several combinations of subsoil conditions and present ground level are present. To limit the number of the indicative calculations the following situations will be analysed. These are encompassing the possible variations:

- Site 1: Polder, GL = NAP + 1 m, top of NUNAWO layer at NAP – 15 m.
- Site 2: GL = NAP + 2.5 m, settlement: NUNAWO layer present, potclay layer.
- Site 3: GL = 2.5 m, top of NUNAWO at NAP – 10 m, potclay layer.

Reasoning behind this selection is that:

- Site 1: a low present ground level will give a large thickness of the additional fill, therefore this situation is considered to be decisive.
- Site 2: here the NUNAWO layer is partly absent, as the situation with the NUNAWO layer is conservative only this situation is considered.
- Site 3: here the top of the NUNAWO layer varies over the area. Since founding the reactor building directly on the thick clay layer is not logical, the situation of a high top level of the NUNAWO layer is not considered.

7.3.3 Building timeline

For the analyses the following timeline will be used:

- Year 0: start preparation site, increase surface level to desired platform height of NAP +8 m by applying a well compacted sand layer.
- Year 1-3: consolidation time, to limit the residual settlements due to backfilling area to required platform height.
- Year 3: start construction of the civil works. (among others: building the concrete structures).
- Year 8: start installation turbine etc.

7.3.4 Calculation methodology

The settlement calculations are performed with the program D-Settlement of Deltares.
The new reactor building is modelled as a vertical load at foundation level (15 m below ground level). This is below ground water level, so the structure experiences an upward force due to the groundwater pressure at foundation level. The applied net load at foundation level is therefore reduced to consider this upward force. The load is applied such that the total vertical stress at foundation level (GL – 15 m) equals the surcharge load.

Figure 7.3 provides the cross sectional setup of the model, while Figure 7.4 provides the top view of the load. The settlements are computed at the centre of the building, i.e. point 2 in Figure 7.4.

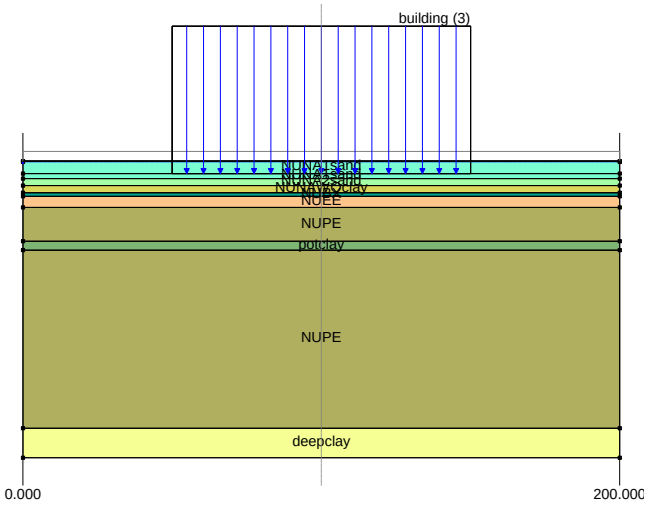

Figure 7.3 Cross section of applied load, modelled depth is 200 m, sediment layering varies for the three locations considered.

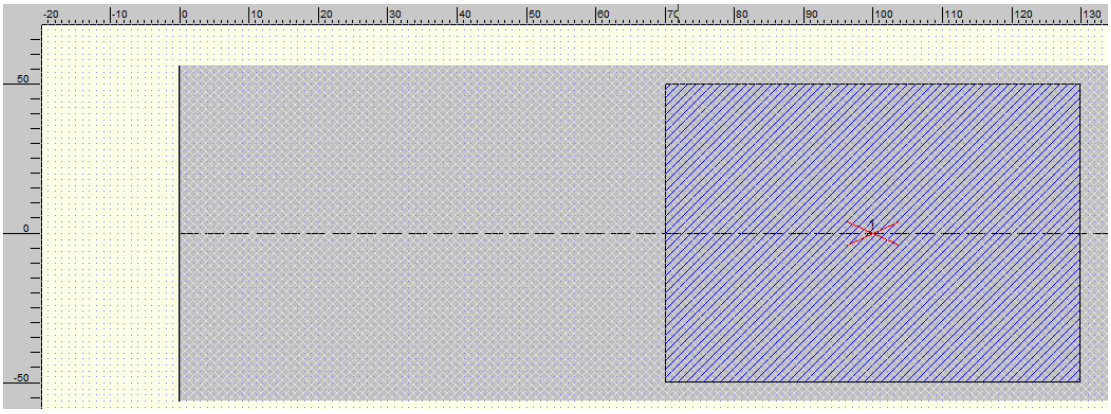

Figure 7.4 Top view of applied load, the red asterisk indicates the point for which the settlements are calculated.

7.3.5 Settlement parameters

The settlement parameters are taken from the geotechnical parameter selection (see Section 6.3). However, the contribution of the deeper clay layers (below NAP – 30 m) cannot be ignored for the calculation of the total settlement. No sufficient information on the properties of these layers is available. Therefore, some assumptions are made.

The depth and thickness of these layers are selected using the geological description. The settlement parameters are selected based on the given soil description and, in absence of a qualitative description, values from NEN-9997-1 for clay are used. The Dutch code NEN-9997-1 combines the Eurocode NEN-EN 1997-1 and the Dutch national annex.

For the Potclay layer no settlement parameters are available. Settlement behaviour of this will greatly depends on the overconsolidation ratio (OCR). As these layers are of older age overconsolidation, e.g. due to aging, is expected to be present.

For the settlement calculations the following parameters for this layer are used:

- A low value for the creep (C_α) is used.
- The clay layers are assumed to be overconsolidated, OCR = 2 is used.
- For CR (= Cc/(1 + e0)) the values for stiff clay are used.
- For RR a value of CR/RR = 5 is selected, this differs from the ratio used in the Dutch code NEN-9997-1, but is believed to better represent the settlement for stresses below the pre-consolidation stress; this resulted in RR = 0.02.

For the Site S1 SE, a layered sand layer between NAP – 4 m and NAP – 23 m. For the calculations a weighted average of the settlement parameters for sand and clay is used, assuming that 20% of the layer consists of clay and 80% of sand.

7.3.6 Calculated settlement

For the settlement calculations, the deep subsurface, to a depth of NAP – 200 m, is modelled, as shown in Figure 7.3. For the top layers the soil layering is taken from the given geotechnical soil profile. The layering of the deeper layers is taken from the geological profiles. No data on the settlement parameters of the deep clay layers are available. For the calculations parameters for a stiff clay are used.

The construction time of the reactor building is taken into account by applying the load in four steps with a 1-year interval. The settlement as function of time at foundation level is shown in Figure 7.5 to Figure 7.7 for the three sites. Figure 7.8 to Figure 7.10 provide the settlement as a function of depth, indicating the contribution of the various soil layers.

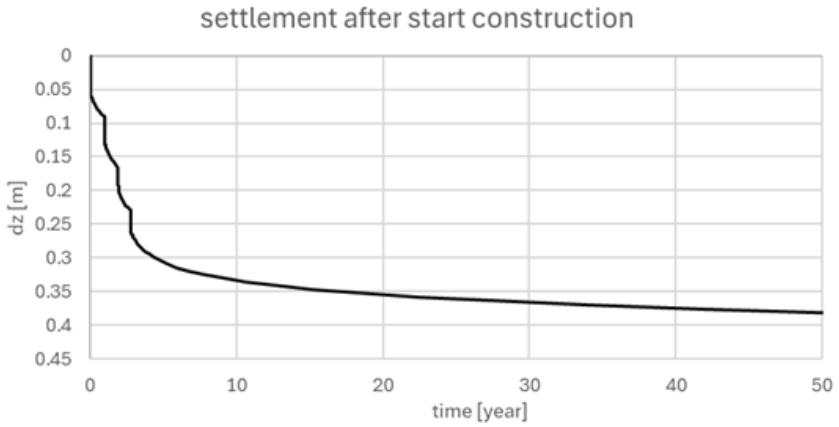

Figure 7.5 Settlement-as function of time at foundation level (z = NAP – 7 m), Site 1. t = 0 years represents the start of the preparation of the site.

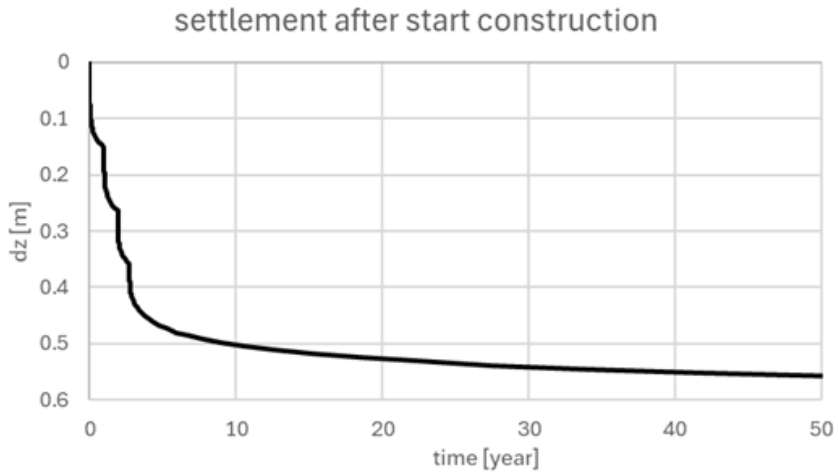

Figure 7.6 Settlement-as function of time at foundation level (z = NAP – 7 m), Site 2. t = 0 years represents the start of the preparation of the site.

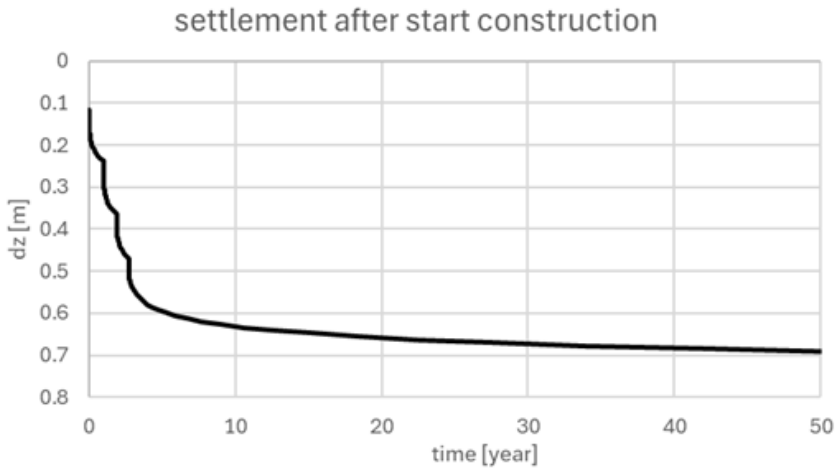

Figure 7.7 Settlement-as function of time at foundation level (z = NAP – 7 m), Site S3. t = 0 years represents the start of the preparation of the site.

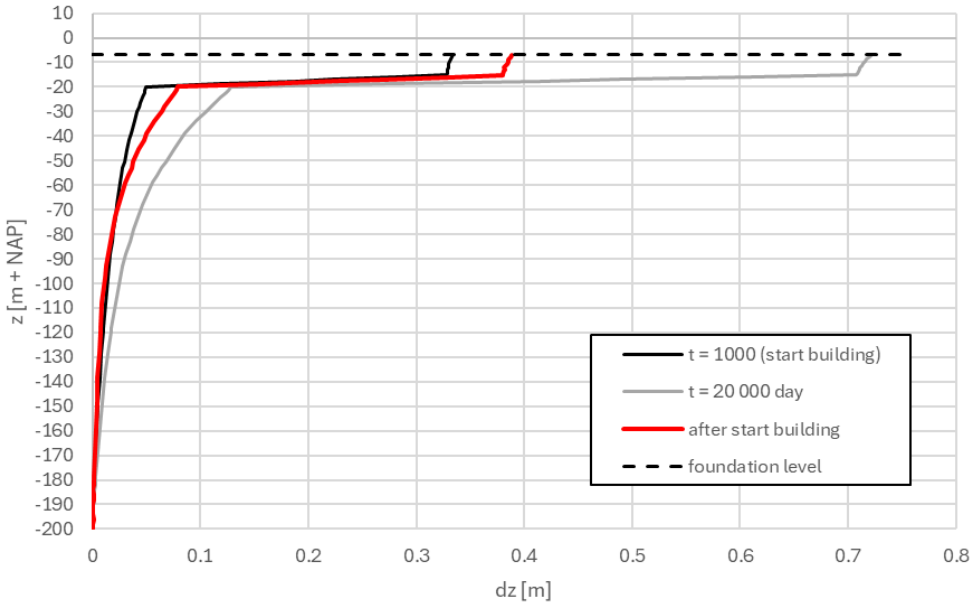

Figure 7.8 Settlement as function of depth, Site 1. The red line indicates the additional settlement since the construction of the building, i.e. the difference between the gray and black lines. The dashed line is the foundation level (NAP – 7 m).

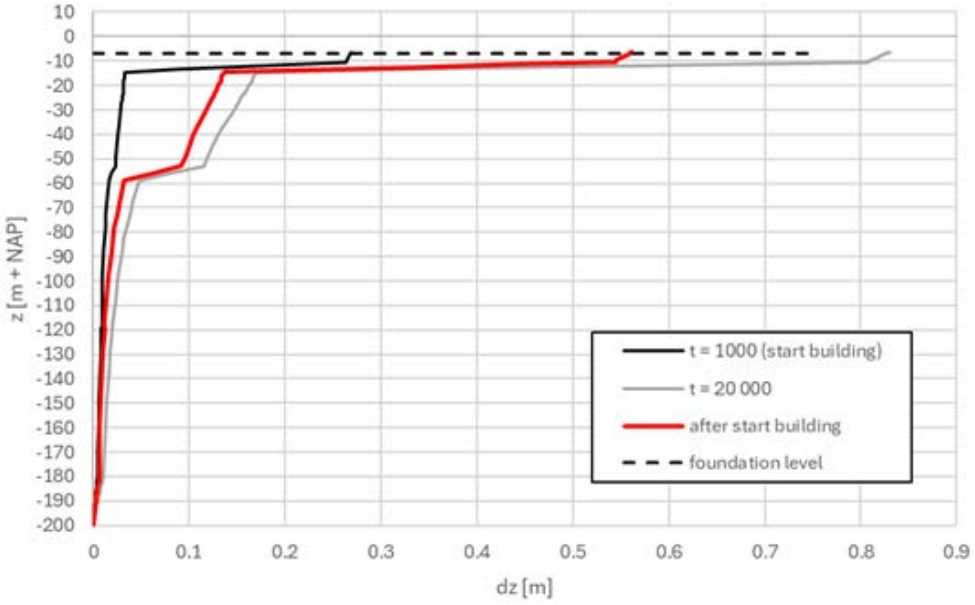

Figure 7.9 Settlement as function of depth, Site 2. The red line indicates the additional settlement since the construction of the building, i.e. the difference between the gray and black lines. The dashed line is the foundation level (NAP – 7 m).

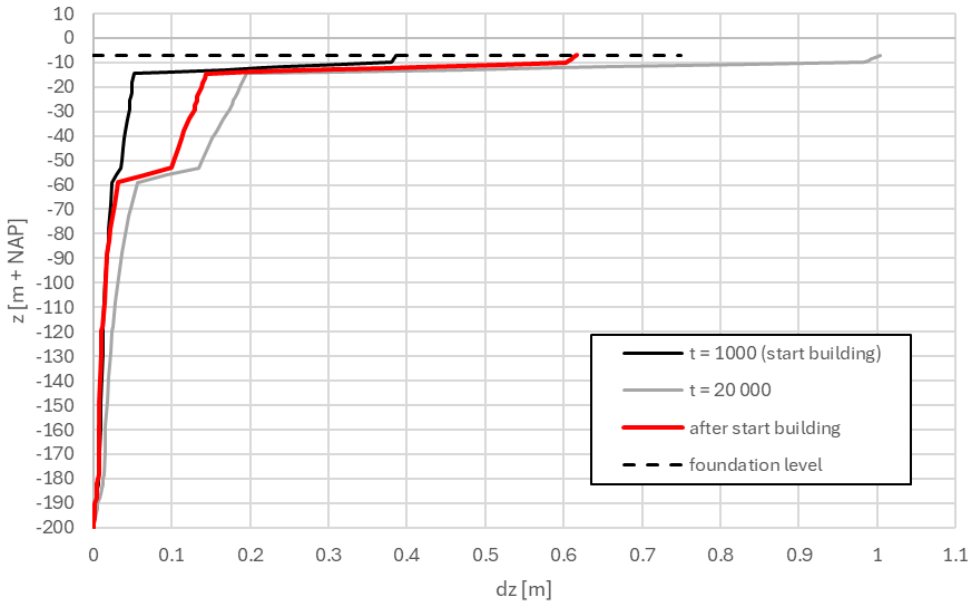

Figure 7.10 Settlement as function of depth, Site S2. The red line indicates the additional settlement since the construction of the building, i.e. the difference between the gray and black lines. The dashed line is the foundation level (NAP – 7 m).

The resulting settlements of the reactor building 30 years after start of building are:

- Site 1, polder: 0.36 m.
- Site 2, situation with NUNAWO layer: 0.53 m.
- Site 3: 0.67 m.

For site 2 there will be a large difference in settlement for the area with and without the NUNAWO layer, which has the largest contribution to the settlements at all three sites. At site 2 large differential settlements are therefore expected when the power plant is constructed. The thickness of the NUNAWO layer varies at site 1 and 3, so differential settlements may also be expected at these locations. For site 2 and 3 the potclay layer contributes about 0.1 m to the total settlement.

7.4 Bearing capacity

The objective of these bearing capacity calculations is to estimate the bearing capacity of the subsurface, and the result may be used to decide whether a non-piled foundation may be used or if a piled foundation is needed.

The assumed building dimensions and building timeline are provided in sections 7.3.1 and 7.3.3

7.4.1 Locations

At the considered locations several combinations of subsoil conditions and present ground level are present, see section 7.3.2. To limit the number of the indicative calculations the following situations will be analysed. These are encompassing the possible variations.

- Site 1: Polder, GL = NAP + 1 m, top of NUNAWO layer at NAP – 15 m.
- Site 2: GL = NAP + 2.5 m, bearing capacity: NUNAWO layer absent.
- Site 3: GL = 2.5 m, top of NUNAWO at NAP – 10 m, potclay layer.

Reasoning behind this selection is that:

- Site 1: a low present ground level will give a large thickness of the additional fill, therefore this situation is considered to be decisive.
- Site 2: here the NUNAWO layer is partly absent, as the situation with the NUNAWO layer is comparable to site 1 only the situation without the NUNAWO layer is investigated.
- Site 3: here the top of the NUNAWO layer varies over the area. Since founding the reactor building directly on the thick clay layer is not logical, the situation of a high top level of the NUNAWO layer is not considered.

7.4.2 Calculation methodology

For the bearing capacity calculations, the foundation of the structure will be considered as a shallow foundation. Bearing capacity will be assessed using the Brinch-Hansen approach, as described in the governing Dutch geotechnical code (NEN-9997-1). In the present calculations any horizontal load, e.g. due to wind, is not taken into account.

According to the Dutch code NEN-9997-1 the settlement of the building should be within certain limits. For this report the check on settlement is omitted when checking the bearing capacity, as these settlements are already calculated in Section 7.3.

The calculations are performed with the software program D-Foundation of Deltares.

7.4.3 Soil parameters

The used soil parameters are taken from the geotechnical parameter selection, see Section 6.4. For the deeper soil layers an estimate is made, using the given soil description.

In the calculations the applicable partial factors, as prescribed in NEN-9997-1, are used. These are:

- Angle of internal friction: 1.15.
- Effective cohesion: 1.6.
- Undrained shear strength: 1.35.

No partial factor on the load is applied as these calculations are for comparative purposes.

7.4.4 Bearing capacity calculation

For the bearing capacity calculations three vertical profiles of sedimentary successions are considered. The difference between the considered vertical profiles is the soft layer at NAP – 15 m, which is not present over the total area. Figure 7.11 (Site 1), Figure 7.12 (Site 2) and Figure 7.13 (Site 3) show the used sedimentary successions and their properties.

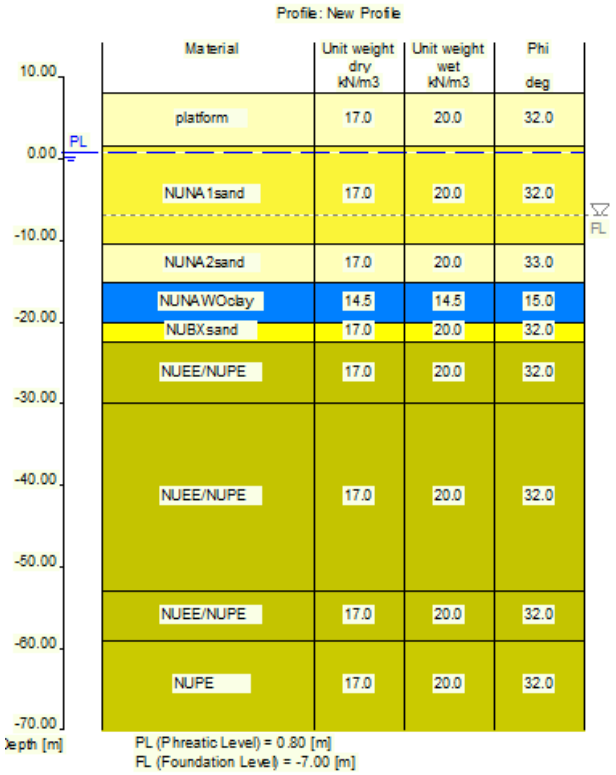

Figure 7.11 Sedimentary layering used in bearing capacity calculation, Site 1.

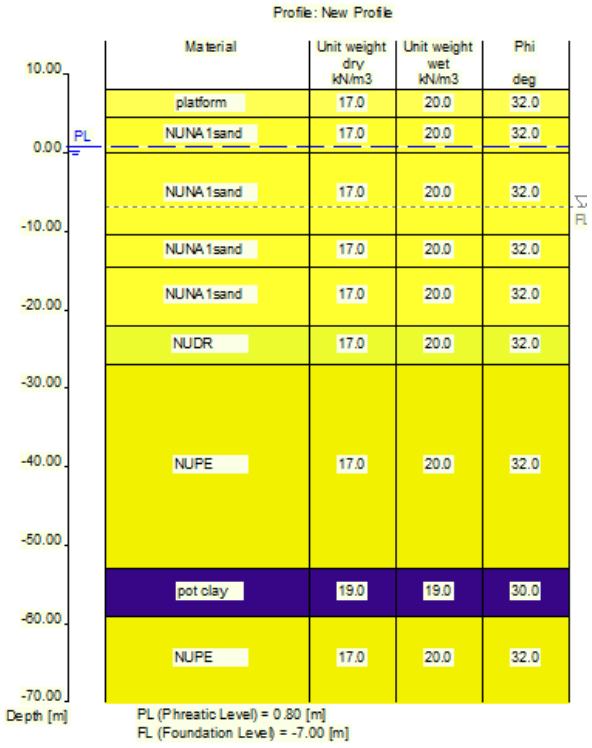

Figure 7.12 Sedimentary layering used in bearing capacity calculation, Site 2.

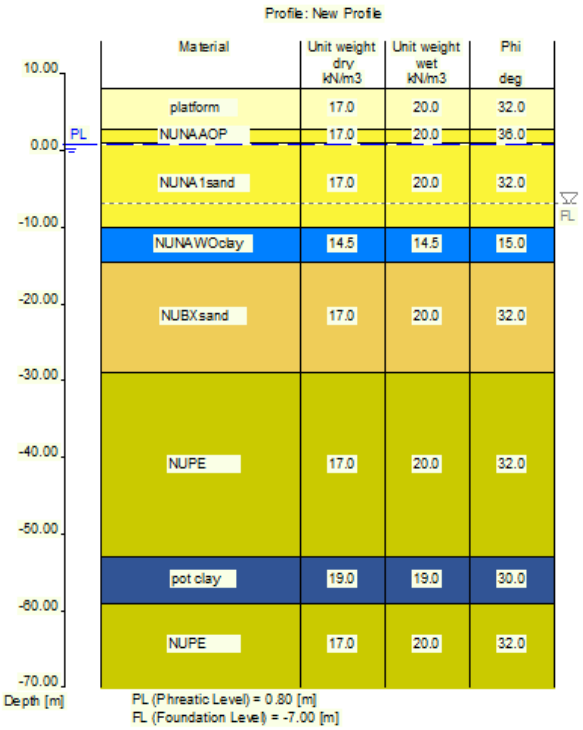

Figure 7.13 Sedimentary layering used in bearing capacity calculation, Site 3.

The following values for the total bearing capacity are calculated:

- Site 1, q = 406 kPa.
- Site 2, q = 1031 kPa (situation without the NUNAWO layer).
- Site 3: q = 392 kPa.

From the calculations it follows that the bearing capacity is governed by the punch-trough mechanism of the soft NUNAWO layer. The bearing capacity is mostly below the required bearing capacity. Only for the part of site 2 where the NUNAWO layer is absent the bearing capacity is sufficient. This implies that ground treatment of the NUNAWO layer is required or that a piled foundation is needed. Such a treatment will also reduce the total expected settlements.

8 Seismic hazards

8.1 Faults in the vicinity of Eemshaven

The Eemshaven site is located on the northern coast of the Netherlands and lies on top of the stable Groningen Platform intra-basinal high (Huis in ‘t Veld and Den Hartog Jager, 2025). This part of the Netherlands is not known as a region with natural seismicity (Dost et al., 2025). However, induced seismicity resulting from gas extraction from the Groningen gas field is prevalent in the region. This chapter represents a short overview of seismicity in a greater regional framework. For a recent, more detailed description of seismicity in the Netherlands, we refer to Dost et al. (2025).

Regionally, the European Fault-Source Model 2020 (EFSM; Basili et al., 2022) does not indicate any nearby naturally active faults. At 200 km distance, the nearest known active faults are the eastern bounding faults of the Roer Valley Graben (RVG) in the southeast of the Netherlands (Figure 8.1). On the eastern side of this actively subsiding region, the Peel Boundary Fault is located 200 km away. The most recent major earthquake along this fault line was in 1992 when near Roermond (250 km from Eemshaven) a 5.8 magnitude earthquake occurred at depths of 15 km. The northernmost end of the Viersen Fault, located to the east of the Peel Boundary Fault close to the border with Germany, is 210 km away and the nearest point of the Gilze-Rijen Fault on the western side of the RVG is located approximately 230 km from Eemshaven.

Within 300 km from Eemshaven, seismicity on the southern North Sea should also be considered. Regional scale tectonic stress patterns for the North Sea are controlled primarily by post-glacial rebound, and far-away drivers such as ridge push forces from the Mid-Atlantic Ridge and subduction forces from the African-Eurasian plate Boundary (Kettlety et al., 2024). Although the North Sea is tectonically in a relatively stable position with few recorded events, some larger events have been recorded (M > 6), particularly in the Norwegian sector. However, the largest earthquakes recorded within 300 km from Eemshaven have reached $M_L = 4$. These events were recorded about 250 km to the northwest of Eemshaven.

Induced seismicity due to gas extraction in the Groningen gas field is important to consider for the Eemshaven sites. The seismicity in the Groningen field is characterized by clustering around large faults in the producing reservoir at a depth of approximately 3 km (Figure 8.2). Over 1500 events of $M_L > 1$ have been linked to gas production since the 1980’s. The most notable event was the Huizinge earthquake in 2012, with a magnitude of $M_L = 3.6$, about 15 km to the southwest of the Eemshaven (Dost et al., 2025). Following this event, a greatly improved seismic monitoring network was installed in the Groningen region, allowing to record smaller magnitude events. In addition, gas extraction from the Groningen gas field was reduced and eventually fully stopped in 2024. Where the probability of an earthquake in the central part of the Groningen field with a magnitude of $M_L > 4$ was 5.5% before 2018, it has since declined to 1% in 2025 (Staatstoezicht op de Mijnen, 2025).

Risks associated with induced seismicity, such as the liquefaction potential, is discussed in the following section.

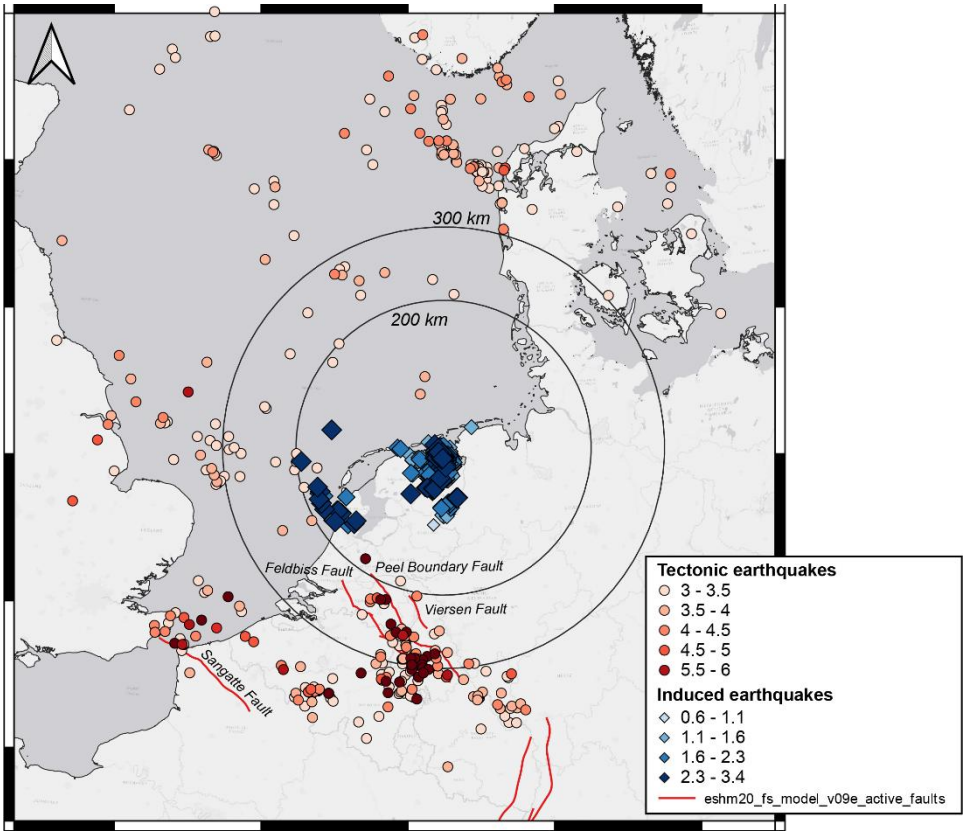

Figure 8.1 Regional map of earthquake activity (colored circles and diamonds) and active faults (red lines). All earthquake intensities (induced and tectonic) are given as Richter scale values. Indicated are 200 km and 300 km equidistance lines surrounding the Eemshaven location.

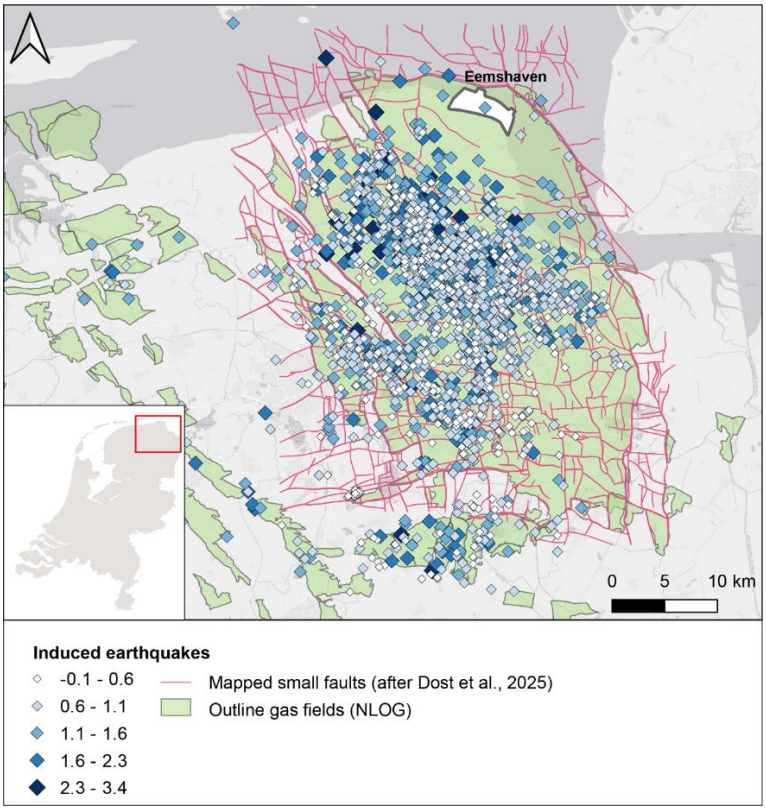

Figure 8.2 Overview of induced seismic events related to the Groningen gas field. Adapted from Dost et al. (2025).

8.2 Initial assessment of liquefaction potential

8.2.1 Induced earthquakes

An extensive investigation was executed in Groningen (including the Eemshaven) to determine the effects of induced earthquakes, where also the impact of liquefaction was studied. The results are summarized by NEN for the NPR 9998 on the online webtool NPR 9998 (NEN, 2020). Due to the stopped gas extraction, the induced earthquake hazard decreases. The current version of the dataset (2020-07-01) includes predictions valid for the time frame 2023 to 2029, with a maximum return period of 2475 years. This return period is equivalent to a 50 yearly probability of exceedance of 0.02 or a yearly probability of exceedance of $4*10^{-4}$. This results in a PGA at ground level between 0.065 and 0.085 g in the vicinity of the Eemshaven, see Figure 8.3.

Figure 8.3 Overview of the PGA at ground level for a return period of 2475 years based on the data of the NPR9998 webtool (NEN, 2020).

The webtool also provides a liquefaction potential analysis based on CPT data, where the liquefaction potential index (LPI) for a return period of 2475 years is provided. LPI is an index reflecting the combined liquefaction potential of all soil layers. Figure 8.4 highlights the results of the data of the webtool. All points in the Eemshaven compute an LPI below 0.5. An LPI of 5 corresponds to a low liquefaction potential, i.e. the liquefaction potential of the Eemshaven is very low. Additionally, most points in the Eemshaven compute an LPI = 0, i.e. none of the layers are prone to liquefaction given a 2475 return period earthquake. No earthquake loads for a longer return period are assessed, but the expected liquefaction potential is low based on the low LPI and the future reduction of induced earthquake loading since the stopped gas extraction.

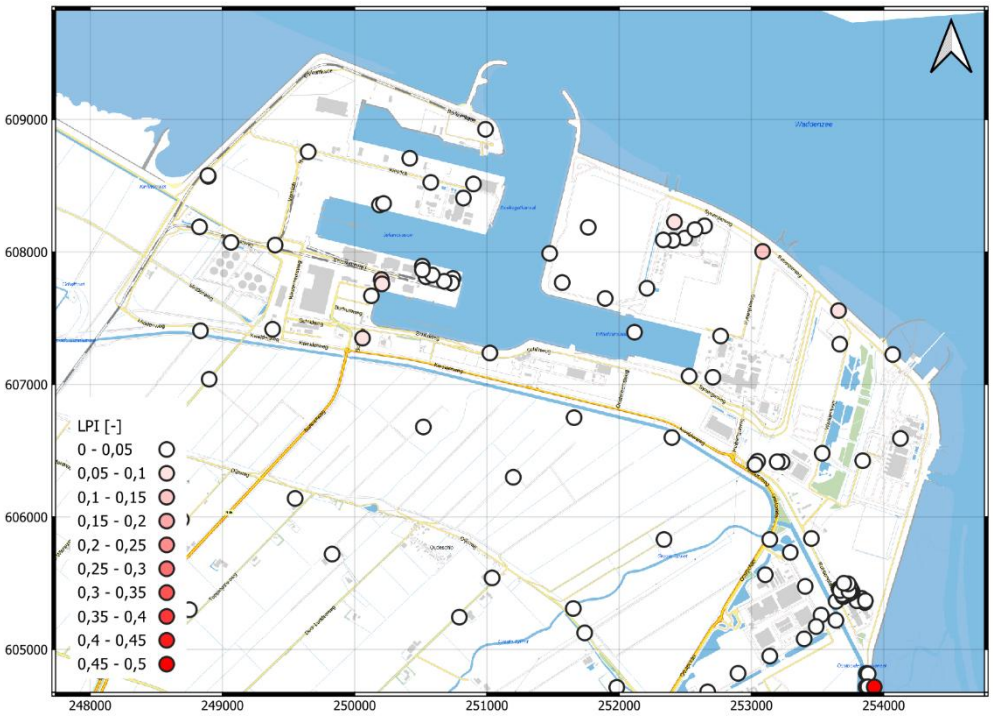

Figure 8.4 Overview of the liquefaction potential index (LPI) for a return period of 2475 years based on the data of the NPR9998 webtool (NEN, 2020). An LPI below 5 indicates a low liquefaction potential.

8.2.2 Tectonic earthquakes

As no results of a recent site-specific seismic hazard analysis are available, indicative values for the seismic loading are used. Note that a full Probabilistic Seismic Hazard Analysis according to the latest scientific standards and SSHAC recommendations is recommended. The properties used are derived from the hazard curve shown in Figure 8.5. The vertical lines indicate a PGA of 0.007, 0.025 and 0.09 g at bedrock level, which correspond to yearly probability of exceedance of 10^{-4},10^{-5} and 10^{-6} respectively. Due to this very low tectonic earthquake loading, especially when compared to the induced earthquakes, no further investigation is performed.

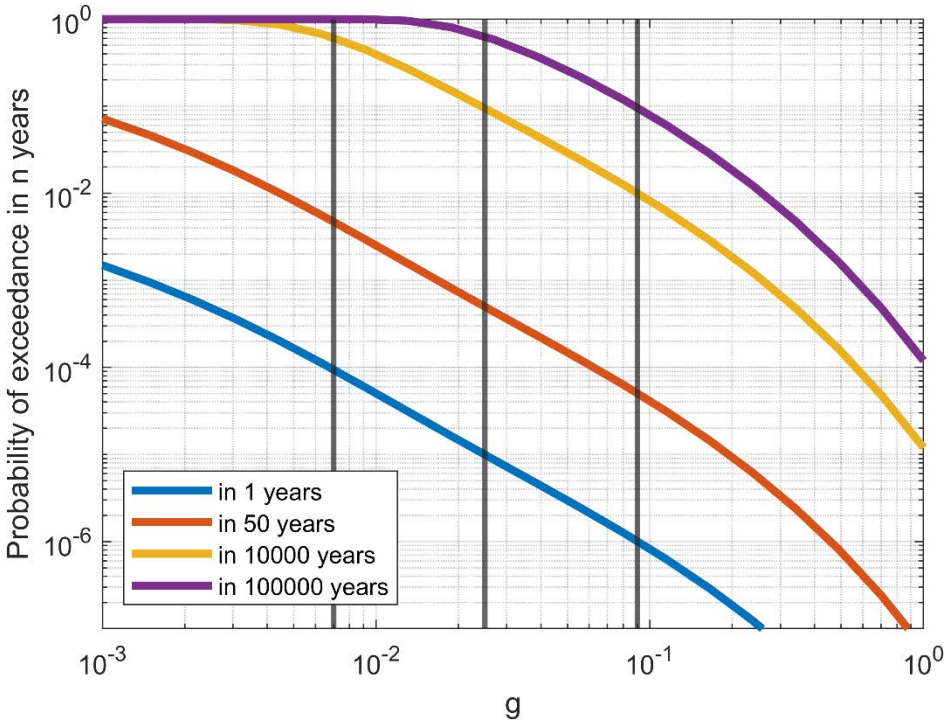

Figure 8.5 PGA Hazard Curves for the Eemshaven. Derived from the publicly available European Seismic hazard model ESHM20 (Danciu et al., 2021). The curves have been derived with the following settings: Longitude 6.782, Latitude 53.400, ESHM20, PGA, rock_vs_30_800ms-1 and the arithmetic mean.

9 Volcanic risks

No volcanic activity is known to have taken place in the Netherlands during the last 10 Ma (Ten Veen et al., 2025). In this section we will discuss the nearest regions that were volcanically active during the Holocene and Pleistocene. This is far from a complete study on all volcanic activity in northwestern Europe, but within the scope of the current report it provides first insights towards a potential volcanic hazard risk assessment for the Eemshaven sites. All volcanic centres that are discussed below are over 350 km from the Eemshaven sites. Only distal effects are likely to reach the Eemshaven site in case of an eruption at one of these known volcanic areas.

9.1 Western and Eastern Eifel Volcanic Fields

The nearest volcanoes are the West and East Eifel Volcanic Fields in Germany. These fields are located respectively 365 km and 340 km to the south of Eemshaven, respectively. The West Eifel Volcanic Field is located southwest of Bonn and the East Eifel Volcanic Field is situated approximately 40 km to the northeast (Van den Bogaard & Schmincke, 1985).

Volcanic activity in the West and East Eifel Volcanic Fields took place during the early parts of the Neogene, approximately until the late Miocene. After a quiet period, volcanic activity restarted in the Quaternary at 850 ka. The last eruption of the East Eifel Volcanic Field was due to the Laacher See volcano at approximately 12.9 ka. The last eruption of the West Eifel Volcanic Field was approximately 11 ka due to the Ulmener Maar (Förster & Sirocko, 2016; Hensch et al., 2019). Given this relatively recent age, these volcanic fields are considered active on geological time scales according to the IAEA guidelines (International Atomic Energy Agency, 2012).

The West Eifel Volcanic Field contains scoria cones, maars (tuff rings) and small stratovolcanoes. The East Volcanic Field contains scoria cones, maars, lava flows and the three larger caldera complexes of Wehr, Rieden and Laacher See volcano (Förster & Sirocko, 2016). Therefore, volcanic phenomena which occurred could be amongst others tephra fall out, lava flows, slumps triggered by volcanic earthquakes or base surges. Tephra fall out is one of the volcanic phenomena which can have relatively large travel distances. During the large eruption of the Laacher See volcano about 20 km^3 of tephra was produced (Global Volcanism Program, 2023). Figure 9.1 shows the different lobes of the tephra deposits of the Laacher See volcano, which can be found close to the border of the province of Limburg in the southeasternmost part of the Netherlands. Maps of the areal distribution of ash layers in Van den Bogaard and Schminke (1985) show similar patterns as in Figure 9.1.

All other volcanically active regions in Europe are schematically indicated in Figure 9.2. These are all located farther from Eemshaven and include the volcanoes at the Massif Central in France (~900 km) and the Icelandic volcanoes (~1800 km). Because historically only minor effects have been recorded in the Netherlands from these locations, we will only briefly mention them.

9.2 Chaîne des Puys

Holocene volcanic activity has taken place in the Chaîne des Puys, situated in the Massif Central, France. This chain consists of 80 cinder cones, maars and lava domes. Latest volcanic activity occurred at approximately 8.6 ka during the eruption of the La Vache and Lassolas cone complex. This was also one of the most powerful eruptions of the Chaîne des Puys. Tephra and lava flow deposits of this eruption were found in the surrounding dozens of kilometers within the Chaîne des Puys (Jordan et al., 2016).

9.3 Icelandic volcanoes

Effects of eruptions of Icelandic volcanoes such as the eruption of the Eyjafjallajökull volcano in Iceland in 2010 were relatively limited in the Netherlands. This eruption led to disruption of the air traffic in Europe due to the large volcanic ash cloud (>8 km height) (Petersen et al., 2012). The size of the ash particles that reached northwestern Europe were only submillimeter to tens of nanometers in size (Gislason et al., 2011).

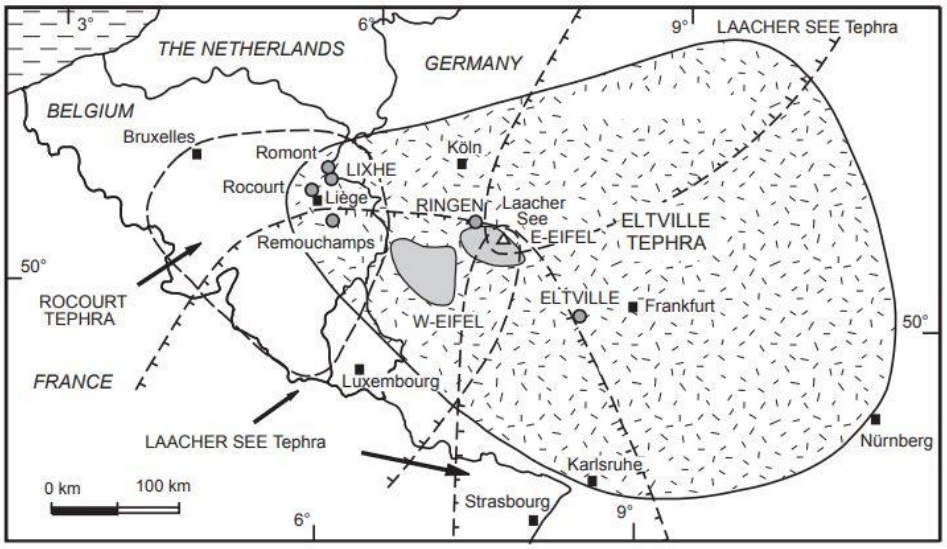

Figure 9.1 Lobes of the Lacher See tephra deposits (Pouclet & Juvinge, 2009).

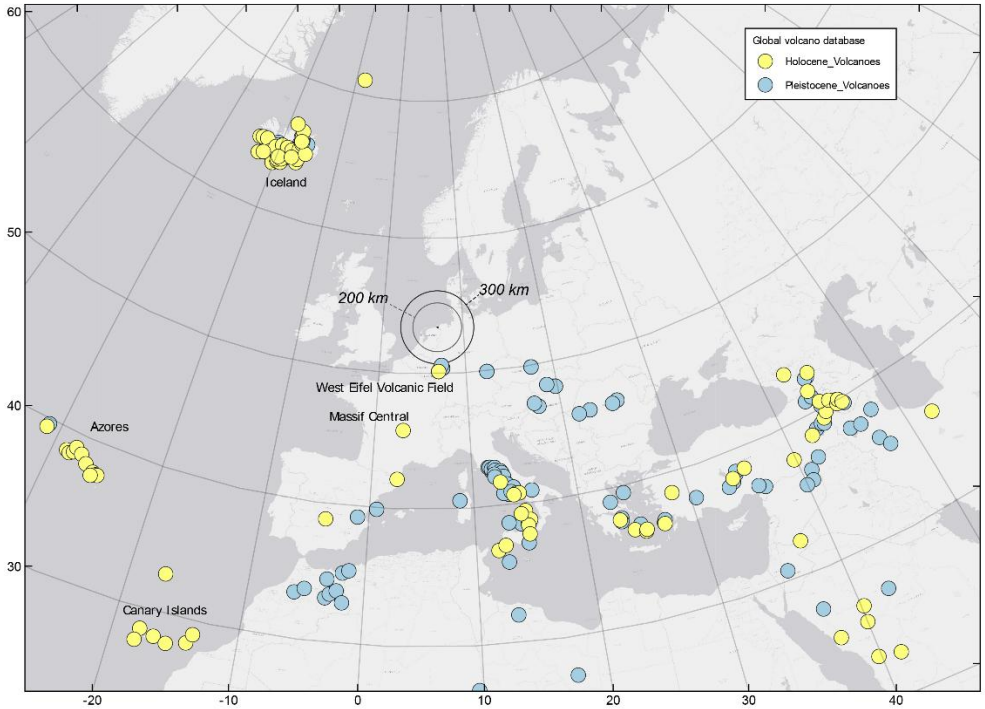

Figure 9.2 Holocene and Pleistocene volcanoes in and around Europe, based on the Smithsonian Institution's Global Volcanism Program database. Indicated are 200 km and 300 km buffers around the Eemshaven sites.

10 Conclusions and recommendations

10.1 General

A combined analysis of available regional geological models, hydrogeological models, boreholes, CPT data and additional sources from literature was carried out to characterize three potential sites in and around the Eemshaven for building a nuclear power plant (NPP). The site evaluation focused on the buildup, geohydrological and geotechnical properties of the subsurface. In addition, we also addressed potential hazards associated with subsidence, seismicity and volcanic activity. With respect to the latter three, no major upfront constraints for the development of Eemshaven were identified.

The results presented in this report should be used as starting point for planning additional subsurface research, for assigning geotechnical properties to geological units and for more advanced geostatistical risk analysis when new data comes in.

10.2 Site characterization

Geological build-up
Marine sediments coarsen upwards from clay to fine to medium sands between -500 and -120 m NAP, followed by predominantly medium to coarse fluvial sands at depths between -120 and -40 m NAP. Between ~ -40 and -20 m NAP there are mainly Late-Pleistocene glaciofluvial, fluvial and aeolian sands that are quite coarse and often contain some gravel. The top 20 m of natural deposits consists of various Holocene tidal deposits and comprises a heterogeneous sequence of mostly fine to medium sand that is more clayey at the base.

Until construction began in the early seventies, the present-day Eemshaven port was located on a mudflat along the Eems-Dollard estuary. This mudflat was reclaimed for the construction of the port and was covered by a landfill of up to 6 m. The land fill material is sand that was locally sourced from the Wadden Sea and Eems-Dollard estuary, but may contain more silty and clayey layers and/or lenses.

Cross sections
A total of six geological cross sections, two for each of the three potential NPP sites, were produced based on an analysis of available CPT, borehole and model data. The cross sections cover the subsurface down to a depth of -40 m NAP. The most important findings based on the cross sections are:

- The early-Holocene Wormer clay layer is thinner (1 - 2 m) and sandier in the west (site 1, cross sections 1 and 2) and thicker and more purely clay in the east. In the South of site 3 (cross section 4) the Wormer clay is up to 10 m thick. This is a new finding that is not properly captured in existing geological models.
- In some places, most notably site 2, the Wormer clay as well as some of the underlying Boxtel sands were completely eroded by Middle-Holocene tidal channels. The presence of these channels is a new finding that is not captured in existing geological models.
- Pleistocene units, despite being distinctly different in terms of their depositional history, are difficult to distinguish in CPTs and boreholes as they mostly consist of (sometimes gravelly) medium to coarse sand.
- Although the Middle to Late Holocene tidal deposits dominantly consist of sand, they are often silty/clayey and/or laminated with thin (cm-scale) silt/clay layers.

Ground motion & seismicity
InSAR measurements of surface motion show subsidence rates of around 3.5 to 6 mm/year for all three potential NPP sites in the Eemshaven area. Subsidence in the area is for the

most part caused by gas extraction from the Groningen gas field. The area has been subjected to about 15 to 20 cm of subsidence since the early sixties when production started, which translates to about 3 mm/year. Although gas production ceased in 2024, the associated subsidence will continue into the foreseeable future with another 4 to 5 cm of subsidence to be expected by 2080. Compaction of clayey strata within the Holocene sequence may contribute to the present and future subsidence. This subsidence may vary both amongst the three potential sites and within individual sites due to marked spatial differences in clay thickness. Glacio-isostatic adjustment is a minor and spatially uniform subsidence component in the area.

Seismicity in the Eemshaven is also related to the Groningen gas field. The seismicity in the Groningen field is characterized by clustering around large faults in the producing reservoir at a depth of approximately 3 km. Over 1500 events of $M_L > 1$ have been linked to gas production since the 1980ies. The most notable event was the Huizinge earthquake in 2012, with a magnitude of $M_L = 3.6$, about 15 km to the southwest of the Eemshaven. The probability of an earthquake in the central part of the Groningen field with a magnitude of $M_L > 4$ was 5.5% before 2018 and has since declined to 1% in 2025.

Geohydrology
Modelling results from the national hydrological model LHM suggest that Site 1 has a clear division in a part with deeper (north) and shallower (south) groundwater levels, which is explained by variations in soil surface level. Also Site 2 shows a large variation in groundwater level depth, with relatively deep levels in the south-west part and shallow levels in the northern part. On average, modelled groundwater levels are deepest at site 3. Absolute groundwater levels (in m NAP) are lowest at site 1 and highest at site 3. Particularly in the east – southeast part of site 3 the groundwater levels are relatively high; this is due to higher resistance of Holocene layer here, because of the presence of the clayey Wormer member.

Particularly the mean yearly highest groundwater levels (GHG) are relevant, as it related to inundation risk. At site 3, the GHG remains well below 1 m.b.s.l. At site 1, however, there are areas where the calculated GHG is shallower than 0.5 m.b.s.l, with most of the terrain having a GHG between 0.5 and 1 m.b.s.l. At site 2 the variation is largest, again due to the large variations in soil surface levels.

It is stressed that the modelling results are uncertain due to the absence of publicly available data (e.g. groundwater level monitoring data) from the sites.

Geotechnical properties
With the exception of the landfill, the sand layers are similar for all subareas. The landfill is dense at site 2 and 3 and loose to medium dense at site 1. The natural sand layers below consist mainly of loose to medium dense sands. The NUNAWO clay layer varies significantly in thickness, and can be absent in site 2 and the northern part of site 3. Differential settlements can be expected due to these variations. The bearing capacity of the NUNAWO layer is too low, which implies that ground treatment of the NUNAWO layer is required or that a piled foundation is needed. Such a treatment will also reduce the total expected settlements and the differential settlements.

Liquefaction due to seismicity is not expected. However, the region is known for static liquefaction of the external slopes of the foreshore. Static liquefaction may need re-evaluation for low likelihood events for a NPP during later design phases.

10.3 Recommendations

Although there was enough data available for the present reconnaissance phase of the project, additional data must be acquired to better model the 3D buildup of the subsurface.

This is especially important for the Early-Holocene Wormer clay layer that varies in thickness and material properties as well as the presence of tidal channels that have incised into this confining clay unit and the underlying Pleistocene units. An accurate mapping of these features will improve our understanding of spatial variation in settlement rates under the load of an NPP. Furthermore, especially the incision of tidal channels is important to accurately map in 3D for hydrological model studies.

No groundwater monitoring wells are present at the potential project sites, which makes the geohydrological evaluation of the sites uncertain. It is advisable to develop and execute a monitoring plan, preferably consisting of multiple monitoring wells per site with filters at different depths, to capture both horizontal and vertical gradients. Monitoring should continue for at least one year to capture seasonal effects. High frequency monitoring would be advisable for at least a short period to capture tidal effects.

For the potential risks associated with seismic hazards a full Probabilistic Seismic Hazard Analysis according to the latest scientific standards and SSHAC recommendations, is recommended. Based on preliminary assumptions it is concluded that the risk of full liquefaction is low. These assumptions need further consideration once the full Probabilistic Seismic Hazard Analysis has been carried out.

11 References

Adriaens, R., Zeelmaekers, E., Fettweis, M., Vanlierde, E., Vanlede, J., Stassen, P., Elsen, J., Srodon, J. & Vandenberghe, N., 2018. Quantitative clay mineralogy as provenance indicator for recent muds in the southern North Sea. Marine Geology 398: 48-58. DOI: 10.1016/j.margeo.2017.12.011

Basili, R., Danciu, L., Beauval, C., Sesetyan, K., Vilanova, S., Adamia, S., Arroucau, P., Atanackov, J., Baize, S., Canora, C., Caputo, R., Carafa, M., Cushing, M., Custodio, S., Demircioglu Tumsa, M., Duarte, J., Ganas, A., Garcia-Mayordomo, J., Gomez de la Pena, L., … Zupancic, P. (2022). *European Fault-Source Model 2020 (EFSM20): online data on fault geometry and activity parameters. Istituto Nazionale di Geofisica e Vulcanologia (INGV)*. https://doi.org/https://doi.org/10.13127/efsm20

Bosch, J. H. A. (2000). *Nederlands Instituut voor Toegepaste Geowetenschappen TNO Standaard Boor Beschrijvingsmethode Versie 5.1 (in Dutch)*.

Boulanger, R.W., Idriss, I.M. (2014). CPT and SPT based liquefaction triggering Procedures. *Center for Geotechnical Modeling, Department of Civil and Environmental Engineering, University of California, Davis, California. Report No. UCD/CGM-14/01,* April 2014

Danciu, L., Nandan, S., Reyes, C. G., Basili, R., Weatherill, G., Beauval, C., ... & Giardini, D. (2021). The 2020 update of the European Seismic Hazard Model-ESHM20: model overview. *EFEHR Technical Report*, *1*.

Dost, B., Ruigrok, E., Spetzler, J., & Kruiver, P. (2025). Natural and induced seismicity. In J. H. ten Veen, G.-J. Vis, J. de Jager, & T. E. Wong (Eds.), *Geology of the Netherlands: Second Edition* (pp. 793–823). Amsterdam University Press. https://doi.org/10.2307/jj.27435714.26

Förster, M. W., & Sirocko, F. (2016). The ELSA tephra stack: Volcanic activity in the Eifel during the last 500,000 years. *Global and Planetary Change*, *142*, 100–107. https://doi.org/10.1016/j.gloplacha.2015.07.012

Gibbard, P. L., & Lewin, J. (2016). Filling the North Sea Basin: Cenozoic sediment sources and river styles (André Dumont medallist lecture 2014). *Geologica Belgica*.

Gislason, S. R., Hassenkam, T., Nedel, S., Bovet, N., Eiriksdottir, E. S., Alfredsson, H. A., Hem, C. P., Balogh, Z. I., Dideriksen, K., Oskarsson, N., Sigfusson, B., Larsen, G., & Stipp, S. L. S. (2011). Characterization of Eyjafjallajökull volcanic ash particles and a protocol for rapid risk assessment. *Proceedings of the National Academy of Sciences*, *108*(18), 7307–7312. https://doi.org/10.1073/pnas.1015053108

Global Volcanism Program. (2023). *[Database] Volcanoes of the World (v. 5.1.0; 9 Jun 2023). Distributed by Smithsonian Institution, compiled by Venzke, E. https://doi.org/10.5479/si.GVP.VOTW5-2023.5.1*.

de Haas, T., & Schepers, M. (2022). Wetland reclamation and the development of reclamation landscapes: A comparative framework. *Journal of Wetland Archaeology*, *22*(1-2), 75-96.

Hensch, M., Dahm, T., Ritter, J., Heimann, S., Schmidt, B., Stange, S., & Lehmann, K. (2019). Deep low-frequency earthquakes reveal ongoing magmatic recharge beneath Laacher See Volcano (Eifel, Germany). *Geophysical Journal International*, *216*(3), 2025–2036. https://doi.org/10.1093/gji/ggy532

Hijma, M. P. & Kooi, H. Bodemdaling in het kustfundament en de getijdenbekkens (deel 2) - Een update, case IJmuiden en kwantificering onzekerheden. (Deltares report 11202190-001-ZKS-0001_v1.0, 2018).

Hijma, M. P., & Cohen, K. M. (2019). Holocene sea-level database for the Rhine-Meuse Delta, The Netherlands: Implications for the pre-8.2 ka sea-level jump. *Quaternary Science Reviews*, *214*, 68–86. https://doi.org/10.1016/j.quascirev.2019.05.001

Hijma, M. P., Cohen, K. M., Hoffmann, G., Van der Spek, A. J. F., & Stouthamer, E. (2009). From river valley to estuary: the evolution of the Rhine mouth in the early to middle Holocene

(western Netherlands, Rhine-Meuse delta). *Netherlands Journal of Geosciences - Geologie En Mijnbouw*, *88*(1), 13–53. https://doi.org/10.1017/S0016774600000986

Hijma, M.P., Bradley, S.L., Cohen, K.M. *et al.* Global sea-level rise in the early Holocene revealed from North Sea peats. *Nature* **639**, 652–657 (2025). https://doi.org/10.1038/s41586-025-08769-7

Huisman, D.J. & Kiden, P., 1998. A geochemical record of Late Cenozoic sedimentation history in the southern Netherlands. Geologie En Mijnbouw 76 (4): 277-292. DOI: 10.1023/A:1003212721020

Huis in 't Veld, R. and Den Hartog Jager, D. (2025). Late Carboniferous. In J. H. ten Veen, G.-J. Vis, J. de Jager, & T. E. Wong (Eds.), *Geology of the Netherlands: Second Edition* (pp. 95–125). Amsterdam University Press. https://doi.org/10.2307/jj.27435714.7

International Atomic Energy Agency. (2012). *Volcanic Hazards in Site Evaluation for Nuclear Installations: Specific Safety Guide*.

Janssen, G., Vermeulen, P., Van Walsum, P., Prinsen, G., Nogueira, G.E.H., Verkaik, J., Delsman, J., Kok, H., Leander, R., Klapwijk, E., Kroon, T., 2025. Veranderingsrapportage LHM 4.3.3 - De nieuwe release van het Landelijk Hydrologisch Model in het voorjaar van 2025, Deltares report 11211537-001-BGS-0001.

Jordan, S. C., Le Pennec, J.-L., Gurioli, L., Roche, O., & Boivin, P. (2016). Highly explosive eruption of the monogenetic 8.6 ka BP La Vache et Lassolas scoria cone complex (Chaîne des Puys, France). *Journal of Volcanology and Geothermal Research*, *313*, 15–28. https://doi.org/10.1016/j.jvolgeores.2015.12.006

Kettlety, T., Martuganova, E., Kühn, D., Schweitzer, J., Weemstra, C., Baptie, B., Dahl-Jensen, T., Jerkins, A., Voss, P. H., Kendall, J. M., & Skurtveit, E. (2024). A unified earthquake catalogue for the North Sea to derisk European CCS operations. *First Break*, *42*(5), 31-36. https://doi.org/10.3997/1365-2397.fb2024036

Kluiving, S.J., Bosch, A.J.H., Ebbing, J.H.J., Mesdag, C.S. & Westerhoff, R.S., 2003. Onshore and offshore seismic and lithostratigraphical analysis of a deeply incised Quaternary buried valley system in the Northern Netherlands. Journal of Applied Geophysics 53(4): 249–271.

Kombrink, H. (2008). *The Carboniferous of the Netherlands and surrounding areas; a basin analysis. Geologica Ultraiectina (294)*. Departement Aardwetenschappen.

Lengkeek, A., de Greef, J., & Joosten, S. (2018). CPT based unit weight estimation extended to soft organic soils and peat. In M. A. Hicks, F. Pisano, & J. Peuchen (Eds.), *Cone Penetration Testing 2018: Proceedings of the 4th International Symposium on Cone Penetration Testing (CPT'18), 21-22 June 2018, Delft, The Netherlands* (pp. 389-394). London: CRC Press.

Lengkeek, A. (2024). CPT based classification with focus on organic soils. In proceedings of the 7th International Conference on Geotechnical and Geophysical Site Characterization, Barcelona. DOI: 10.23967/isc.2024.154.

Lunne, T., Christoffersen, H.P., (1983). Interpretation of cone penetrometer data for offshore sands. *Proceedings OTC 1983*, OTC 4464.

Meijles, E. (2015). A geological history of Groningen's subsurface.

Munsterman, D. K., ten Veen, J. H., Menkovic, A., Deckers, J., Witmans, N., Verhaegen, J., ... & Busschers, F. S. (2019). An updated and revised stratigraphic framework for the Miocene and earliest Pliocene strata of the Roer Valley Graben and adjacent blocks. *Netherlands Journal of Geosciences*, *98*, e8.

NAM, 2020. Bodemdaling door aardgaswinning - Statusrapport 2020 en Prognose tot het jaar 2080. Report No. EP202011201629: 58 pp.

NEN. (2020). Webtool NPR 9998: Bepaling van de seismische belasting. https://seismischekrachten.nen.nl/

Petersen, G. N., Bjornsson, H., & Arason, P. (2012). The impact of the atmosphere on the Eyjafjallajökull 2010 eruption plume. *Journal of Geophysical Research: Atmospheres*, *117*(D20). https://doi.org/10.1029/2011JD016762

Pierik, Harm Jan & Leuven, Jasper & Busschers, F.s & Hijma, Marc & Kleinhans, Maarten. (2022). Depth-limiting resistant layers restrict dimensions and positions of estuarine channels and bars. The Depositional Record. 9. 10.1002/dep2.184.

Pouclet, A., & Juvinge, E. (2009). The Eltville Tephra, a Late Pleistocene widespread tephra layer in Germany, Belgium and the Netherlands; symptomatic compositions of the minerals. *Geologica Belgica*, *12*(1–2), 93–103.
Reise, K. (2013). *A natural history of the Wadden Sea*. Wadden Academy.
Staatstoezicht op de Mijnen. (2025). *Staat van de veiligheid in Groningen 2024*. Staatstoezicht op de Mijnen. Retrieved from https://www.sodm.nl/documenten/rapporten/2025/04/07/staat-van-de-veiligheid-in-groningen-2024
STOWA (2020) Deltafact bodemdaling. Bodemdaling versie 3.1 (feb 2020).pdf
Ten Veen, J. H., Vis, G.-J., de Jager, J., & Wong, T. E. (Eds.). (2025). *Geology of the Netherlands: Second Edition*. Amsterdam University Press. https://doi.org/10.2307/jj.27435714
TNO-GDN. (2023). *Geologische Kaart van het Koninkrijk der Nederlanden 1:600 000*.
TNO & Deltares, 2022. KEM-19 - Evaluation of post-abandonment fluid migration and ground motion risks in subsurface exploitation operations in the Netherlands. Final report Phase 2 Simulations and case studies of fluid migration, leakage, and ground motion threats in selected hydrocarbon areas in the Netherlands. KEM-19 Report: 161 pp
Van Adrichem Boogaert, H.A. & Kouwe, W.F.P., 1993–1997. Stratigraphic nomenclature of the Netherlands. Mededelingen Rijks Geologische Dienst 50
Van den Bogaard, P., & Schmincke, H.-U. (1985). Laacher See Tephra: A widespread isochronous late Quaternary tephra layer in central and northern Europe. *Geological Society of America Bulletin*, *96*(12), 1554. https://doi.org/10.1130/0016-7606(1985)96<1554:LSTAWI>2.0.CO;2
Van Onselen, E.P., 2021. Nationale erosieresistente lagen kaart, Deltares rapport 11206794-003-ZKS-0005, 12 pp
VEN, 2020. Bodemdaling Statusrapport 2020 - Drenthe Overijssel Friesland, versie 1.1. Vermilion Energy Netherlands B.V. (VEN): 101 pp.
Vis, G. J., Houben, A. J., Debacker, T. N., & Geel, C. R. (2025). The geological foundation of the Netherlands: the early Carboniferous, Devonian and older. *Geology of the Netherlands, second edition. Amsterdam University Press (Amsterdam)*, 53-93.
Vos, P. C., & Van Heeringen, R. M. (1997). Holocene geology and occupation history of the Province of Zeeland. *Mededelingen Nederlands Instituut Voor Toegepaste Geowetenschappen TNO*, *59*(5), 109.
Vos, P., Van der Meulen, M., Weerts, H., & Bazelmans, J. (2020). *Atlas of the Holocene Netherlands*.
Wallinga, Jakob & Törnqvist, Torbjörn & Busschers, F.s & Weerts, H.J.T.. (2004). Allogenic forcing of the late Quaternary Rhine-Meuse fluvial record: the interplay of sea-level change, climate change and crustal movements. Basin Research. 16. 535-547. 10.1111/j.1365-2117.2003.00248.x.

A Lithological description of the geological units

In this section, characteristics of each of the geological units will be described in detail. This includes the depositional age, lithology and related depositional environments, defining characteristics of the lower and upper boundaries of each unit, the thickness and typical depths at the Eemshaven sites. In addition, defining characteristics of these units in cone penetration test (CPT) results are discussed in combination with specific points of attention related to geotechnical investigations. The geological formations will be discussed from young to old.

For the current report we limit ourselves to the formations that make up the top 200 m of subsurface at Eemshaven, because that is the depth range that is covered by boreholes.

A.1 Naaldwijk Formation

A.1.1 Undifferentiated (NUNA)

- Link to Dutch stratigraphic nomenclature

https://www.dinoloket.nl/stratigrafische-nomenclator/formatie-van-naaldwijk

- Age

Holocene, varying per site location. Site 1: Boreal to present (~9000 BP - present). Site 2 and 3: Atlantic to present (~8000 BP - present). Southernmost tip of site 3: Atlantic to present (~7000 BP - present).

- Lithological description

(Silty) fine to coarse grey sand. Sometimes alternating with layers of silty or sandy clay (especially at site 1). Shells and shell fragments occur in varying quantities.

- Depositional environments

Tidal basin. Diverse range of intertidal and subtidal environments including mudflats, tidal bars, channels and creeks.

- Lower boundary

Stratigraphically above the Wormer Member of the Naaldwijk Formation. If present, above the Hollandveen member of the Nieuwkoop Formation (only the case in the southernmost tip of the site 3 area). In places where a tidal channel has incised, NUNA may be bounded by Late-Pleistocene units such as the Boxtel Formation, Drenthe Formation or even Peelo formation.

- Upper boundary

Covered by anthropogenically reworked sediment or exposed at the surface.

- Thickness indication and typical depth interval

Thickness up to 20 m at site 1 and in places with NUNA-filled tidal channel incisions (mainly site 2) down to 4 m in the southern half of the site 3 area. Depth interval at site 1 typically between -20 and 0 m NAP and between -10 and 0 m NAP at site 2 and 3.

- CPT characteristics

Variable cone resistance (qc) and friction ratio (rf). Peaks in qc are related to tidal channel deposits (>20 MPa) or to sandy tidal flats (10 – 20 MPa). This is alternated by lower values of qc and higher values of rf (approximately 2 – 4 %), related to more clayey sediments, which are interpreted as mudflats. A peak in rf (>5 %) with very low values of qc indicates the occurrence of peat/organic rich clay, but these are rarely present.

- Points of attention

This unit is very heterogenous due to the dynamic nature of the intertidal and subtidal zone it was part of throughout most of the Holocene. Thickness of the unit may change abruptly due to incised tidal channels.

A.1.2 Wormer Member (NUNAWO)

- Link to Dutch stratigraphic nomenclature

https://www.dinoloket.nl/en/stratigraphic-nomenclature/wormer-member

- Age

Holocene, varying per site location. Site 1: Pre-Boreal to Boreal (9500 - 8500 BP); Site 2: Boreal (8500 - 8000 BP); Site 3: Boreal to Atlantic (8500 - 7000 BP)

- Lithological description

Grey silty or sandy calcareous clay. The clay can be organic-rich. The Wormer Member is locally sandy (e.g. site 1). It may contain shells and shell fragments.

- Depositional environments

Tidal basin. Intertidal mudflats to supratidal salt marshes.

- Lower boundary

Typically, a sharp and possibly erosive contact with sand of the Boxtel Formation. Otherwise a sharp contact with Basal Peat of the Nieuwkoop Formation.

- Upper boundary

Stratigraphically below the undifferentiated later-Holocene Naaldwijk Formation.

- Thickness indication and typical depth interval

Typically 1 - 4 m at a depth interval of -14 to -10 m NAP. Found deeper at site 1, around -18 m NAP. Thicker deposits, up to 10 m, are found in the southeast of the Eemshaven area between - 14 and - 4 m NAP.

- CPT characteristics

High rf values (2 – 5 %) and low qc values (around 1 MPa), associated with the occurrence of (organic) clay. Occasionally higher qc and lower rf values when the Wormer Member is sandy.

- Points of attention

Locally absent due to incision of later channels.

A.2 Nieuwkoop Formation

A.2.1 Undifferentiated (NUNI)

- Link to Dutch stratigraphic nomenclature

https://www.dinoloket.nl/en/stratigraphic-nomenclature/hollandveen-member

- Age

Holocene, Subboreal - early Subatlantic.

- Lithological description

Brown to black peat, with occasionally traces of sand in the upper part. The peat can be spongy to very loose.

- Depositional environments

Eutrophic to mesotrophic coastal marsh.

- Lower boundary

A sharp, but non-erosive contact with the tidal clay and sand of the Wormer Member.

- Upper boundary

Sharp erosive contact with deposits of the (undifferentiated) Naaldwijk Formation.

- Thickness indication and typical depth interval

Only seen in the southeasternmost tip of the Eemshaven area where it is locally found as a 10 - 50 cm thick layer around -4 m NAP.

- CPT characteristics

Rf with values >5 % and corresponding very low (1 MPa) values of qc.

- Points of attention
  1. The peat can be spongy to very loose.
  2. Widespread peat layers formed in coastal peat areas are typically counted to the Hollandveen Member of the Nieuwkoop Formation. Here we chose to not use this classification as the peat found at site 3 appears to be local or is at best indicating proximity to a coastal peat area further to the south.

A.2.2 Basal Peat Bed (NUNIBA)

- Link to Dutch stratigraphic nomenclature

https://www.dinoloket.nl/en/stratigraphic-nomenclature/basisveen-bed

- Age

Early Holocene. The age of the Basal Peat Bed corresponds with the vertical position with respect to the paleo-groundwater level.

- Lithological description

Brown to black stiff and compact peat.

- Depositional environments

Eutrophic lowland marsh subjected to a rising groundwater level.

- Lower boundary

A relatively gradual contact with the Late Pleistocene very fine sand of the Boxtel Formation.

- Upper boundary

The Basal Peat Bed commonly has a sharp contact with the clay and sand of the Wormer Member. Alternatively a sharp contact with the (undifferentiated) Naaldwijk Formation is possible if a tidal channel has eroded deposits belonging to the Naaldwijk Wormer Member.

- Thickness indication and typical depth interval

Thickness < 0.5 m at depths of around -14 m NAP (site 2 and 3) or around -18 m NAP (site 1).

- CPT characteristics

Typically expressed as a peak in rf with values >5 % and corresponding very low (1 MPa) values of qc.

- Points of attention

None.

A.3 Boxtel Formation (NUBX)

- Link to Dutch stratigraphic nomenclature

https://www.dinoloket.nl/en/stratigraphic-nomenclature/boxtel-formation

- Age

Late-Pleistocene (Weichselian)

- Lithological description

Very fine to very coarse sand. Coarse sands are dominant, sometimes with gravel admixture. Sometimes clay or rarely a very thin layer of peat.

- Depositional environments

Fluvial environments: local, small-scale braided river system and brooks. Mainly channel beds (sand) and less frequently overbank deposits (clayey sand, silt and clay). Also Periglacial aeolian sands

- Lower boundary

Either diffuse in case of aeolian deposits or sharp, sometimes erosive contact in case of channel deposits. Can be bounded by the Eem, Drenthe and Peelo Formation depending on their presence.

- Upper boundary

Gradual contact with the peat of the Basal Peat Bed or with the tidal clay of the Wormer Member. Sharp contact possible with younger incised Naaldwijk tidal channels.

- Thickness indication and typical depth interval

Locally up to 15 m thick, but typically in the range of 5 - 10 m. Can be found between -12 and -28 m NAP.

- CPT characteristics

Low rf values of approximately 1 % with peaks in qc up to 40 MPa. Typical qc range is 10 - 30 MPa. Thin layers of finer-grained material may have rf values up to 4 in combination with a low (1 - 2 MPa) cone resistance.

- Points of attention

The lower boundary of the Boxtel Formation is difficult to determine accurately;
Hard to distinguish from Peelo and Drente Formation based on CPTs alone;
The Boxtel formation in this area is atypically a very coarse sandy, sometimes even gravelly unit.

A.4 Eem Formation (NUEE)

- Link to Dutch stratigraphic nomenclature

https://www.dinoloket.nl/en/stratigraphic-nomenclature/eem-formation

- Age

Late-Pleistocene (Eemian)

- Lithological description

Grey fine to coarse sand, calcareous and may contain shells and fragments.

- Depositional environments

Tidal flats and channels, shallow marine.

- Lower boundary

Sharp, possibly erosive contact with Peelo or Drente Formation.

- Upper boundary

Either diffuse in case of aeolian Boxtel sands or sharp, sometimes erosive contact in case of Boxtel channel deposits.

- Thickness indication and typical depth interval

Less than 5 m, if present (only at site 1), found between -20 and -30 m NAP.

- CPT characteristics

No data from the Eemshaven area available.

- Points of attention

No boreholes in the Eemshaven describe the Eem Formation. It is believed to be only present at site 1, but the exact boundaries are highly uncertain.

A.5 Drente Formation (NUDR)

- Link to Dutch stratigraphic nomenclature

https://www.dinoloket.nl/en/stratigraphic-nomenclature/drente-formation
https://www.dinoloket.nl/en/stratigraphic-nomenclature/schaarsbergen-member

- Age

Late Middle Pleistocene (Saalian).

- Lithological description

Fine to very coarse sand and gravel, though mostly coarse sand and upward.

- Depositional environments

Glaciofluvial (proglacial sandur, stratified sand)

- Lower boundary

Sharp, unconformable contact with sand belonging to the Formation of Peelo.

- Upper boundary

Diffuse or erosive contact with the Boxtel Formation (see Boxtel Formation lower boundary). Possibly, albeit unlikely a sharp erosive contact with an incised Naaldwijk channel.

- Thickness indication and typical depth interval

Typically less than 5 m at depths between -20 and -30 m NAP

- CPT characteristics

High cone resistance typically in the range of 20 - 40 MPa with rf values of ~1%.

- Points of attention

Not many interpreted boreholes that describe characteristics of the Drente Formation. May also consist of glacial till (Gieten member). Hard to distinguish from Peelo and Boxtel Formation based on CPTs alone.

A.6 Peelo Formation (NUPE)

- Link to Dutch stratigraphic nomenclature

https://www.dinoloket.nl/en/stratigraphic-nomenclature/peelo-formation

- Age

Middle-Pleistocene (Elsterian)

- Lithological description

Mostly light grey, yellowish grey and brownish grey very fine to very coarse sand. In the Eemshaven area overall finer-grained than, the Drente Formation. Possibly also grey to black or brownish black (very) firm clay (‘potclay’), most likely to the east of the Eemshaven.

- Depositional environment

Glaciofluvial and glaciolacustrine.

- Lower boundary

Sharp contact with fluvial sand of the Appelscha formation.

- Upper boundary

Unconformable contact with the Eem, Drente or Boxtel Formation.

- Thickness indication and typical depth interval

~20 m typically between -30 and -50 m NAP.

- CPT characteristics

For glaciofluvial sands low rf and cone resistance likely in the range of 10 - 40 MPa, but there is little CPT data to confirm this.

- Points of attention

A tunnel valley associated with the Peelo Formation runs just to the east of the Eemshaven. Potclay is more likely to be found here as opposed to the glaciofluvial sands under the Eemshaven. Hard to distinguish from Drente and Boxtel Formation based on CPTs alone.

A.7 Appelscha Formation (NUAP)

- Link to Dutch stratigraphic nomenclature

https://www.dinoloket.nl/en/stratigraphic-nomenclature/appelscha-formation

- Age

Middle Pleistocene (Bavelian to Cromerian C)

- Lithological description

Light grey to light yellow medium to very coarse sand, non-calcareous, gravelly.

- Depositional environment

Fluvial, braided river system.

- Lower boundary

Gradual contact with fluvial sand of the Peize formation.

- Upper boundary

Sharp, erosive contact with fluvial sand of the Peelo formation.

- Thickness indication and typical depth interval

~10 m between -60 and -50 m NAP

- CPT characteristics

No data, but stable low friction ratios (~1%) alongside high cone resistance (~10 - 30 MPa) expected.

- Points of attention

No local CPT data available. Is absent in the eastern half of the area.

A.8 Peize Formation (NUPZ)

- Link to Dutch stratigraphic nomenclature:
https://www.dinoloket.nl/en/stratigraphic-nomenclature/peize-formation

- Age
Late Pliocene - early Pleistocene.

- Lithological description
Light grey to white fine to very coarse quartz-rich sand.

- Depositional environment
Fluvial, braided river system. The bottom of the unit may also have developed in a deltaic environment (delta top and delta front).

- Lower boundary
Sharp contact with marine deposits of the Oosterhout formation.

- Upper boundary
Gradual transition into Appelscha Formation or sharp erosive contact with the Peelo Formation.

- Thickness indication and typical depth interval
Up to 100 m to the west of the Eemshaven (between -60 and -160 m) down to 20 m thick to the west where the Peelo tunnel valley has eroded most of the Peize Formation deposits.

- CPT characteristics
No data, but stable low friction ratios (~1%) alongside high cone resistance (~10 - 30 MPa) expected.

- Points of attention
No local CPT data available.

A.9 Oosterhout Formation (NUOO)

- Link to Dutch stratigraphic nomenclature
https://www.dinoloket.nl/en/stratigraphic-nomenclature/oosterhout-formation

- Age
Pliocene (Piacenzian).

- Lithological description
Fine to coarse, light grey to greyish green sand with abundant shells. Trace amounts of glauconite can be present.

- Depositional environment
Shallow-marine, littoral zone.

- Lower boundary
Sharp contact with finer, shell-poor, glauconitic, green sand of the Breda Formation.

- Upper boundary
Unconformable contact with the bottom of the Peize Formation.

- Thickness indication and typical depth interval
~100 m thick, typically between -150 and -270 m NAP.

- CPT characteristics

No data from the Eemshaven area available. In general the Oosterhout Formation is characterized by a stable very low (>1 %) rf and a very high qc (peaks in qc can be 45 – 65 MPa).

- Points of attention

Traces of glauconite can be present.

A.10 Breda Formation (NUBR)

- Link to Dutch stratigraphic nomenclature

https://www.dinoloket.nl/en/stratigraphic-nomenclature/breda-formation

- Age

Middle Miocene (Langhian – early Serravallian).

- Lithological description

Clay, very sandy to moderately silty and poorly graded, greenish black, fine to medium sand with abundant glauconite.

- Depositional environment

Subtidal offshore below storm wave base.

- Lower boundary

Middle North-Sea group

- Upper boundary

Sharp contact with coarser, shell-rich, greyish sand of the Oosterhout Formation. The Oosterhout Formation sand is also less glauconite-rich.

- Thickness indication and typical depth interval

Up to 150 m thick, typically between -250 and -400 m NAP below the Eemshaven.

- CPT characteristics

No local CPT data available.

- Points of attention

Glauconite is present in high amounts (up to 50 %) in the sandstones of the Breda Formation.

B Additional information geotechnical parameters

B.1 Layer boundaries

Table C.1 Layer boundaries for CS1.

Length along cross section (m)	Layer boundaries (m)					
	1	2	3	4	5	6
0	1.2	-10.5	-15.6	-20	-22	-30
200	1.3	-10.5	-15.5	-19	-22	-29
400	1.3	-10.5	-15	-19	-22	-28
600	1.3	-10.5	-14.5	-18	-23	-26
800	1.4	-10.5	-14	-17.4	-23	-24
1000	1.4	-10.5	-16.4	-18.2	-23	-23
1200	1.5	-10.5	-16.4	-17.6	-23	-23
1400	1.6	-10.5	-15	-22	-24	-24
1600	1.7	-10.5	-15	-22.8	-24	-24
1650	1.7	-10.5	-15	-22.8	-24	-24

Table C.2 Layer boundaries for CS3.

Length along cross section (m)	Layer boundaries (m)					
	1	2	3	4	5	6
0	4.5	0.5	-10.5	-15	-22	-28
200	4.5	0.5	-10.5	-15	-22	-28
300	4.5	0.2	-11.5	-14.5	-22	-28
500	4.5	0.2	-11.5	-16	-23	-27.5
700	4.5	0	-19.5	-19.5	-23	-27.5
1100	4.5	0	-23.5	-23.5	-24	-27.5
1180	4.5	-0.1	-23	-23	-24	-27.4
1201	4.5	-0.2	-15	-15	-24	-27.3
1250	4.5	-0.3	-10.5	-15	-24	-27
1400	4.5	-0.5	-10.5	-15	-25	-27

Table C.3 Layer boundaries for CS3.

Length along cross section (m)	Layer boundaries (m)				
	1	2	3	4	5
0	2.7	1.2	-3.5	-14	-28
200	2.7	1.2	-3.5	-14	-28.3
300	2.7	1.2	-3.5	-14	-28.7
500	2.7	0.8	-4.5	-15	-29.2
700	2.7	0.8	-5.5	-14	-29.7
1100	2.7	0.8	-9	-14	-30

Length along cross section (m)	Layer boundaries (m)				
	1	2	3	4	5
1250	2.7	0.8	-10	-14	-30
1400	2.7	0.8	-11	-14	-30
1600	2.7	0.8	-11	-14.5	-30
1800	2.7	0.8	-11.5	-14	-30
2000	2.7	0.8	-10.5	-14	-30
2100	2.7	0.8	-11.5	-14	-30

B.2 NEN9997 Interpolation table

Table C.4 Interpolation table for all layers except the NUNAWO layer.

$q_{c,norm}$	phi (degrees)	E100 (MPa)	$C_c/(1+e_0)$	C_α	$C_{sw}/(1+e_0)$
0.1	15	0.2	0.46	0.023	0.1533
0.5	15	1	0.23	0.0115	0.0767
0.7	22.5	1.5	0.23	0.0092	0.0767
1.0	27.5	2	0.092	0.0037	0.0307
2	27.5	3	0.0511	0.0020	0.017
5	30	15	0.0115	0	0.0038
15	32.5	45	0.0038	0	0.0013
25	35	75	0.0023	0	0.0008
45	40	110	0.0015	0	0.0005

Table C.4 Interpolation table the NUNAWO layer.

$q_{c,norm}$	phi (degrees)	E100 (MPa)	$C_c/(1+e_0)$	C_α	$C_{sw}/(1+e_0)$
0.1	15	0.2	0.46	0.023	0.1533
0.2	15	0.5	0.3067	0.0153	0.1022
0.5	15	1	0.23	0.0115	0.0767
1	15	2	0.1533	0.0077	0.0511
2	27.5	3	0.0511	0.002	0.017
5	30	15	0.0115	0	0.0038
15	32.5	45	0.0038	0	0.0013
25	35	75	0.0023	0	0.0008
45	40	110	0.0015	0	0.0005

Deltares is an independent institute for applied research in the field of water and subsurface. Throughout the world, we work on smart solutions for people, environment and society.

Deltares

www.deltares.nl